Influence of upper limb ischaemia-reperfusion injury on the regulation of cutaneous blood flow during local thermal hyperaemia

Gregory Walter McGarr, MSc

Submitted in partial fulfillment of the requirements for the degree
Doctor of Philosophy
(Health BioSciences)

Faculty of Applied Health Sciences, Brock University
St. Catharines, ON
Canada

ABSTRACT

The present research was developed to investigate the effects of acute upper limb ischaemia- reperfusion (I-R) on neurovascular and endothelial control of the cutaneous micro-circulation in the forearm and finger by evaluating its influence on the magnitude and kinetics of the vasodilatory response to local skin heating. Study 1 investigated between-day reliability of the local heating response in non-glabrous and glabrous index finger skin. Study 2 investigated the effects of I-R on the local heating response in non-glabrous and glabrous skin of the index finger. Study 3 investigated within- and between-day reliability of the local heating response in non-glabrous forearm skin. Study 4 investigated the effects of I-R on the local heating response in non-glabrous forearm skin, as well as the contribution of sensory nerves in mediating the magnitude and kinetics of this response. When data were normalized for blood pressure and expressed as cutaneous vascular conductance (CVC) reliability was generally comparable across all skin sites. In non-glabrous skin reliability was superior when CVC was normalized to maximum heating. At all skin sites, normalizing CVC to baseline produced poor results. Vasodilatory onset time and time to initial peak during local heating produced moderate to good reliability for all skin sites in Studies 1 and 3. In the finger, I-R did not influence the magnitude of the local heating response for the initial peak or plateau phases in either skin type. However, I-R did cause a ~23% delay in vasodilatory onset time and a ~16% delay in time to initial peak in non-glabrous skin. In the forearm, I-R attenuated the initial peak and plateau phases by ~31% and

~34%, respectively. Vasodilatory onset time was also delayed by 34% post-ischaemia. The contribution of sensory nerves in mediating the initial peak and vasodilatory onset time were significantly reduced post-ischaemia, while sensory nerves did not influence the plateau. It is concluded that upper limb I-R impairs the local heating response in non-glabrous forearm and index finger skin. A combination of cutaneous sensory nerve impairment and reduced nitric oxide bioavailability appear to be responsible for attenuating the vasodilatory response to local skin heating under these conditions.

KEYWORDS: laser-Doppler, microcirculation, oxidative stress, sensory nerves, skin blood flow

ACKNOWLEDGEMENTS

I would like to start by thanking my supervisor Dr. Stephen S. Cheung for giving me the opportunity to join the Environmental Ergonomics Laboratory and enter the exciting field of environmental physiology. You have provided me with numerous opportunities to explore various avenues of research in the laboratory and in field settings, all while giving me the freedom to chart my own course by pursuing those areas that interested me the most. Your passion for science, high standards, and remarkable work ethic, has provided a great example of how to conduct myself as an independent scientist. Finally, your continued support and encouragement through the many ups and downs of this long process have been greatly appreciated by me.

I would like to thank Drs. Deborah O'Leary, Michael Plyley, and Gary Hodges for their valuable contributions as members of my thesis committee. Debbie and Mike have been involved from the beginning, starting with my comprehensive exams and throughout the many iterations of my thesis. Your thoughtful critiques of my ideas as well as your enthusiasm and positive attitudes during this process have been greatly appreciated. Gary has been an invaluable resource for learning about all aspects of skin blood flow control in humans, including designing and running experiments, analyzing data, and developing a detailed understanding of the underlying physiological mechanisms. His passion for this area of research and tremendous energy has made our time in the lab together over the last few years very productive and a lot of fun.

Throughout my extended tenure as a PhD Candidate at Brock University I have had the pleasure of working with many other great people over the years that have made the long hours spent in the lab a great place to work and learn. They include: Mike Taber, Geoffrey Hartley, Matt Smith, Nikki Zouros, Leah Rosso, Dessi Zaharieva, Roger Montgomery, Glen Selkirk, Isabelle Kim, Anais Masbou, Phil Wallace, Matt Mallette, Janae Vlaar, Nico Coletta, Steve Ferguson, Des Stewart, and Paul Davison.

I need to thank all of my family and friends for their continual support and encouragement throughout this process. In particular, I would like to thank my parents Rick and Carol Ann McGarr, my sister and brother in law, Sarah and Harris Nepon, and my friends Joe and Brittany Orlando.

Of course, I could not have completed this work without the individuals who participated in my experiments. I greatly appreciate those who generously and enthusiastically gave up their time to let me run pilot tests and experiments on them in order to complete my research. I also appreciate that some of them even trusted me enough to take a nap while I cut off blood flow to their arm for 20 minutes. Apparently my sense of self preservation is much stronger than others.

Finally, during the course of my doctoral studies I was financially supported by an Ontario Graduate Scholarship in Science and Technology, Brock University, and by additional support from Dr. Cheung's grant funding.

TABLE OF CONTENTS

LIST OF TABLES

LIST OF FIGURES

LIST OF ABBREVIATIONS

Adenosine triphosphate	ATP
Ambient room temperature	T_{amb}
Analysis of variance	ANOVA
Angiotensin-II	ANG-II
Arbitrary perfusion units	APU
Arteriovenous anastomosis	AVA
Calcitonin gene related peptide	CGRP
Calcium-activated potassium	KCa
Cluster of differentiation 11b/18	CD11b/CD18
Coefficient of variation (%)	%CV
Confidence interval	CI
Cutaneous vascular conductance	CVC
Endothelial derived hyperpolarizing factor	EDHF
Endothelial nitric oxide synthase	eNOS
Epoxyeicosatrienoic acid	EET
Hydrogen peroxide	H_2O_2
Inducible nitric oxide synthase	iNOS
Intercellular adhesion molecule-1	ICAM-1
Intraclass correlation coefficient	ICC
Ischaemia-reperfusion	I-R
Laser-Doppler flowmetry	LDF
Laser-Doppler imaging	LDI
Laser Speckle Contrast Imaging	LSCI
Local skin temperature	T_{loc}
Local thermal hyperaemia	LTH
Magnitude-based inference	MBI
Molecular oxygen	O_2
Neurokinin-A	NKA
Neurokinin-1	NK-1
Neuropeptide Y	NPY
N^G-nitro-L-arginine methyl ester	L-NAME
Null hypothesis significance testing	NHST
Nicotinamide adenine dinucleotide phosphate	NADPH
Nitric oxide	NO
Nitric oxide synthase	NOS
Neuronal nitric oxide synthase	nNOS
Post-occlusive reactive hyperaemia	PORH
Reactive oxygen species	ROS
Substance P	SP
Superoxide	O_2^-
Superoxide dismutase	SOD
Tetraethylammonium	TEA

Transient receptor potential	TRP
Transient receptor potential vanilloid	TRPV
Xanthine oxidase	XO
Xanthine dehydrogenase	XDH

Chapter 1: Introduction

Cutaneous sensory nerves play a vital role in mediating several physiological and pathophysiological processes at the tissue level including those associated with ischaemia and reperfusion. During ischaemia a significant depletion of cellular energy stores occurs, followed by an increase in oxidative stress and inflammation, which both contribute to microcirculatory impairment upon blood flow restoration. Sensory nerves exert their influence by releasing highly potent neuropeptides into the surrounding tissue, which promotes blood flow following ischaemia, but may also contribute to an exaggerated inflammatory response to the injury in some cases. In addition, persistent stimulation of sensory nerves under these conditions may also impair axonal conduction and/or desensitize neuropeptide receptors, which could render them unresponsive to further stimulation and hinder their ability to generate an appropriate increase in blood flow during a subsequent vasodilatory challenge.

Elevations in either local skin or core body temperature also require proper sensory nerve function to initiate an appropriate vasodilatory response. However, the physiological strain associated with acute and chronic cases of ischaemia and reperfusion may impair the function of sensory nerves, hindering their ability to regulate cutaneous blood flow in response to a subsequent heating challenge. In turn, this may prolong tissue hypoxia beyond the initial ischaemic insult and potentiate tissue injury when skin and vessel temperature are not adequately controlled. With that in mind, the primary purpose of this thesis is to examine the effects of an acute exposure to ischaemia and reperfusion injury of the upper limb in a group of healthy young males, on the subsequent vasodilatory response to local heating in the skin. A particular focus is placed on the early phase of the local heating response, which is predominantly controlled by sensory nerves. However, the response to sustained local heating, which is primarily nitric oxide (NO)-mediated, is also examined due to the well-established influence of reperfusion injury on NO bioavailability. Since non-glabrous (hairy) and glabrous (non-hairy)

skin are characterized by differences in neurovascular control and microcirculatory organization, comparisons between skin types are also evaluated.

Chapter 2 provides a review of the literature, starting with a general overview of the pathophysiology of ischaemia and reperfusion injury and its effects on microcirculatory blood flow. From there, a detailed description of the cutaneous microcirculation and its neural control mechanisms in human non-glabrous and glabrous skin is provided. This is followed by an examination of the role that cutaneous sensory nerves play in regulating vasodilatation and inflammation at the tissue level, culminating in an examination of the beneficial and deleterious effects of sensory nerve stimulation during ischaemia and reperfusion. The latter part of the review discusses the various measurement techniques and functional microvascular reactivity tests available for examining the cutaneous microcirculation and concludes with a thorough examination of the mechanisms that regulate the response to local heating in non-glabrous and glabrous skin in humans.

Chapter 3 outlines the main objectives and hypotheses for the experiments that follow in Chapters 5-8. Chapter 4 provides a detailed overview of common experimental methods, measurement techniques, and data analysis procedures used for all of the experiments.

Establishing reliability of the local skin heating protocol is vital prior to systematically investigating the effects of ischaemia and reperfusion on the response. Therefore, Chapter 5 examines the between-day reliability of the local heating response in non-glabrous and glabrous skin of the index finger using single-point laser-Doppler flowmetry. Several commonly used forms of data expression are assessed and test-retest reliability is evaluated in order to define the threshold values for minimally important positive and negative effects for the relevant skin sites in the subsequent experiment. Chapter 6 examines the influence of ischaemia and reperfusion injury on the vasodilatory response to local skin heating in the finger and compares the effects between non-glabrous and glabrous skin.

Chapter 7 examines the within-day and between-day reliability of the local skin heating response in non-glabrous skin of the forearm using single-point laser-

Doppler flowmetry. Similar to Chapter 6, several commonly used forms of data expression are assessed and test-retest reliability is evaluated in order to define the threshold values for minimally important positive and negative effects for the relevant skin sites in the subsequent experiment. Chapter 8 examines the influence of ischaemia and reperfusion injury on the vasodilatory response to local skin heating of the forearm. The influence of ischaemia and reperfusion on the contribution of sensory nerves in mediating the local skin heating response is also evaluated.

Chapter 9 is a general discussion. It integrates the experimental findings, provides conclusions in relation to the objectives and hypotheses outlined in Chapter 3, describes limitations of the previous experiments, and ends with directions for future research.

Chapter 2: Literature Review

2.1 Introduction

Human skin is densely populated with sensory nerves, which are intimately involved in several physiological and pathophysiological processes including cell growth, immunity, inflammation, wound healing, and the responses to itching and pain (Roosterman *et al.*, 2006). Stimuli such as heat and pain induce the release of highly potent neuropeptides from sensory nerve endings into the surrounding tissue, which are capable of activating adjacent immune cells and blood vessels in order to modulate the local inflammatory and microcirculatory responses to injury (Roosterman *et al.*, 2006).

Ischaemia and subsequent reperfusion are associated with several pathophysiological changes including the significant depletion of cellular energy stores during ischaemia, followed by an increase in oxidative stress and inflammation during reperfusion, which both contribute to microcirculatory impairment upon restoration of blood flow (Granger, 1999; Eltzschig & Collard, 2004; Kalogeris *et al.*, 2012). Both ischaemia and reperfusion are also associated with significant pain and a heightened activation of sensory nerve fibres and the consequent release of vasoactive neuropeptides. These neuropeptides play an important role in promoting blood flow following ischaemia, but may also contribute to an exaggerated inflammatory response to the injury in some cases. In addition, persistent stimulation of sensory nerves under these conditions may also impair axonal conduction and/or desensitize neuropeptide receptors, which could render them insensitive to further stimulation and hinder their ability to generate an appropriate increase in blood flow during a subsequent vasodilatory challenge (Wong *et al.*, 2005; Wong & Minson, 2011).

Sensory nerves in the skin also play a major role in mediating the initiation of cutaneous vasodilator responses to both local (Minson *et al.*, 2001) and whole body (Wong, 2013) heating. Since increasing temperature also increases metabolic demand on the tissue, an adequate increase in microcirculatory blood flow is

necessary to supply sufficient oxygen and nutrients under these conditions. Furthermore, an increase in core body temperature also requires an adequate increase in cutaneous perfusion in order to produce an appropriate thermoregulatory response to avoid overheating. However, impairments in sensory nerve conduction and/or depletion of vasoactive sensory neuropeptide stores associated with acute and chronic cases of ischaemia and reperfusion may inhibit the skin's response to a subsequent heating challenge. Acutely, this could result in persistent hypoxic stress following the original ischaemic insult if tissue temperature is not properly controlled, which may prolong recovery. In chronic wounds, which are associated with repeated cycles of ischaemia and reperfusion, elevated local skin temperature may exacerbate the tissue dysfunction and cellular breakdown that occurs over time, increasing the likelihood of ulcer formation (Mustoe, 2004). In addition, chronic tissue ischaemia in people with conditions such as diabetes may contribute to the impaired sensory nerve function associated with this disease (Lennertz *et al.*, 2011) and an altered neurovascular response to an elevation in core body temperature may contribute to their predisposition for heat related illness (Semenza *et al.*, 1999).

The purpose of the following review is to examine these relationships with the ultimate aim of providing a greater understanding of the potential influence of ischaemia and reperfusion on sensory nerve control of local heating in human skin. To accomplish this goal the review begins with a general overview of ischaemia and reperfusion injury followed by a description of the primary cellular and molecular responses with information derived from various *in vitro* and animal model experiments. The primary focus of this section is on the contributions of oxidative stress and inflammation to microcirculatory impairment. From there the review provides a detailed anatomical description of the cutaneous microcirculation and its innervation in both hairy and non-hairy human skin. This is followed by an examination of cutaneous sensory nerves and their influence on oedema formation, inflammation, and microcirculatory function from studies in both rodents and humans. This section ends by examining the role of sensory nerve responses to ischaemia and reperfusion, which, due to the limited information available in the

skin, necessitates an exploration of findings from several organ systems in rodents to provide a clear picture. The latter part of the review provides a brief description of techniques for examining skin blood flow and the use of functional reactivity tests to look at specific aspects of cutaneous microcirculatory function in humans before concluding with a comprehensive examination of the mechanisms involved in regulating the response to local heating in human hairy and non-hairy skin.

2.2 Ischaemia and reperfusion injury

It is commonly understood that restricting blood flow to a region of tissue for a protracted period of time results in tissue injury. The ultimate consequence of prolonged oxygen deprivation resulting from ischaemia is cellular necrosis in the affected area if blood flow is not restored in a timely fashion. What may be less intuitive, however, is that the vital act of tissue reperfusion, which restores blood flow to the affected area, may augment tissue injury beyond that of the ischaemia itself. In support of this, histological examinations of cat intestine (Parks & Granger, 1986) and human liver (Varadarajan *et al.*, 2004) have demonstrated that tissue damage caused by 3-hours of ischaemia followed by 1-hour of reperfusion is much greater than the injury observed following an equivalent duration (4-hours) of ischaemia alone. This process, which is now commonly referred to as reperfusion injury, is defined as the cellular damage that occurs after reperfusion of previously viable ischaemic tissues (Carden & Granger, 2000).

Reperfusion injury is a pervasive clinical problem that contributes to poor outcomes in a variety of pathological conditions such as frostbite and non-freezing cold injuries, hemorrhagic shock, myocardial infarction, and stroke. It is also a common operative concern following organ transplantation, free tissue transfers, limb replantations, and reconstructive surgeries (Wang *et al.*, 2011; Eisenhardt *et al.*, 2012; Schmidt *et al.*, 2012). Aside from acute cases of ischaemia, chronic conditions such as pressure ulcers, venous leg ulcers, diabetic neuropathic ulcers, and chronic limb insufficiency, among others, are associated with repeated cycles of ischaemia and reperfusion with the concomitant build up and distribution of toxic metabolites

and free radicals that contribute to progressive tissue dysfunction and cellular breakdown over time (Mustoe, 2004; Loerakker *et al.*, 2011).

Reperfusion following prolonged ischaemia initiates a number of pathophysiological processes within the microcirculation and surrounding tissue upon restoration of blood flow. These include the production of reactive oxygen species (ROS) in the blood, activation of the complement system, which induces the release of cytokines into the blood stream to activate and recruit leukocytes to the affected area, a reduction in endothelium-dependent vasorelaxation, increased capillary permeability and impaired perfusion contributing to further tissue hypoxia, leukocyte-endothelial cell interactions, and development of platelet-leukocyte aggregates (Eltzschig & Collard, 2004; Kalogeris *et al.*, 2012; Widgerow, 2014).

The immune system plays a major role in reperfusion-induced tissue damage. Local inflammation in the previously ischaemic tissue impairs normal perfusion and deposition of free radicals by leukocytes further exacerbates cellular dysfunction. If the ischaemic insult is great enough, the ensuing inflammatory response that occurs during blood flow restoration may be so profound that signs of reperfusion injury develop in remote organs that were not previously ischaemic (Carden & Granger, 2000; Eltzschig & Collard, 2004), and in the most severe cases this injury progresses to the systemic inflammatory response syndrome and multiple organ dysfunction syndrome, which are associated with high mortality rates (Carden & Granger, 2000; Eltzschig & Collard, 2004).

2.2.1 Ischaemic tolerance

Both the duration and magnitude of an ischaemic insult directly influence the reversibility of the response to injury, which ultimately determines tissue survival (Wang *et al.*, 2011; Schmidt *et al.*, 2012; Granger & Kvietys, 2015). Ischaemic tolerance differs greatly among various cell types and is directly associated with the metabolic demand, energy substrate requirements, and antioxidant capacity of the tissue in question (Eltzschig & Collard, 2004; Kalogeris *et al.*, 2012). On one extreme, the brain, which is the most sensitive organ to reductions in blood supply, will

succumb to irreversible injury when exposed to less than 20 minutes of ischaemia (Ordy *et al.*, 1993; Kalogeris *et al.*, 2012). In contrast, tissues such as the cornea, which contain little to no natural blood supply, have tremendous ischaemic tolerance. Indeed, corneal transplants can survive in cultures for up to three weeks with minimal cellular injury (Smith & Johnson, 2010; Kalogeris *et al.*, 2012).

Acute limb ischaemia is generally well tolerated in otherwise healthy individuals, with tissues such as skin and skeletal muscle sustaining several hours of oxygen deprivation before irreversible injury is present (Sapega *et al.*, 1985; Kalogeris *et al.*, 2012). In orthopaedic and vascular surgery of the limb, tourniquet time is generally limited to two hours under normothermic conditions (Turchanyi *et al.*, 2005). This duration of limb ischaemia is often associated with functional reductions in muscle contractile force for several days post-operatively (Suzuki *et al.*, 1995; Racz *et al.*, 1997; Joneschild *et al.*, 1999). However, overt signs of cellular damage are typically absent upon histological examination (Racz *et al.*, 1997; Turchanyi *et al.*, 2005). What is consistent among cell types is that all will eventually succumb to cellular necrosis following prolonged periods of anoxia or tissue hypoxia if adequate blood flow is not restored (Eltzschig & Collard, 2004; Kalogeris *et al.*, 2012).

2.2.2 Pathophysiology of ischaemia and reperfusion injury

The cellular and molecular responses to ischaemia and reperfusion are extremely complex and a complete examination of these mechanisms is far beyond the immediate scope of the current review. For an in depth exploration of ischaemia-reperfusion (I-R) injury from a cellular and molecular perspective, the reader is referred to other excellent reviews on the topic by Eltzschig and Collard (2004), Kalogeris *et al.* (2012), Widgerow (2014), and Granger and Kvietys (2015).

The onset of ischaemia initiates a reduction in oxidative phosphorylation and a transition to anaerobic metabolism in all affected cells, impairing their ability to resynthesize a sufficient amount of energy rich phosphates such as adenosine triphosphate (ATP) and phosphocreatine. Under these conditions ionic balance between the intracellular and extracellular environments becomes disrupted due to

reduced functioning of ATP-dependent membrane ionic pump function (Kalogeris *et al.*, 2012; Widgerow, 2014). Tissue pH is also reduced due to the accumulation of hydrogen ions inside the cell. In response, the sodium-proton exchange pump is activated in order to buffer this excess of hydrogen ions by driving them into the extracellular space, resulting in a large influx of sodium into the cell (Kalogeris *et al.*, 2012; Widgerow, 2014). The depletion of ATP further contributes to sodium overload within the cell by inhibiting the sodium pump and interfering with ATPases such as the sodium/potassium-ATPase. As a consequence, the active efflux of calcium from the cell and its reuptake by the endoplasmic reticulum are both impaired, the combined result of which is calcium overload within the cell (Kalogeris *et al.*, 2012; Widgerow, 2014). These changes are also associated with the opening of the mitochondrial permeability transition pore, which eliminates the normal mitochondrial membrane potential, further hindering ATP production (Kalogeris *et al.*, 2012; Widgerow, 2014). Ultimately, if the ischaemic insult is not interrupted, the combination of elevated intracellular calcium, pH alterations, and ATP depletion, results in cell death.

2.2.3 Development of reperfusion injury

The act of reperfusion replenishes the supply of oxygen and substrates necessary for aerobic ATP production and also restores normal tissue pH by flushing out excess hydrogen ions (Kalogeris *et al.*, 2012). However, the re-establishment of blood flow also initiates a detrimental chain of events. The molecular processes associated with reperfusion injury begin immediately upon restoration of blood flow to the affected tissue since the metabolic changes that have taken place during the preceding period of ischaemia have already primed the system for these pathological processes to develop upon reperfusion (Kaminski *et al.*, 2002; Eltzschig & Collard, 2004). The process of reperfusion injury is characterized by a variety of metabolic and molecular responses including a rapid increase in ROS production, leukocyte recruitment, increased membrane permeability and oedema, vascular thrombosis, as well as cellular apoptosis, which is a hallmark of reperfusion injury (Eltzschig & Collard, 2004; Widgerow, 2014).

2.2.4 Reactive oxygen species

Hearse *et al.* (1973) were the first to propose the idea that a rapid reintroduction of molecular oxygen (O_2), to previously energy- and oxygen-starved tissue results in a unique injury response that is not present during the initial period of hypoxic stress. It is now well established that restoration of blood flow is associated with an immediate and rapid increase of ROS production in the affected tissue that is sustained over the first few minutes of the response (Granger & Kvietys, 2015). Cellular enzymes that are built up during the preceding period of ischaemia are the source of this initial burst of ROS, which initiates the injury caused by reperfusion. Several potential enzymatic sources of ROS have been identified in the context of reperfusion injury, with the most prominent and well characterized being xanthine oxidase (XO), nicotinamide adenine dinucleotide phosphate (NADPH) oxidase, mitochondria, and uncoupled nitric oxide (NO) synthase (Granger & Kvietys, 2015). While one source of ROS will typically dominate the reperfusion injury response in a given tissue, the specific enzymatic source varies depending on the species and tissue type in question, and it has recently been argued that multiple sources are likely to contribute to reperfusion injury simultaneously due to the fact that redox signaling enables ROS from one enzymatic source to activate and enhance production by other sources (Granger & Kvietys, 2015).

In the majority of vascular beds including those found in skin and skeletal muscle, XO appears to be the primary enzymatic source of ROS (Carden & Granger, 2000; Granger & Kvietys, 2015). Xanthine oxidoreductase is a complex enzyme that regulates the rate-limiting step in the hydroxylation of xanthine to uric acid during ischaemia. In mammals, this enzyme exists in two interchangeable forms, xanthine dehydrogenase (XDH) and XO, with the dehydrogenase form of the enzyme dominating in healthy tissue. Granger (1988) provided the classical description for the theory of XO-derived ROS production during reperfusion. Under this paradigm, a period of ischaemia is associated with the conversion of ATP, via its progressive dephosphorylation, into hypoxanthine, while XDH is simultaneously converted to its oxidase form, XO. This is a crucial step because, unlike XDH, which uses the coenzyme NAD^+ as its terminal electron acceptor, the XO form of the enzyme uses

O_2, thus giving it the capacity for ROS generation (Granger, 1988; Carden & Granger, 2000).

Immediately upon reperfusion, the newly reintroduced O_2 then reacts with XO to catalyze the conversion of hypoxanthine to xanthine (and subsequently uric acid) and also produces ROS such as superoxide (O_2^-) and hydrogen peroxide (H_2O_2) as byproducts of this reaction. These ROS can then further interact with each other and with NO to produce secondary forms of ROS as well (Granger *et al.*, 1981; McCord, 1985; Granger & Kvietys, 2015). This process effectively shifts the normal NO/O_2^- balance, from one that is dominated by NO in healthy tissue to a state where NO bioavailability is reduced and the concentration of O_2^- is much higher, promoting cellular injury, inflammation, and arteriolar vasoconstriction (Carden & Granger, 2000). Interestingly, more recent evidence suggests that conversion from XDH to XO is not necessarily required for ROS production under these circumstances since the tissue is converted from an oxidative to a reduced state during ischaemia, which is known to increase the generation of O_2^- directly from XDH when xanthine is present (Lee *et al.*, 2014; Granger & Kvietys, 2015).

The immune system also responds rapidly to this initial tissue insult by depositing natural antibodies, activating the complement system and recruiting leukocytes into the affected area (Eltzschig & Collard, 2004; Kalogeris *et al.*, 2012). It is this inflammatory response that ultimately dominates the pathophysiology of reperfusion injury beyond that induced within the first few minutes. Indeed, following the initial burst of ROS from enzymatic sources, leukocytes become the dominant source for a much larger and persistent ROS production in the affected tissue and they also contribute directly and indirectly to impaired blood flow in the microcirculation. Of course, the magnitude of this inflammatory response is ultimately associated with the volume of tissue affected and the duration of the preceding ischaemic insult, as well as the sensitivity of the tissue in question to oxygen deprivation (Kalogeris *et al.*, 2012). Due to the intimate relationship between activated leukocytes and their interactions with capillaries and post-capillary venules, further discussion of the inflammatory component of reperfusion

injury will be detailed in the following sections as part of the examination of microcirculatory responses.

2.2.5 The microcirculation and reperfusion injury

The microcirculation is composed of the arterioles, capillaries, shunt vessels, and post-capillary collecting venules. In healthy tissues, local regulation of blood flow is tightly controlled at the microcirculatory level in order to deliver oxygen and other nutrients, and remove carbon dioxide and other waste products across the capillary walls, in accordance with local metabolic requirements (De Backer *et al.*, 2010). Along with metabolic regulation, the arteriolar side of the microcirculation plays a major role in the regulation of vascular resistance, influencing blood flow both locally and systemically, while the venous side passively adjusts to arteriolar changes in order to regulate perfusion pressure through the capillaries (Rowell, 1993). Fluid shifts between the intra- and extra-vascular compartments also take place across the capillary membrane (Landis, 1930; Hargens *et al.*, 1981) as well as through post-capillary venules during an inflammatory response (Granger, 1999).

The endothelium is a dynamic cellular structure comprising a single layer of cells that makes up the inner lining of blood vessels in all segments of the vascular tree, including the microcirculation. The integrity of this monolayer is vital for the regulation of normal blood flow as these cells are crucial for signaling between different vascular segments as well as the production of various vasodilator and vasoconstrictor agents that influence vascular tone. Intercellular communications along the vessel wall and between microvessel and parenchymal cells further contribute to the proper regulation of tissue blood flow in order to closely match perfusion with the metabolic requirements of the tissue (Kuo *et al.*, 1992; Segal, 1994).

An impaired regulation of blood flow at the microcirculatory level has long been recognized as an early and rate-determining feature in the pathophysiology of reperfusion injury (Granger, 1999; Carden & Granger, 2000). The deleterious effects of this response on each segment of the microcirculation are unique due to the distinct functional and structural properties of arterioles, capillaries, and post-

capillary venules. However, a unifying factor of this microvascular compromise is the impairment of endothelial cell integrity, which is initiated by the ischaemic insult and amplified during the subsequent reperfusion period (Granger, 1999; Carden & Granger, 2000). The following sections provide an overview on the effects of I-R injury on the microvascular endothelium as well as the arterioles, capillaries, and post-capillary venules. For a more thorough examination of this topic the reader is referred to reviews by Granger (1999) and Carden and Granger (2000).

2.2.5.i Effects of ischaemia and reperfusion on the endothelium

Endothelial cells are particularly vulnerable to the deleterious effects of both ischaemia and reperfusion (Granger, 1999; Carden & Granger, 2000). As with other cell types, ischaemia threatens endothelial cell integrity by depleting energy reserves and compromising the functional and structural integrity of the cellular membrane. This occurs along with a reduction of NO and prostaglandin production and a shift toward the production of vasoconstrictor agents such as endothelin and pro-thrombotic mediators such as thromboxane A2 by these cells (Carden & Granger, 2000; Eltzschig & Collard, 2004). Pro-inflammatory gene production is also stimulated with a concomitant suppression of genes that improve blood flow (Carden & Granger, 2000; Eltzschig & Collard, 2004; Kalogeris *et al.*, 2012). Much of these responses to ischaemia are exacerbated by the subsequent reperfusion, resulting in rapid endothelial cell dysfunction upon restoration of blood flow. Indeed, as described earlier, the immediate response to reperfusion is the rapid production of various ROS species, causing a further reduction in NO bioavailability through redox signaling (Harrison, 1997; Carden & Granger, 2000). This further compromises tissue function by creating an imbalance between these vasoregulatory mediators and a shift towards an increase in vasoconstrictor tone at a time when restoration of blood flow to the tissue is crucial for maintaining viability (Carden & Granger, 2000). Importantly, these functional changes occur despite the absence of overt morphological damage to endothelial cells (Granger, 1999; Carden & Granger, 2000).

2.2.5.ii Effects of ischaemia and reperfusion on arterioles

The arteriolar response to reperfusion is an elevation in vasoconstrictor tone due to an impairment of vascular smooth muscle relaxation. This effect appears to be NO-mediated and endothelium-dependent, as evidenced by an impaired vasodilator response to acetylcholine following ischaemia and reperfusion in superior mesenteric arteries of mice (Banda *et al.*, 1997). In contrast, the vascular smooth muscle itself does not appear to be negatively impacted by ischaemia and reperfusion, as indicated by maintenance of vasodilatation in response to the endothelium-independent vasodilator sodium nitroprusside (Banda *et al.*, 1997). Antioxidants such as superoxide dismutase (SOD) effectively restore the vasodilatory response of arterioles following ischaemia, suggesting that the rapid production of ROS within endothelial cells is an important factor in reducing endothelium-dependent vasodilatation, through their potent NO scavenging action (Harrison, 1997). Furthermore, activated and adherent leukocytes represent another important ROS source that contributes to impaired endothelium-dependent vasodilation during reperfusion. This has been demonstrated by the fact that mice, which are genetically deficient in either the leukocyte cell surface adhesion molecule cluster of differentiation 11b/18 (CD11b/CD18), or endothelial cell surface adhesion molecules, including P-selectin and intercellular adhesion molecule-1 (ICAM-1), maintain arteriolar vasodilator capacity during reperfusion, in contrast to their wild-type counterparts, which do not (Banda *et al.*, 1997).

2.2.5.iii Effects of ischaemia and reperfusion on capillaries

Reperfusion injury impairs blood flow through capillaries by a combination of increased fluid filtration into the surrounding tissue as well as a reduction in the number of perfused vessels (Granger, 1999; Carden & Granger, 2000). When examining fluid filtration in isolated rat mesenteric capillaries following ischaemia and reperfusion, Harris and Granger (1996) identified an increase in capillary fluid filtration rate through the capillary wall. Since they did not observe a significant change in microvessel pressure following reperfusion injury these authors argued that this increased fluid filtration was more likely due to an increase in hydraulic

conductivity (i.e. increased permeability) of the endothelial barrier rather than an elevation of intra-capillary pressure. Using a similar experimental model with rat mesenteric capillaries, Harris (1997) subsequently provided indirect evidence that the reduced bioavailability of NO following ischaemia-reperfusion may also contribute to the increased capillary filtration rate since reduction of NO with the NO synthase (NOS) inhibitor *N^G-nitro-L-arginine methyl ester* (L-NAME) in healthy capillaries also produced increases in capillary filtration rate in the absence of elevated intra-capillary pressure, similar to that found previously with reperfusion injury. Furthermore, this response appeared to be elevated in the presence of neutrophils, demonstrating that leukocyte binding is also an important contributor to the increased capillary fluid filtration rate (Harris, 1997).

A reduction in the number of capillaries exhibiting normal perfusion is a hallmark of reperfusion injury that has been identified in many organs and is often referred to as the "no-reflow" phenomenon (Eltzschig & Collard, 2004). This stagnation of blood flow in certain capillaries impairs oxygen delivery during reperfusion in sections of tissue surrounding these dysfunctional vessels due to the limited capacity for passive diffusion of oxygen. Multiple contributing factors have been implicated in this response.

In severe cases, swelling of endothelial cells and their partial detachment from the underlying basement membrane may contribute to perfusion impairment by reducing luminal diameter and increasing flow resistance (Carden & Granger, 2000). Similarly, flow resistance is also known to be elevated in small diameter capillary tubes by the slow passage of large activated leukocytes, which are more rigid in their activated state, implicating inflammation in this response (Skalak & Skalak, 1995). Interactions between circulating leukocytes and the endothelium in post-capillary venules also restrict the movement of blood through these outflow vessels, increasing flow resistance in upstream capillaries (Horie *et al.*, 1998). Furthermore, post-ischaemic oedema formation caused by leukocyte migration into the tissue through the vessel walls of downstream post-capillary venules, has also been implicated in capillary no-reflow, due to the resulting external compression on these vessels (Jerome *et al.*, 1994). All of these factors may contribute to blood flow

stasis and the development of a pro-thrombotic environment generating blood clots and platelet-leukocyte aggregates during reperfusion (Eltzschig & Collard, 2004).

Consistent with these findings, mice that are genetically deficient in either leukocyte or endothelial cell adhesion molecules exhibit a relative maintenance of capillary perfusion during ischaemia-reperfusion compared to their wild-type counterparts (Horie *et al.*, 1998). A build up of ROS also contributes to the reduction in the number of perfused capillaries as evidenced by studies demonstrating a relative maintenance of capillary perfusion in mutant mice that overexpress the SOD enzyme (Horie *et al.*, 1998).

2.2.5.iv Effects of ischaemia and reperfusion on post-capillary venules

Post-capillary venules are the primary site of the inflammatory response associated with reperfusion injury. Here, a complex process of leukocyte-endothelial cell interactions and subsequent migration of leukocytes through the vessel wall into the surrounding tissue occurs. This passage of white blood cells into the tissue is associated with the accumulation of leukocyte-platelet aggregates, protein extravasation, and an elevation of ROS within the local environment (Granger, 1999). Resident leukocytes, such as mast cells and macrophages, serve to intensify the inflammatory response by releasing mediators such as cytokines into the interstitial space of the surrounding tissue, further stimulating endothelial cells and contributing to the recruitment of circulating leukocytes such as neutrophils (Kubes & Granger, 1996). Studies examining the interactions between post-hypoxic human umbilical vein endothelial cell monolayers and human neutrophils have suggested that elevated leukocyte trafficking in post-capillary venules is largely the result of increased expression of adhesion molecules on leukocytes and on endothelial cells in this region of the microcirculation (Ichikawa *et al.*, 1997; Carden & Granger, 2000). This relationship has also been directly observed with intravital microscopy in rat mesenteric post-capillary venules and is associated primarily with the adhesion molecules CD11b/CD18 located on activated neutrophils and ICAM-1 on the venular endothelium (Kurose *et al.*, 1994).

The impact of oxidative stress on endothelial cells is particularly strong in post-capillary venules due to the fact that ROS production in this segment of the microcirculation following ischaemia is derived from enzymatic sources in the endothelial cells themselves during the initial ROS burst as well as from the activated leukocytes interacting with the endothelium here, which sustains the high level of oxidative stress over longer periods of time (Granger, 1999). Indeed, pretreatment with the XO-inhibitor, allopurinol, in cultured post-hypoxic endothelial cell monolayers and post-ischaemic venules reduces the oxidant stress from this enzymatic source, which dominates in the first few minutes of reperfusion (Ratych *et al.*, 1987). Moreover, in rats, treatment of post-ischaemic mesenteric venules with monoclonal antibodies to block either leukocyte or endothelial cell adhesion molecules reduced the oxidative stress (Salas *et al.*, 1999).

As mentioned previously, endothelial barrier dysfunction in post-capillary venules is an important contributor to reperfusion-induced microcirculatory impairment. The reduction in the restrictive properties of the vessel wall during reperfusion has been observed directly using intravital microscopy of FITC-albumin extravasation through post-capillary venules (Granger, 1988). Observations of elevated whole organ estimates of radiolabelled albumin accumulation, and a reduced osmotic reflection coefficient of plasma proteins during reperfusion lend further support to these microscopy findings (Granger, 1988). This increase in venular permeability is strongly associated with the inflammatory response as evidenced by the fact that agents targeting endothelial cell and leukocyte ROS production, such as SOD, or antibodies for specific endothelial cell adhesion molecules such as ICAM-1, generally minimize this increased permeability (Granger, 1988). In support of this, Kurose *et al.* (1994) demonstrated a strong correlation between albumin leakage in post-ischaemic venules and the number of leukocytes traversing the vessel wall into the tissue in the mesenteric microcirculation. Furthermore, these authors showed that antibodies for CD11b/CD18 and ICAM-1 were both effective in reducing this albumin leakage by restricting leukocyte adhesion and migration (Kurose *et al.*, 1994).

2.3 Cutaneous microcirculation

In humans, cutaneous perfusion primarily serves a thermoregulatory purpose as metabolic activity in this tissue is typically very low and nutritional requirements are easily accommodated by a small fraction of the total blood flow (Burton, 1939). The majority of the body's surface is covered in non-glabrous (hairy) skin, including the limbs, head and trunk (Johnson *et al.*, 2014). A smaller portion of the body is covered in glabrous skin, which is naturally devoid of hair. These areas include the ventral side of the fingers and palms of the hand, the soles of the feet, areas of the face including the lips, ears, and tip of the nose, as well as the glans penis and labia minora (Taylor *et al.*, 2014). Distinct differences exist between these two types of skin in their microvascular organization and neural control, which will be discussed in the following sections.

2.3.1 Cutaneous blood vessel organization

The structural organization of the circulation in non-glabrous skin and histological examination of its constituent blood vessels in humans were largely a mystery until the anatomical studies of Braverman and Yen beginning in the 1970s. This body of work has been reviewed extensively in Braverman (1997) and Braverman (2000). The cutaneous circulation is divided into two physiologically important blood vessel networks, the deep and superficial horizontal vascular plexuses, that both run parallel to the skin's surface (Braverman, 1997). Perpendicular vascular segments provide connections between deeper vascular structures and the two horizontal plexuses, creating one contiguous system of vessels. The deep horizontal plexus lies at the interface between the dermis and subcutaneous fat. Perforating vessels from deeper structures, including the subcutaneous fat and underlying muscles, form this lower plexus, which gives rise to arterioles and venules that connect directly with the upper plexus along with lateral blood vessels supplying hair follicles, and sweat glands (Braverman & Kehyen, 1981; Braverman, 1989, 1997). The superficial plexus consists entirely of microvessels such as the high-resistance terminal arterioles, the papillary loops, which are true nutritive capillaries, and post-capillary venules. The majority of these vessels lie

within 1-2 mm of the skin's surface (Yen & Braverman, 1976; Braverman & Yen, 1977; Braverman, 1989, 1997).

Papillary (nutritive capillary) loops are located near the dermal-epidermal junction and blood flow through these loops is regulated by highly innervated terminal arterioles originating in the superficial horizontal plexus (Braverman, 1997). Initially, an ascending limb extends perpendicular toward the skin's surface. This limb may extend directly into an individual dermal papilla or it may subdivide as much as three times prior to becoming a terminal ascending limb. Within each dermal papilla the loop transitions into a hairpin turn and then into the descending limb as it leaves the papilla and finally connects to a post-capillary venule back in the superficial horizontal plexus (Braverman & Yen, 1977).

Both non-glabrous and glabrous skin contain the previously mentioned vascular plexuses and papillary loops, however, glabrous skin is also rich in vessels known as arteriovenous anastomoses (AVA), which are located in both the deep and superficial horizontal vascular plexuses (Hurley & Mescon, 1956; Daanen, 2003; Taylor *et al.*, 2014). These vessels are richly innervated and contain thick muscular walls that lie deep in the skin relative to the more superficial papillary loops (Sherman, 1963; Daanen, 2003). The AVAs are direct vascular connections between arterioles and venules that function as low-resistance (i.e. large diameter) vascular shunts, allowing blood to effectively bypass the higher-resistance arterioles and capillary loops (Sherman, 1963; Daanen, 2003). As such, they do not contribute to nutritional blood flow in the skin and instead function as thermoregulatory structures that are capable of rapidly controlling blood volume in the appendages to regulate heat exchange with the surrounding environment (Flavahan, 2015). The pads and nail beds of the fingers and toes are the most abundant sites of AVAs, however, they are also present in other areas of the hands and feet including the palms and soles, as well as in areas of the face including the cheeks, ears, eyelids, forehead, lips, and nose (Mescon *et al.*, 1956; Taylor *et al.*, 2014).

While AVAs dilate in response to heat stress and constrict during mild to moderate cold stress, their primary role appears to be in mediating local vascular tone during prolonged, direct cold exposure (Daanen, 2003). AVA vasodilatation

delivers warm blood to maintain tissue temperature and thus preserve tissue viability through what is known as "cold-induced vasodilatation" (Daanen, 2003; Taylor *et al.*, 2014).

2.3.2 Ultrastructure of cutaneous microvascular segments

Arterioles and venules in the deep horizontal plexus and lower dermis are typically much larger than those in the superficial plexus with external diameters of ~50 μm and wall thicknesses in the range of 10-16 μm (Braverman, 1997). In the superficial horizontal plexus, the higher resistance terminal arterioles are typically smaller, with external diameters ranging from 17-26 μm (Yen & Braverman, 1976). In contrast, AVAs vary widely in size, with internal diameters ranging between 25-125 μm (Taylor *et al.*, 2014).

The high resistance terminal arterioles in the superficial horizontal plexus eventually merge with arterial capillaries, which have external diameters of ~10-12 μm and internal diameters of only ~4-6 μm (Yen & Braverman, 1976). The venous sides of these capillaries connect with post-capillary venules, the majority of which have external diameters in the range of 18-23 μm and internal diameters of ~10-15 μm (Braverman, 1997).

Within capillary loops, the ascending limb shares the same structural characteristics as other arteriolar capillaries mentioned above. At the apex of each loop, the presence of endothelial cells is reduced and capillary wall thickness may be as narrow as 11-30 nm. In the descending limb there is a distinct change in vessel wall characteristics in the region starting at the edge of the papillary and extending 10-30 μm beyond the papillary border itself. Here the vessel becomes much larger in diameter and takes on the characteristics of a typical cutaneous venule before connecting with the superficial horizontal plexus (Braverman & Yen, 1977).

2.3.3 Spatial organization of the cutaneous microcirculation

In non-glabrous skin of the limbs, measurement of blood flow is associated with significant spatial variation (Tenland *et al.*, 1983). Topographical studies of blood flow in the forearm have explained this phenomenon by demonstrating that a strong correlation exists between the variation in blood flow measurements and the

spatial heterogeneity of microvessel distribution in the underlying tissue (Braverman & Schechner, 1991; Braverman *et al.*, 1992; Wardell *et al.*, 1994). Based on these examinations, the ascending arterioles, which generate vasomotor activity in the skin, appear to be randomly spaced at intervals of 1.5-7.0 mm in the forearm (Braverman & Schechner, 1991). Regions dominated by the presence of capillaries or post-capillary venules surrounding these arterioles have also been identified, as well as relatively avascular areas of the skin (Braverman & Schechner, 1991).

Due to the smaller surface area of the fingers and toes, spatial variation is generally considered to be less of a concern when examining skin blood flow in these areas (Roustit *et al.*, 2010). In support of this assertion, corrosion casting of the cutaneous vasculature from a cadaver finger has revealed that on the volar side of the distal phalanx (finger pad), cutaneous microvessels in the papillary layer are uniformly distributed with two parallel rows of vessels ~200 μm apart that follow the patterning of the fingerprint (Sangiorgi *et al.*, 2004). The capillary loops extending vertically from these structures toward the skin surface were also evenly spaced at a distance of ~70 μm (Sangiorgi *et al.*, 2004). This is in contrast to the heterogeneous distribution observed on the dorsal side of the finger, which was more similar to the forearm skin with certain regions dominated by capillaries or post-capillary venules, mixed with relatively avascular areas (Braverman & Schechner, 1991; Sangiorgi *et al.*, 2004). As such, the distribution of capillary loops were much more variable here, ranging between 70-180 μm (Sangiorgi *et al.*, 2004).

2.4 Cutaneous neuroanatomy

2.4.1 Autonomic innervation

While sensory nerves are the most abundant nerve type in the skin, autonomic nerves are also found in large numbers and consist primarily of sympathetic noradrenergic and sympathetic cholinergic fibres (Hurley & Mescon, 1956; Montagna *et al.*, 1964; Breathnach, 1977; Munger & Ide, 1988; Nolano *et al.*, 2013). Autonomic fibres are only found in the dermal and subdermal regions where they innervate blood and lymph vessels, AVAs, erector pili muscles, hair follicles, and sweat glands (Roosterman *et al.*, 2006; Johnson *et al.*, 2014). Cutaneous

postganglionic autonomic nerves release classical neurotransmitters such as norepinephrine and acetylcholine along with a multitude of other important peptide and non-peptide based co-transmitters such as atrial natriuretic peptide, galanin, neuropeptide Y (NPY), peptide histidine methionine, pituitary adenylyl cyclase activating peptide, and vasoactive intestinal polypeptide (Roosterman *et al.*, 2006).

A unique feature of non-glabrous skin in humans is the presence of a dual sympathetic neural system controlling vasomotor tone. A noradrenergic system controls vasoconstriction while a non-adrenergic (cholinergic) system actively controls vasodilatation (Johnson *et al.*, 2014). This dual sympathetic control system is primarily associated with maintaining thermal balance, initiating vasoconstriction to prevent excessive body cooling and actively initiating vasodilatation to prevent hyperthermia (Johnson *et al.*, 2014). Evidence for the existence of an active vasodilator system in non-glabrous skin is well-established. Early work by Grant and Holling (1938) identified the presence of active vasodilatation by demonstrating that sympathectomy or nerve blockade prevented the large increase in forearm skin blood flow that occurs during heat stress. In addition, nerve blockade during established heat stress reversed this vasodilatory response (Grant & Holling, 1938). These data were subsequently confirmed by Edholm *et al.* (1957) and Roddie *et al.* (1957) with application of local anaesthetic to the skin. Later, presynaptic pharmacological blockade of noradrenergic nerves with bretylium tosylate in forearm skin was shown to eliminate the cutaneous vasoconstriction caused by cold stress while having no influence on the vasodilatory response to heat stress, confirming the non-adrenergic sympathetic source of active vasodilatation (Kellogg *et al.*, 1989).

Unlike non-glabrous skin, there does not appear to be any strong evidence of an active cholinergic vasodilator system in glabrous skin (Gaskell, 1956). Instead, noradrenergic vasoconstrictor nerves are primarily responsible for controlling vasomotor tone in cutaneous arterioles and AVAs in this skin type. In regions where glabrous skin is present blood flow is mainly driven by thermoregulatory demands via fluctuations in vasoconstrictor activity and by the direct influence of local skin temperature (Johnson *et al.*, 2014). Similar to non-glabrous skin, noradrenergic

vasoconstrictor nerves in glabrous skin release norepinephrine and associated peptide and non-peptide based co-transmitters (Hashim & Tadepalli, 1995; Padilla *et al.*, 1997; Wallengren, 1997; Heath, 1998).

2.4.2 Sensory innervation

Sensory nerves represent the dominant neural input in the skin and are found in all layers of the tissue. Afferent sensory nerve fibres emanate from dorsal root ganglia to innervate the skin, which release active neuropeptides into the local environment upon stimulation (Steinhoff *et al.*, 2003). Four distinct anatomical groups of cutaneous sensory nerves exist in both non-glabrous and glabrous skin, including the highly myelinated Aα-fibres, the moderately myelinated Aβ-fibres, the thinly myelinated Aδ-fibres, and the unmyelinated C-fibres (Roosterman *et al.*, 2006). The Aα-fibres are associated with muscle spindles and tendons involved in hair movement and the Aβ-fibres are broadly associated with different touch sensations such as tapping, buzzing, and pressure (Roosterman *et al.*, 2006).

Both the Aδ - and C-fibres respond to a broad range of physical (trauma, heat, pain, cold, distension and pressure, and ultraviolet light) and chemical (allergens, proteases, microbes, and toxins) stimuli (Steinhoff *et al.*, 2003); additionally, these fibres are also stimulated by several endogenous mediators such as hydrogen ions, hormones, cytokines, proteinases and kinins (Steinhoff *et al.*, 2003). Of these, the unmyelinated C-fibres are the most abundant, making up roughly 45% of all cutaneous afferent nerves (Roosterman *et al.*, 2006). The unmyelinated C-fibres can be further classified as either mechano-sensitive fibres or chemo-sensitive (mechano-insensitive) fibres, which respond to temperature and chemical stimulation (Schmidt *et al.*, 1995). These afferent neurons are present throughout the epidermis, dermis, and subcutaneous tissue innervating blood vessels, hair follicles, and sweat glands. They are also abundantly present as free nerve endings (Roosterman *et al.*, 2006).

Transient receptor potential (TRP) ion channels are located on sensory neurons in the skin and other organs throughout the body and they respond to and transmit a wide variety of stimuli, acting as non-selective, calcium-permeable signal

transduction channels that sense mechanical, chemical, and temperature changes (Roosterman *et al.*, 2006). These TRP channels are comprised of six subfamilies known as the canonical, melastatin, polycystin, mucolipin, TRPA, and vanilloid (TRPV) channels (Clapham, 2003). Of these, the TRPV subfamily, and in particular, the TRPV-1 ion channel has been studied most extensively in relation to stimulation of unmyelinated, chemo-sensitive C-fibres, in the skin and other organs. Several stimuli are known to directly or indirectly activate TRPV-1 channels, including local heating (>43°C), low pH, and other stimuli including eicosanoids, histamine, bradykinin, ATP, and a variety of neurotrophins (Roosterman *et al.*, 2006). Interestingly, hydrogen ions, which are commonly found in excess during inflammation and ischaemia, indirectly influence TRPV-1 channels by reducing the receptor threshold for stimulation, which can make typically comfortable temperature sensations become noxious, and produce a pain response (Caterina & Julius, 2001).

The function of chemo-sensitive C-fibre afferents has been extensively evaluated by examining their response to the vanilloid alkaloid compound capsaicin and for this reason they are also commonly referred to as capsaicin-sensitive C-fibres. Capsaicin is the com-pound derived from the chili pepper fruit that elicits a rapid, burning response upon acute application, which occurs through the selective activation of these unmyelinated C-fibres and subsequent release of neuropeptides from their nerve endings (Steinhoff *et al.*, 2003). In contrast to acute application, desensitization of C-fibres occurs with chronic applications of capsaicin, which renders them insensitive to subsequent stimulation at higher concentrations. This response is believed to be the result of neuropeptide depletion from the nerve endings, mediated by repeated TRPV-1 stimulation (Holzer, 1991; Roosterman *et al.*, 2006). For these reasons acute and chronic administration of capsaicin are often used as experimental techniques to specifically stimulate or inhibit these chemo-sensitive C-fibres, respectively, in order to evaluate their role in various physiological responses.

2.5 Cutaneous sensory nerves stimulate vasodilatation and inflammation

Beyond their obvious role in tactile sensation and the detection of other stimuli from the surrounding environment, cutaneous sensory nerves have long been recognized as important regulators of vasodilatation and inflammation in the skin. Early work by Bayliss (1901) described the vasodilatory response following electrical stimulation of centrally cut sensory dorsal roots in the hind limb of the dog. Other studies subsequently confirmed the role of sensory nerves in the cutaneous response to inflammation using the same experimental model (Chapman & Goodell, 1964; Jancso *et al.*, 1967; Foreman & Jordan, 1984). Capsaicin-sensitive C-fibres are primarily responsible for initiating these responses, while the thinly myelinated-Aδ fibres are also involved to a lesser extent (Szolcsanyi, 1996; Roosterman *et al.*, 2006). The functional importance of cutaneous sensory nerves in regulating vasodilatation and inflammation is directly related to their capacity to release potent neuropeptides upon stimulation that interact with cell surface receptors located on adjacent microvessels and resident leukocytes, which are both found in close proximity to these neurons within the tissue (Steinhoff *et al.*, 2003; Roosterman *et al.*, 2006; Zegarska *et al.*, 2006).

In several species a variety of stimuli capable of inducing neuropeptide release from cutaneous sensory nerves have been identified including electrical stimulation, ether, formalin, toluene diioscyanate, leukotrienes, prostaglandins, bradykinin, histamine, capsaicin, cigarette smoke, low tissue pH, and exposure to cold and heat (Roosterman *et al.*, 2006; Zegarska *et al.*, 2006). A multitude of sensory neuropeptides have also been identified in the skin of various species including calcitonin gene-related peptide (CGRP), Substance P (SP), neurokinin-A (NKA), neurokinin-B, neuropeptide-K, NPY, somatostatin and galanin (Steinhoff *et al.*, 2003; Roosterman *et al.*, 2006), with NKA, SP, and CGRP, being the most established contributors to neurogenic inflammation in humans (Schmelz & Petersen, 2001).

2.5.1 Neurogenic inflammation

Neurogenic inflammation is the term used to describe the vascular response to sensory nerve stimulation, which involves the release of sensory neuropeptides into the skin and a resulting combination of vasodilatation and plasma/protein extravasation into the tissue (Zegarska *et al.*, 2006). In response to a variety of stimuli such as application of thermal, mechanical, and chemical stressors, neurogenic inflammation initiates what is known as the so-called "triple response", which was first described by Lewis (1927). This response begins with erythema (redness), resulting from vasodilatation that first appears at the site of injury, followed by the development of a circular pattern of oedema emanating from the original site, and finally the development of a flared rim around the edge of the circle (Lewis, 1927).

According to the axon reflex hypothesis, neurogenic inflammation is the result of a combination of central and peripheral sensory nerve impulses. An orthodromic reflex transmits the stimulus immediately following tissue damage via local sensory nerves, through the sensory dorsal root ganglion, to the central nervous system, providing the conscious perception of pruritis (itching) and/or pain (Roosterman *et al.*, 2006; Zegarska *et al.*, 2006). Conversely, an antidromic reflex transmits the sensory nerve signal in the opposite direction, initiating the direct release of neuropeptides in the peripheral tissue independent from central nervous system input (Roosterman *et al.*, 2006; Zegarska *et al.*, 2006).

The neuropeptides involved serve a dual function, acting as neurotransmitters directing signals to the spinal cord and brain as part of the orthodromic reflex, while also acting in a paracrine fashion, serving as local modulators of vasodilatation and inflammation by stimulating adjacent microvascular and immune cells, via the antidromic reflex (Scholzen *et al.*, 1999; Schmelz & Petersen, 2001; Scholzen *et al.*, 2003). A broad spectrum of immune and non-immune cells in the skin contain receptors for these neuropeptides, including keratinocytes, which are the dominant cell type in the skin, along with Merkel cells, Langerhans cells, fibroblasts, eosinophils, mast cells, mononuclear cells, neutrophils and microvascular endothelial cells, which underlies their importance in regulating vasodilatation and

inflammation in the skin (Lotti *et al.*, 1995; Schaffer *et al.*, 1998; Steinhoff *et al.*, 2003; Zegarska *et al.*, 2006).

2.5.3 Influence on oedema, protein extravasation, and inflammation

The sensory neuropeptides NKA and SP play similar roles in neurogenic inflammation and they are both regulated primarily through the neurokinin (NK)-1 receptor (Quinlan *et al.*, 1998; Zegarska *et al.*, 2006). In the bovine brain, Nawa *et al.* (1983) demonstrated that NKA and SP are derived from the same precursor molecule and examination of various tissue types (spinal cord, sensory ganglion, dermis, epidermis) in the rat has demonstrated that they coexist in capsaicin-sensitive C-fibres (Dalsgaard *et al.*, 1985), consistent with their close functional relationship in neurogenic inflammation in human skin (Wallengren & Hakanson, 1987). In rodents, these neurokinins are potent contributors to oedema formation, which is caused by their influence on microvascular permeability. Microvascular permeability is increased by NKA through its effects on NK-1 receptors to induce plasma leakage into the surrounding tissue (Brain & Williams, 1989). Like NKA, plasma leakage is also mediated by SP via its effect on NK-1 receptors in rat skin, however, SP also directly stimulates mast cells to release mast cell amines such as histamine, which directly contribute to oedema formation themselves by increasing microvascular permeability to proteins and circulating leukocytes (Devillier *et al.*, 1986).

As with rats, protein extravasation and vasodilatation with secondary histamine release have also been demonstrated with SP administration in humans (Foreman *et al.*, 1983; Devillier *et al.*, 1986; Wallengren & Hakanson, 1987). However, Weidner *et al.* (2000) subsequently showed that protein extravasation and vasodilatation associated with exogenous administration of SP only occurred at very high concentrations in healthy human skin (10^{-8}M) and the involvement of secondary histamine release was only present at even higher levels (10^{-5}M). Furthermore, exogenous administration of CGRP at varying concentrations (10^{-8}-10^{-5}M) elicited vasodilatation with no protein extravasation or histamine release (Weidner *et al.*, 2000). Consistent with these findings, stimulation of sensory nerves in healthy

human skin by either acute capsaicin application (Petersen, 1998) or electrical stimulation (Sauerstein *et al.*, 2000; Weber *et al.*, 2001) failed to induce any protein extravasation or histamine release, however, a marked vasodilatory response was present in all studies (Petersen, 1998; Sauerstein *et al.*, 2000; Weber *et al.*, 2001). Combined, these data suggest that in humans, cutaneous microcirculatory responses to sensory nerve stimulation are dominated by the vasodilatory effects of neuropeptides acting directly on blood vessels, with minimal effects on oedema and protein extravasation (Schmelz & Petersen, 2001).

Beyond the influence of SP on microvascular permeability and histamine release, this neuropeptide can also stimulate the production and release of a variety of cytokines from leukocytes such as resident mast cells, lymphocytes, and macrophages (Campos & Calixto, 2000; Black, 2002), and along with NKA, from human keratinocytes as well (Kiss *et al.*, 1999; Steinhoff *et al.*, 2003). In human dermal microvascular endothelial cells, leukocyte-endothelial cell interactions are also directly influenced by SP through its role in regulating the expression of cellular adhesion molecules on the surface of endothelial cells including ICAM-1 and vascular cell adhesion molecule-1 (Quinlan *et al.*, 1998; Quinlan *et al.*, 1999b) as well as pro-inflammatory gene expression (Quinlan *et al.*, 1999a).

2.5.4 Influence on microcirculatory blood flow

Although the primary effect of exogenous administration of SP is oedema formation through its effect on increasing microvascular permeability (Siney & Brain, 1996), it is also known to have a potent acute vasodilatory effect in human skin (Wallengren & Hakanson, 1987). Studies in the rat by Whittle *et al.* (1989) demonstrated that systemic hypotension caused by SP administration was NO-dependent. Conversely, similar work by Santicioli *et al.* (1993), demonstrated that NO blockade did not prevent the hypotension caused by SP administration, which may suggest that NO does not influence SP-induced vasodilatation in all tissues. Using intravital microscopy to examine the microcirculation in the hamster cheek pouch, Hall and Brain (1994) demonstrated that exogenous administration of SP induced a transient, NO-dependent arteriolar vasodilatation. Consistent with this

finding, in human skin exogenous administration of SP also induces a transient vasodilatory effect that is maximal within the first 5 minutes and then begins to subside despite further administration (Fuller *et al.*, 1987; Weidner *et al.*, 2000; Schlereth *et al.*, 2016).

In contrast to the transient effects of SP and NKA on blood flow in the cutaneous microcirculation, exogenous administration of CGRP produces a powerful and long lasting vasodilatation in isolated blood vessels from multiple rodent species (Brain *et al.*, 1985), and in intact rat skin (Brain & Williams, 1989). The same effect has been consistently demonstrated in healthy human skin (Brain *et al.*, 1985; Fuller *et al.*, 1987; Wallengren & Hakanson, 1987; Weidner *et al.*, 2000; Schlereth *et al.*, 2016). This sustained vasodilatation occurs via CGRP-induced relaxation of vascular smooth muscle (Brain *et al.*, 1985). As with SP, the involvement of NO in CGRP-induced vasodilatation is not consistent among different blood vessel types. In isolated rat thoracic aorta, the vasodilatation caused by exogenous administration of CGRP is mediated by NO (Gray & Marshall, 1992a, b), which appears to be in contrast to the mechanism of action in the microcirculation. In an interesting study by Hughes and Brain (1994) examining the cutaneous microcirculation in rabbits, the authors demonstrated that the NOS inhibitor L-NAME impaired vasodilatation induced by acute capsaicin stimulation of sensory nerves while NO-blockade had no influence on vasodilatation induced by exogenous administration of CGRP, suggesting that the endogenous release of CGRP from sensory nerves, but not its ultimate mechanism of vasodilator action on cutaneous microvessels, is NO-dependent. In support of these findings, examination of isolated smooth muscle cells from rabbit mesenteric arteries demonstrated that CGRP stimulated adenylyl cyclase, resulting in an increase of cyclic adenosine monophosphate, which activates protein kinase A, and ultimately results in the opening of ATP-sensitive potassium channels in these cells (Quayle *et al.*, 1994). Combined, these data indicate that CGRP may have a direct relaxing effect on arteriolar smooth muscle that is independent of endothelial mediators such as NO, through the direct opening of potassium channels in these cells.

The individual actions of SP and CGRP on vasodilatation are modified by co-administration of the two peptides in human skin. Several studies have demonstrated that exogenous administration of SP has an inhibitory effect on the long lasting vasodilatation of previously administered CGRP, resulting in a vasodilator response that is characterized by a transient peak followed by a return to baseline (Fuller *et al.*, 1987; Brain & Williams, 1988; Schlereth *et al.*, 2016). This response is believed to be the result of SP-induced mast cell degranulation and the consequent release of proteases that inhibit the biological activity of CGRP (Brain & Williams, 1988; Xu *et al.*, 1992; Wallengren & Wang, 1993). While earlier studies failed to show an effect of exogenously administered CGRP on previously administered SP in the skin (Fuller *et al.*, 1987; Weidner *et al.*, 2000), a recent study by Schlereth *et al.* (2016) did demonstrate an inhibitory influence of CGRP on SP-induced vasodilatation in humans. This discrepancy lies in the much higher concentration of CGRP administered in the latter study (Schlereth *et al.*, 2016). These authors suggested that the inhibitory effect of CGRP on SP could have been due to competitive interactions with the NK-1 receptor or via the release of peptidases that break down the SP molecule, although these conclusions were largely speculative.

2.5.5 Sensory nerve responses to ischaemia and reperfusion

A multitude of studies in rodents have demonstrated that capsaicin-sensitive C-fibre afferents play a significant role in mediating the responses to both ischaemia and reperfusion via the modulating effects of SP, CGRP, and other neuropeptides, on tissue blood flow and inflammation. This has been confirmed in several organs including the brain (Miyanohara *et al.*, 2015), lung (Wang *et al.*, 2012; Ji *et al.*, 2013), heart (Ustinova & Schultz, 1994b; Ustinova *et al.*, 1995; Wang & Wang, 2005), liver (Harada *et al.*, 2002), intestine (Souza *et al.*, 2002), kidney (Mizutani *et al.*, 2009), skeletal muscle (Turchanyi *et al.*, 2005), and skin (Gherardini *et al.*, 1996), underlying the ubiquitous role of sensory nerves in modulating blood flow and inflammation at the tissue level under these conditions.

Studies in the rat myocardium have demonstrated that the onsets of ischaemia and reperfusion are both associated with an increased activation of cardiac, vagal C-fibre afferents (Ustinova & Schultz, 1994b), which primarily causes the release of SP as well as other neuropeptides into the tissue (Ustinova *et al.*, 1995). Ustinova and Schultz (1994a) demonstrated that capsaicin-sensitive C-fibres (and not mechano-sensitive C-fibres) are specifically activated in the heart under these circumstances, which is consistent with the direct stimulatory effects of low pH (Franco-Cereceda *et al.*, 1993) and ROS (Ustinova & Schultz, 1994b, a) on this fibre subtype. Specifically, during reperfusion, O_2^-, H_2O_2, and hydroxyl radicals from XO production have been shown to contribute to ROS mediated C-fibre activation in the rat heart (Ustinova & Schultz, 1994b, a). The release of SP during ischaemia and reperfusion has been shown to be cardioprotective, which is evident by the fact that capsaicin pre-treatment of rats can impair recovery following ischaemia and exogenous SP administration reverses this effect and also improves cardiac recovery in control animals (Ustinova *et al.*, 1995). Consistent with these findings, Wang and Wang (2005) showed that isolated hearts from TRPV-1 knockout mice and hearts from wild-type mice with acute capsazepine blockade of TRPV-1 receptors, both demonstrated poor recovery post-ischaemia, which was improved by exogenous administration of either SP or CGRP.

Sensory nerve inhibition using various experimental techniques has produced similar results to those described in the heart by Ustinova *et al.* (1995) and Wang and Wang (2005) for several other organs including the lung (Wang *et al.*, 2012; Ji *et al.*, 2013), liver (Harada *et al.*, 2002), kidney (Mizutani *et al.*, 2009), and skeletal muscle (Turchanyi *et al.*, 2005). Collectively, these studies demonstrate an impairment in post-ischaemic recovery when capsaicin-sensitive C-fibre afferent function was blocked.

Furthermore, like the heart (Wang & Wang, 2005), several studies have demonstrated an association between increased tissue levels of CGRP and improved post-ischaemic recovery. In both the liver (Harada *et al.*, 2002) and kidney (Mizutani *et al.*, 2009), exogenous application of CGRP improved tissue blood flow during reperfusion and also reduced inflammation via enhanced endothelial prostaglandin

synthesis in rats. Similarly, in the rabbit lung acute stimulation of sensory nerves with capsaicin was associated with a reduction in the inflammatory response and markers of oxidative stress, which was directly related to an increase in tissue CGRP levels (Wang *et al.*, 2012). Consistent with these results, Gherardini *et al.* (1996) demonstrated a direct relationship between tissue viability, increased microcirculatory blood flow, and elevated levels of tissue CGRP expression ten days following harvesting of skin flaps in rats.

Importantly, the functional benefit of sensory nerve stimulation during ischaemia and reperfusion appears to be influenced by the severity of the ischaemic insult. In support of this, Turchanyi *et al.* (2005) compared the effects of selective deafferentation of nociceptive C-fibre afferents in the sciatic nerve with capsaicin pretreatment on muscle recovery following one- and two-hour hind limb ischaemia in the rat. These authors demonstrated that sensory nerve inhibition was associated with improved isometric contractile force of the extensor digitorum longus muscle during recovery within one hour and up to seven days post-occlusion following two-hour hind limb ischaemia. Conversely, when the ischaemic period was limited to one-hour, contractile force was actually weaker between one and seven days post-occlusion in the animals with sensory nerve impairment. In the brain, which has very poor ischaemic tolerance, Miyanohara *et al.* (2015) demonstrated reductions in neurological and motor deficits and reduced cerebral infarct size following ischaemia in wild-type mice treated acutely with the TRPV-1 antagonist capsazepine, as well as in TRPV-1 knockout mice, indicating a significant pathophysiological role of sensory nerves in the response to ischaemia in this tissue.

Despite the beneficial effects of SP previously discussed, its release from sensory nerves has also been implicated in the pathophysiological response to ischaemia and reperfusion. Studies of myocardial reperfusion injury in isolated rat (Kramer *et al.*, 1997) and guinea pig (Chiao & Caldwell, 1996) hearts have demonstrated that antagonism of NK-1 receptors, which inhibits the actions of NKA and SP, is associated with a reduction in oxidative stress and an improvement in functional recovery; findings which are in direct contrast to those reported by Ustinova *et al.* (1995). Consistent with the notion of SP having a detrimental effect

on tissue recovery post-ischaemia, a study in rats using occlusion of the superior mesenteric artery, a reperfusion injury model that is associated with a significant inflammatory response as well as local (intestine) and remote (lung) organ injury (Souza *et al.*, 2000; Souza *et al.*, 2002), has demonstrated that NK-1 receptor antagonism, had a dose-dependent effect on reducing vascular permeability and neutrophil recruitment in local and remote organs following mild (30 min) ischaemia and additionally reduced cytokine release and intestinal hemorrhage following severe (120 min) ischaemia (Souza *et al.*, 2002). However, mortality during severe ischaemia was ultimately not improved by NK-1 inhibition in that study.

Together, these data suggest that stimulation of capsaicin-sensitive C-fibre afferents is beneficial during ischaemia and reperfusion, due to the strong vasodilatory actions of SP and CGRP on the microcirculation in situations where a significant inflammatory response is not expected to develop; as would be the case in tissues with higher ischaemic tolerance that are exposed to shorter occlusion times. However, in tissues with lower tolerance to oxygen deprivation or in cases of longer occlusion times, release of SP/NKA by sensory nerves may also contribute to the pathophysiology of reperfusion injury by amplifying the immune response during these more severe ischaemic insults.

2.7 Techniques for assessment of skin blood flow in humans

A variety of measurement devices are available for examining skin blood flow in humans. For a detailed overview of the strengths and limitations of these techniques the reader is referred to reviews by De Backer *et al.* (2010), Roustit and Cracowski (2012), Roustit and Cracowski (2013), and Johnson *et al.* (2014). Although many options are available, due to the complexity of the microvessel arrangement and the difficulty of optical devices to penetrate the surrounding connective tissue, the cutaneous microcirculation in humans is not easily assessed at an individual vessel level as it can be with intravital microscopy examinations from animal preparations such as the hamster cheek pouch model or the bat wing (Braverman, 2000).

The exception to this is the examination of blood flow in individual nail-fold capillaries of the fingers or toes. This can be achieved via traditional capillaroscopy with a light microscope or through more modern hand-held derivatives such as Orthogonal Polarization Spectral Imaging and Sidestream Dark Field Imaging, which both provide superior image contrast between the vessel wall and surrounding tissue (Mathura *et al.*, 2001; Goedhart *et al.*, 2007). However, blood flow in the nail folds is strongly influenced by environmental conditions and it is not generally representative of other body regions (Braverman, 1997).

Optical coherence tomography is a relatively new technique that allows for a non-invasive, three-dimensional structural examination of the microcirculation that can be combined with ultrasound or laser-Doppler techniques to assess blood flow within the volume of tissue as well (Mahmud *et al.*, 2013). Although this technique shows great promise it is still in the early stages of development for use in the skin and issues with measurement resolution still remain, making examination of the nutritive capillary supply difficult. Its extremely high cost and current lack of validation may also hinder its widespread adoption.

Due to the limitations of the previous approaches, examination of blood flow in the cutaneous microcirculation in humans is most commonly performed by measuring red blood cell flux with laser-Doppler flowmetry (LDF), which provides an index of skin blood flow (Johnson *et al.*, 1984; Saumet *et al.*, 1988). With this technique, laser light of a fixed wavelength penetrates the skin. When the light comes into contact with moving blood cells within the measurement field its frequency is altered, which is known as the Doppler shift. The ratio of Doppler shifted to non-Doppler shifted light is directly related to the number of moving cells within the laser's path. Blood perfusion is reported as the product of the relative number of moving cells, which cause the Doppler shift, and the relative velocity of these cells within the measurement field (Roustit & Cracowski, 2012). Only relative values are obtained since a precise quantification of blood flow cannot be determined, however, this signal is linearly correlated with skin blood flow (Ahn *et al.*, 1987). Probes often consist of a single laser unit that may or may not be surrounded by a heating unit to control local skin temperature. To address the issue

of spatial heterogeneity in non-glabrous skin, integrating-probe units have also been developed that provide an average signal from an array of seven, evenly spaced lasers.

Full-field variations on this technique are also available, which have the advantage of scanning much larger areas of skin without being in direct contact with the tissue, allowing for two-dimensional blood flow maps to be created. While laser-Doppler imaging (LDI) generally improves measurement reliability due to averaging over larger areas, this technique operates very slowly, which hinders its ability to capture rapid blood flow changes that may occur during functional reactivity tests (Roustit & Cracowski, 2013). Another full-field technique is Laser Speckle Contrast Imaging (LSCI), which operates much faster than LDI over large surface areas making this approach more useful to assess blood flow changes during reactivity tests. The main drawback of this technique is the relatively shallow measurement depth (~300μm) compared to laser-Doppler devices (~1-1.5mm), which have better tissue penetration (O'Doherty *et al.*, 2009). As such, laser-Doppler systems are capable of measuring blood flow in both the ascending arterioles and entire superficial horizontal vascular plexus including the nutritive papillary loops while LSCI is likely only to capture the capillary loops and part of the superficial vascular plexus (Braverman, 1997). Neither technique is capable of capturing blood flow directly from the deep horizontal vascular plexus (Braverman, 1997).

The main limitation of using LDF or LSCI is that only a global assessment of microvascular blood flow is obtained for a given volume of tissue, consisting of arterioles, capillaries, shunts, and venules. Since alterations in microvascular flow are heterogeneous, these changes cannot be identified when only assessing total blood flow (De Backer *et al.*, 2010). Due to differences in skin and subcutaneous fat thickness and skin pigmentation, the depth of light penetration is not always consistent and, as such, the volume of tissue sampled can also vary among different body regions and between individuals (Roustit & Cracowski, 2013). The main advantage of these techniques lies in the ability to assess dynamic regional microcirculatory responses to physiological stressors due to their high sampling

frequency, which can detect skin blood flow changes on a beat by beat basis (De Backer *et al.*, 2010; Roustit & Cracowski, 2013).

2.8 Microvascular reactivity tests

Due to the widespread availability of laser-Doppler equipment and its ease of operation, it has been used extensively to examine cutaneous blood flow responses to a variety of functional microvascular reactivity tests and pharmacological manipulations, often in combination. Several of these functional tests have been developed to examine various aspects of cutaneous microcirculatory function, although the depth of our current mechanistic understanding of the response to each test varies considerably. Although several reactivity tests are available, only a few of them have a well-established cutaneous sensory nerve component including post-occlusive reactive hyperaemia (PORH), pressure-induced vasodilatation, current-induced vasodilatation, and local thermal hyperaemia (LTH) (Roustit & Cracowski, 2013; Johnson *et al.*, 2014). For a thorough examination of the neurovascular and biochemical mediators involved in several of these tests, the reader is referred to the review by Roustit and Cracowski (2013). For an in depth examination of thermal reactivity tests in particular, the reader is referred to the review by Johnson *et al.* (2014).

Of the reactivity tests that have a well-established sensory nerve component, LTH has undergone the most extensive mechanistic evaluation with respect to its neurovascular regulation (Johnson *et al.*, 2014). In addition, this test also provides an excellent assessment of endothelial function (Johnson *et al.*, 2014), which, as described earlier, plays an important role in the pathophysiology of reperfusion injury. Neurovascular and/or endothelial impairments in the response to local skin heating have been demonstrated in primary aging (Minson *et al.*, 2002) and in a multitude of clinical conditions including end-stage renal disease (Kruger *et al.*, 2006), diabetes (Khan *et al.*, 2000; Sokolnicki *et al.*, 2007), metabolic syndrome (Kraemer-Aguiar *et al.*, 2008), hypertension (Holowatz & Kenney, 2007), rheumatoid arthritis (Boignard *et al.*, 2005), and systemic sclerosis (Boignard *et al.*, 2005; Roustit *et al.*, 2008; Blaise *et al.*, 2014). Early impairment in the cutaneous

response to local heating has also been identified as an independent prognostic indicator of mortality for patients with end-stage renal disease (Kruger *et al.*, 2006) and for digital ulcer development in patients with systemic sclerosis (Blaise *et al.*, 2014), which underscores the sensitivity and clinical utility of this reactivity test to identify microcirculatory impairment.

2.9 Local cutaneous thermal hyperaemia

The mechanisms regulating the vasodilatory response to local heating of the skin in humans are complex and consist of a variety of neural and biochemical interactions affecting the endothelium and vascular smooth muscle of cutaneous arterioles. Several excellent reviews (Charkoudian, 2003; Johnson & Kellogg, 2010; Roustit & Cracowski, 2013; Johnson *et al.*, 2014; Smith & Johnson, 2016) have provided detailed descriptions of our current mechanistic understanding of this process and the sections that follow are largely adapted from these prior works.

The classic vasodilatory pattern that occurs from a non-painful local heating stimulus in non-glabrous skin is characterized by a biphasic increase in skin blood flow, beginning with an initial peak that occurs within the first five minutes, which is primarily under neural control, followed by a brief nadir and a secondary rise in blood flow characterized by a sustained plateau phase (~20-30min) that is greater in magnitude than the initial peak and is dominated by the release of NO and other local chemical mediators from the endothelium. Prolonged heating during the plateau phase (~50-60min), may result in the so-called “die away” phenomenon, whereby skin blood flow begins to return toward baseline levels even though the local heating stimulus persists (Barcroft & Edholm, 1943; Minson *et al.*, 2001; Hodges *et al.*, 2009).

2.9.1 The role of sensory nerves

Sensory nerves, acting through a local axon reflex, appear to be the primary mediator of the initial vasodilatory peak during local skin heating. Magerl and Treede (1996) demonstrated vasodilatation during brief bouts of rapid local heating at skin sites up to 30 mm from the heating source, indicating the involvement of local sensory nerves in spreading the vasodilatation to distal skin sites, a response

that is highly characteristic of neurogenic inflammation. These authors also demonstrated that nociceptive C-fibre activation was responsible for initiating vasodilatation rather than activation of warm-sensitive fibres, even when a conscious perception of pain was absent (Magerl & Treede, 1996).

Stephens *et al.* (2001) examined the effects of acute capsaicin application on the cutaneous blood flow response to gradual local heating of the skin. The addition of capsaicin caused a dramatic leftward shift (~6°C) in the local temperature-skin blood flow response curve, clearly demonstrating that the stimulus threshold for cutaneous nociceptive C-fibre activation is an important contributor to the onset time of the vasodilatory response during gradual local heating.

Minson *et al.* (2001) demonstrated a significant (>50%) reduction in the initial vasodilatory peak during rapid, non-painful local skin heating when blocking sodium conduction in cutaneous sensory nerves with a topical anaesthetic cream (EMLA®: 2.5% lidocaine, 2.5% prilocaine). Interestingly, in the same study, when a proximal nerve block was used to inhibit all afferent sensory and efferent sympathetic activity, it had no effect on the vasodilatory response to local heating at a distal skin site (Minson *et al.*, 2001). Combined, these data indicate that cutaneous sensory nerves acting through a local axon reflex are sufficient to initiate cutaneous vasodilatation in response to local heating while a perception of skin heating by the central nervous system is not necessary (Magerl & Treede, 1996; Minson *et al.*, 2001; Stephens *et al.*, 2001).

The TRPV-1 channel is generally believed to be sensitive to temperatures above ~43°C (Caterina *et al.*, 1997), which is consistent with the range (42-44°C) of maximum temperatures typically applied in human studies of rapid and gradual local skin heating (Johnson *et al.*, 2014). Using the TRPV-1 antagonist capsazepine, Wong and Fieger (2010) demonstrated a significant reduction in the initial peak during local skin heating, as well as a modest reduction during the sustained plateau phase, indicating an important role for the TRPV-1 receptor in both phases of the rapid, non-painful local heating response.

To date there is minimal direct evidence to support the role of sensory neuropeptide release in the vasodilatory response to local heating in human skin.

However, SP and CGRP are believed to be involved since, as previously discussed, they are the dominant vasodilatory neuropeptides released from sensory nerves in human skin and their combined application produces a transient peak followed by a return to baseline as opposed to the longer lasting vasodilatation of CGRP alone (Fuller *et al.*, 1987; Brain & Williams, 1988; Schlereth *et al.*, 2016); a response that is very similar to that which occurs during the initial phase of rapid, non-painful local skin heating (Johnson *et al.*, 2014). Wong and Minson (2011) provided indirect support for the involvement of these neuropeptides by demonstrating that pretreatment of a skin site with SP, which desensitizes NK-1 receptors upon secondary stimulation (Wong *et al.*, 2005), rendered the initial peak and nadir phases indistinguishable from each other during a rapid, non-painful local heating stimulus, while leaving the secondary plateau unaffected. Since a painful local heating stimulus is characterized by a sustained vasodilatory response with no initial peak phase, similar to the response of CGRP alone, these authors argued that the relative concentrations of SP and CGRP released may be involved in the distinct blood flow responses to these two different heating protocols (Wong & Minson, 2011).

There also appears to be an interactive effect of NO on the sensory nerve response to gradual local skin heating. Indeed, Houghton *et al.* (2006) demonstrated an increased temperature threshold for the initial peak in four participants and a complete absence of the initial peak in 12 others at skin sites treated with the NO inhibitor L-NAME. These results were later confirmed by Hodges *et al.* (2008), who also identified both norepinephrine and NPY as important modulators of the axon reflex during gradual local heating. Consistent with these findings, inhibition of TRPV-1 receptors demonstrated a modest inhibitory effect on the secondary plateau during rapid, non-painful local skin heating, which is primarily mediated by NO release (Wong & Fieger, 2010). Furthermore, prior desensitization of NK-1 receptors, in combination with the NOS inhibitor L-NAME, partially restored the secondary plateau that was eliminated by application of L-NAME alone (Wong & Minson, 2011). Although the precise mechanisms involved in these NO-sensory nerve interactions during local skin heating in humans have not yet been fully

resolved, the existence of an interactive effect is consistent with animal studies examining the relationship between NO and exogenous applications of SP (Whittle *et al.*, 1989; Santicioli *et al.*, 1993; Hall & Brain, 1994) and CGRP (Hughes & Brain, 1994; Quayle *et al.*, 1994), and warrant further investigation.

2.9.2 The role of adrenergic nerves

The contribution of sympathetic adrenergic nerves in the vasodilatory response to local skin heating has been demonstrated in several studies. In a series of experiments, Drummond (1998) demonstrated that norepinephrine reduces the skin temperature at which the thermal pain threshold to capsaicin application occurs. He later showed that alpha-1 adrenoceptors contribute to axon reflex-mediated vasodilatation during local skin heating (Drummond, 2009a, b). Charkoudian *et al.* (2002) demonstrated that the initial vasodilatory peak failed to develop during local skin heating in a group of surgical patients tested within five years of a sympathectomy, lending further support for an adrenergic contribution to the early phase of local skin heating.

Using a gradual local skin heating protocol, Houghton *et al.* (2006) demonstrated that pretreatment with bretylium, a presynaptic inhibitor of norepinephrine and its co-transmitters, abolished the axon reflex component of the local heating response. To examine this idea further, Hodges *et al.* (2008) demonstrated that intradermal administration of both alpha- and beta-adrenergic receptor antagonists, as well as pharmacological blockade of Y_1 receptors for the sympathetic adrenergic co-transmitter NPY, all shifted the axon reflex response to a higher local temperature. When both alpha- and beta-adrenergic receptors and the co-transmitter NPY were blocked at the same skin site the axon reflex component of the gradual local heating response was completely abolished (Hodges *et al.*, 2008). In contrast, when a rapid, non-painful local heating protocol was used, the axon reflex component of the local skin heating response was restored even with blockade of sympathetic neurotransmitters (Hodges *et al.*, 2009). Taken together, these findings suggest that the sympathetic adrenergic system may not be a

necessary component of the initial vasodilatation during local skin heating, but that it does contribute to the sensitivity of the response (Johnson *et al.*, 2014).

2.9.3 The role of nitric oxide

It is now well established that NO plays a critical role in the vasodilatory response during rapid, non-painful heating and gradual local skin heating. However, the contribution of NO in this response appears to be multifaceted and elucidating its various roles is still an active area of investigation. Kellogg *et al.* (1999) were the first to examine the role of NO in local skin heating. These authors demonstrated a ~50% blood flow reduction during the secondary plateau phase when L-NAME was administered at a local skin temperature of 40°C, after the plateau had been established. This finding was later elaborated on in a study by Minson *et al.* (2001) who infused L-NAME into the skin both prior to and during local heating at different sites. These authors confirmed the findings of Kellogg *et al.* (1999) by showing that L-NAME inhibited the vasodilatory response during the plateau phase when local heating had already been established and also demonstrated that L-NAME infusion prior to the start of local heating at another skin site blunted not only the plateau phase but the initial peak response as well by roughly 20-30%. These findings were subsequently confirmed by Gooding *et al.* (2006), although these authors demonstrated a smaller reduction in skin blood flow with L-NAME. Participants in this study were also given an oral dose of sildenafil, which is a phosphodiesterase 5 inhibitor that impairs the breakdown of cyclic guanosine monophosphate, a downstream signaling molecule of the NO pathway. This effectively prolonged the vasodilatory response in the skin following removal of the heating stimulus, further implicating NO as a major source of vasodilatation during the secondary plateau phase of local heating (Gooding *et al.*, 2006).

Beyond its function as a vasodilating agent, NO also plays an important role in counteracting the effects of increased sympathetic activity under conditions of whole body cold stress (Durand *et al.*, 2005) and lower body negative pressure (Shibasaki *et al.*, 2007). Additionally, Wingo *et al.* (2009) demonstrated that NO counteracted the effects of exogenous norepinephrine administration during local

skin heating. Importantly, when NOS was blocked during local heating, sympathetic vasoconstriction was no longer inhibited, indicating that NO is not only a potent vasodilating agent, but it also appears to have a direct sympathoinhibitory effect.

In order to identify the specific enzymatic source(s) of NO involved in local skin heating, several studies have been conducted in order to determine the effects of the endothelial NOS (eNOS), inducible NOS (iNOS), and neuronal NOS (nNOS), isoforms of the enzyme on local skin heating. Kellogg and colleagues conducted a series of experiments using selective inhibitors of eNOS and nNOS during both local and whole body heating. These authors found that using the nNOS specific inhibitors 7-nitroindazole and N^{ω}-propyl-L-arginine had no influence on the skin's response to local heating, but they did reduce the reflex increase in skin blood flow during whole body heating (Kellogg *et al.*, 2008a; Kellogg *et al.*, 2009). The eNOS specific inhibitor N^{G}-amino-L-arginine, on the other hand, had no influence during whole body heating and yet it did attenuate the vasodilatory response to local skin heating by roughly 50% (Kellogg *et al.*, 2008b; Kellogg *et al.*, 2009). No interactive effects between these two NOS isoforms were present during either local skin heating or whole body heating (Kellogg *et al.*, 2009). The lack of a role for nNOS in the response to local skin heating was subsequently confirmed by Bruning *et al.* (2012) using the nNOS inhibitor N^{ω}-propyl-L-arginine. These authors also observed a modest reduction in the initial peak response to local skin heating when they infused the iNOS inhibitor 1400W, but no reduction in the secondary plateau phase was evident.

Although the above findings indicate a primary role for eNOS in the local skin heating response, conflicting data by Stewart *et al.* (2007) does exist. These authors examined the local heating response in skin sites receiving the nNOS antagonist N^{ω}-nitro-L-arginine-2,4-L-diaminobutyric amide or the non-specific NOS inhibitor nitro-L-arginine. Interestingly, in these experiments, which utilized a heat-reheat protocol on the same skin site, both NOS inhibitors reduced the vasodilatory response to local skin heating during the reheating period to the same extent relative to local heating at those skin sites prior to drug infusion, leading the authors to suggest that nNOS was the isoform responsible for local thermal hyperaemia (Stewart *et al.*, 2007). According to Johnson *et al.* (2014), if heat directly stimulates

the NOS enzyme then these findings would be consistent with a greater reliance on nNOS over eNOS during local skin heating since nNOS is known to be more temperature sensitive (Venturini *et al.*, 1999). However, many other substances that are released during local skin heating could also stimulate eNOS, which is generally considered to be the suspected pathway during local skin heating (Johnson *et al.*, 2014).

Ultimately, the reason for these discrepant findings remains unclear. The study by Stewart *et al.* (2007) was performed in the calf skin since the aim of these investigators was to examine alterations in lower limb skin blood flow in patients with Postural Tachycardia Syndrome and several studies have since demonstrated that regional differences in cutaneous responses to local skin heating do exist between the forearm and leg (Hodges & Del Pozzi, 2014; Hodges *et al.*, 2015; Hodges *et al.*, 2016). The use of a heat-reheat protocol has also been shown to desensitize the skin's response to local heating, which may also contribute to the discrepancy in findings (Ciplak *et al.*, 2009; Frantz *et al.*, 2012; Del Pozzi & Hodges, 2015) and the specificity of drugs used in these studies could be another possible explanation (Johnson *et al.*, 2014). Regardless of the specific NOS isoform(s) involved, it is evident that NO plays a major role in the response to local skin heating.

Oxidative stress also has an important influence on the skin during heating through the NO scavenging effects of ROS. Indeed, acute supplementation with the antioxidant ascorbate, alone or in combination with arginase inhibition, improves the attenuated cutaneous vasodilatory response to whole body heating seen in hypertensive patients (Holowatz & Kenney, 2007) and in aged human skin (Holowatz *et al.*, 2006). The attenuated secondary plateau phase observed during local skin heating in hypercholesterolemic patients was also augmented with ascorbate supplementation, alone or in combination with arginase inhibition (Holowatz & Kenney, 2011; Holowatz *et al.*, 2011). To further elucidate the role of ROS in response to heating, Medow *et al.* (2011) examined the effects of various antioxidant mediators during local skin heating. The O_2^- inhibitor tempol and the NADPH oxidase inhibitor apocynin had no influence, while the XO inhibitor allopurinol improved the entire local heating response and the H_2O_2 inhibitor

ebselen actually suppressed the heating plateau (Medow *et al.*, 2011). The addition of angiotensin-II (ANG-II), which is known to increase ROS production through NADPH oxidase and XO pathways, significantly attenuated the entire heating response, which was partially restored by application of each of the antioxidant mediators tested (Medow *et al.*, 2011). Other likely effectors of NO during the local skin heating response such as histamine (Wong *et al.*, 2006), prostaglandins (McCord *et al.*, 2006; Holowatz *et al.*, 2009), and heat shock protein 90 (Shastry & Joyner, 2002) have also been evaluated, although each has been shown to contribute only modestly, if at all, to local skin heating.

2.9.4 The role of endothelial derived hyperpolarizing factors

Endothelial derived hyperpolarizing factors (EDHFs) are a class of factors that cause vasodilatation by hyperpolarization of vascular smooth muscle. Most EDHFs act by stimulating calcium-activated potassium (KCa) channels. Small and intermediate KCa channels are located in the endothelial cell membrane and large conducting KCa channels are found in vascular smooth muscle. Hyperpolarization of endothelial cells spreads via gap junctions to vascular smooth muscle, which also contributes to vasodilatation (Feletou & Vanhoutte, 2009).

Prior evidence for the involvement of KCa channels in human skin had been demonstrated during reactive hyperaemia (Lorenzo & Minson, 2007) and application of external pressure (Garry *et al.*, 2005), while Brunt and Minson (2012) were the first to identify an important role for EDHFs in the response to local skin heating. These authors blunted all vasodilatory responses to local skin heating through combined application of L-NAME and the KCa channel blocker tetraethylammonium (TEA). To further identify the particular EDHF involved, the authors used sulfaphenazole to block the human isoform of cytochrome P450, which acts by catalyzing the conversion of epoxyeicosatrienoic acid (EET) from arachidonic acid in the endothelium. This led to the discovery that EDHFs are responsible for a large fraction of the initial vasodilatory peak as well as the remaining 40-50% of the sustained plateau phase that is not abolished by NOS inhibition. Of the EDHF-dependent vasodilatory component, EETs were found to be

responsible for roughly half of the plateau response, the rest being attributed to EDHFs acting through KCa channels such as lipoxygenase derivatives and H_2O_2 (Brunt & Minson, 2012). Consistent with these findings, Medow *et al.* (2011) demonstrated a blunting of the plateau phase during local skin heating following application of the H_2O_2 scavenger ebselen, which also acts to inhibit lipoxygenases. Furthermore, the study by Brunt and Minson (2012) also suggests that cross-talk between EDHF and NO pathways is important in regulating vasodilatation during the plateau phase as the application of TEA or sulfaphenazole alone produced smaller inhibitory effects on skin blood flow than when either EDHF blocker was given in combination with L-NAME.

2.9.5 Local heating in glabrous skin

Despite its important role in thermoregulation (Taylor *et al.*, 2014) and its selective association with pathological conditions such as Raynaud's phenomenon (Flavahan, 2015) and systemic sclerosis (Boignard *et al.*, 2005; Roustit *et al.*, 2008; Blaise *et al.*, 2014), relatively little is known about the mechanisms regulating blood flow in glabrous skin. This is likely due to a combination of the technical difficulties involved in conducting pharmacological studies specific to regions with glabrous skin in humans and the greater emphasis placed on examining the responses to heating in non-glabrous skin, which covers the majority of the body's surface.

As with non-glabrous skin, the vasodilatory response to a rapid, non-painful, local heating stimulus in glabrous skin begins with an initial peak that occurs within the first five minutes, which is primarily under sensory nerve control (Roustit *et al.*, 2008). However, a unique characteristic of glabrous skin is that a sustained secondary plateau phase does not always develop and when present, it is not always greater in magnitude than the initial peak (Roustit *et al.*, 2010; Metzler-Wilson *et al.*, 2012).

Several studies have identified this paradoxical phenomenon of heating-induced vasoconstriction in glabrous skin using venous occlusion plethysmography when submerging the finger or entire hand in warm water (Nagasaka *et al.*, 1987a; Nagasaka *et al.*, 1987b; Hirata *et al.*, 1988; Nagasaka *et al.*, 1990), and during highly

localized heating of the skin using LDF with integrated heater units (Roustit *et al.*, 2010; Metzler-Wilson *et al.*, 2012). The reason behind this difference in vasodilatory profile between skin types remains unclear, however it has been suggested that differences in neural innervation between non-glabrous and glabrous skin, or either the presence of AVAs or less reliance on NO during local heating in glabrous skin may be responsible (Metzler-Wilson *et al.*, 2012).

The AVAs have extensive sympathetic input and they are controlled by bursts of efferent sympathetic activity (Taylor *et al.*, 2014). To date, the available evidence suggests that a complex interaction between local skin temperature and this sympathetically mediated control of AVA vasomotor tone may be responsible for the paradoxical vasoconstriction during local heating observed in some individuals. Hales *et al.* (1985) demonstrated a biphasic relationship between local skin temperature and AVA blood flow in sheep skin whereby blood flow was reduced as local skin temperature was increased from 36°C to 42°C and then rose again at maximal heating to 44°C. Consistent with this finding, in human non-glabrous skin Wingo *et al.* (2009) demonstrated that adrenergically mediated vasoconstriction was not affected during local heating to 40°C through either pre- or post-synaptic mechanisms in the absence of NO. Furthermore, in isolated cutaneous canine veins, Cooke *et al.* (1984) showed that warming directly enhanced vascular smooth muscle contractility while simultaneously suppressing the response of the vessel to sympathetic nerve stimulation via inhibition of post-junctional α_2-adrenoceptors during warming from 37°C to 41°C. Combined, these studies suggest a complex interaction between the effects of local temperature on smooth muscle relaxation and responsiveness to sympathetic nerve stimulation that may or may not be modified by NO in the glabrous skin, which may be responsible for the individual differences in the response to local heating in this skin type.

2.10 Statement of the problem

It has been established that sensory nerves play an important role in the response to ischaemia and reperfusion. However, the physiological strain associated with this process may desensitize these nerves, hindering their ability to regulate

cutaneous blood flow in response to a subsequent heating challenge, which may potentiate tissue injury both acutely and chronically. With that in mind, the primary purpose of the experiments that follow is to examine the effects of an acute exposure to ischaemia and reperfusion injury of the upper limb in a group of otherwise healthy, young males, on the subsequent neurovascular response to local heating in non-glabrous and glabrous skin.

2.11 References

Ahn H, Johansson K, Lundgren O & Nilsson GE. (1987). In vivo evaluation of signal processors for laser doppler tissue flowmeters. *Med Biol Eng Comput* **25,** 207-211.

Banda MA, Lefer DJ & Granger DN. (1997). Postischemic endothelium-dependent vascular reactivity is preserved in adhesion molecule-deficient mice. *Am J Physiol-Heart Circul Physiol* **273,** H2721-H2725.

Barcroft H & Edholm OG. (1943). The effect of temperature on blood flow and deep temperature in the human forearm. *J Physiol-London* **102,** 5-20.

Bayliss WM. (1901). On the origin from the spinal cord of the vaso-dilator fibres of the hind-limb and on the nature of these fibres. *J Physiol-London* **26,** 173-209.

Black PH. (2002). Stress and the inflammatory response: A review of neurogenic inflammation. *Brain Behav Immun* **16,** 622-653.

Blaise S, Roustit M, Carpentier P, Seinturier C, Imbert B & Cracowski JL. (2014). The digital thermal hyperemia pattern is associated with the onset of digital ulcerations in systemic sclerosis during 3 years of follow-up. *Microvasc Res* **94,** 119-122.

Boignard A, Salvat-Melis M, Carpentier PH, Minson CT, Grange L, Duc C, Sarrot-Reynauld F & Cracowski JL. (2005). Local hyperhemia to heating is impaired in secondary Raynaud's phenomenon. *Arthritis Res Ther* **7,** R1103-R1112.

Brain SD & Williams TJ. (1988). Substance-P regulates the vasodilator activity of calcitonin gene-related peptide. *Nature* **335,** 73-75.

Brain SD & Williams TJ. (1989). Interactions between the tachykinins and calcitonin gene-related peptide lead to the modulation of edema formation and blood flow in rat skin. *British Journal of Pharmacology* **97,** 77-82.

Brain SD, Williams TJ, Tippins JR, Morris HR & Macintyre I. (1985). Calcitonin gene-related peptide is a potent vasodilator. *Nature* **313,** 54-56.

Braverman IM. (1989). Ultrastructure and organization of the cutaneous microvasculature in normal and pathologic states. *J Invest Dermatol* **93,** S2-S9.

Braverman IM. (1997). The cutaneous microcirculation: Ultrastructure and microanatomical organization. *Microcirculation-London* **4,** 329-340.

Braverman IM. (2000). The cutaneous microcirculation. *J Invest Dermatol Symp Proc* **5,** 3-9.

Braverman IM & Kehyen A. (1981). Ultrastructure of the human dermal microcirculation .3. The vessels in the mid dermis and lower dermis and subcutaneous fat. *J Invest Dermatol* **77,** 297-304.

Braverman IM & Schechner JS. (1991). Contour mapping of the cutaneous microvasculature by computerized laser doppler velocimetry. *J Invest Dermatol* **97,** 1013-1018.

Braverman IM, Schechner JS, Silverman DG & Kehyen A. (1992). Topographic mapping of the cutaneous microcirculation using 2 outputs of laser-Doppler flowmetry - flux and the concentration of moving blood cells. *Microvascular Research* **44,** 33-48.

Braverman IM & Yen A. (1977). Ultrastructure of human dermal microcirculation .2. Capillary loops of dermal papillae. *J Invest Dermatol* **68,** 44-52.

Breathnach AS. (1977). Electron-microscopy of cutaneous nerves and receptors. *J Invest Dermatol* **69,** 8-26.

Bruning RS, Santhanam L, Stanhewicz AE, Smith CJ, Berkowitz DE, Kenney WL & Holowatz LA. (2012). Endothelial nitric oxide synthase mediates cutaneous vasodilation during local heating and is attenuated in middle-aged human skin. *Journal of Applied Physiology* **112,** 2019-2026.

Brunt VE & Minson CT. (2012). KCa channels and epoxyeicosatrienoic acids: major contributors to thermal hyperaemia in human skin. *J Physiol-London* **590,** 3523-3534.

Burton AC. (1939). The range and variability of the blood flow in the human fingers and the vasomotor regulation by body temperature. *Am J Physiol* **127,** 437-453.

Campos MM & Calixto JB. (2000). Neurokinin mediation of edema and inflammation. *Neuropeptides* **34,** 314-322.

Carden DL & Granger DN. (2000). Pathophysiology of ischaemia-reperfusion injury. *J Pathol* **190,** 255-266.

Caterina MJ & Julius D. (2001). The vanilloid receptor: A molecular gateway to the pain pathway. *Annu Rev Neurosci* **24,** 487-517.

Caterina MJ, Schumacher MA, Tominaga M, Rosen TA, Levine JD & Julius D. (1997). The capsaicin receptor: a heat-activated ion channel in the pain pathway. *Nature* **389,** 816-824.

Chapman LF & Goodell H. (1964). Participation of nervous system in inflammatory reaction. *AnnNY AcadSci* **116,** 990-&.

Charkoudian N. (2003). Skin blood flow in adult human thermoregulation: how it works, when it does not, and why. *Mayo Clin Proc* **78,** 603-612.

Charkoudian N, Eisenach JH, Atkinson JLD, Fealey RD & Joyner MJ. (2002). Effects of chronic sympathectomy on locally mediated cutaneous vasodilation in humans. *Journal of Applied Physiology* **92,** 685-690.

Chiao H & Caldwell RW. (1996). The role of substance P in myocardial dysfunction during ischemia and reperfusion. *Naunyn-Schmiedebergs Arch Pharmacol* **353,** 400-407.

Ciplak M, Pasche A, Heim A, Haeberli C, Waeber B, Liaudet L, Feihl F & Engelberger R. (2009). The Vasodilatory Response of Skin Microcirculation to Local Heating is Subject to Desensitization. *Microcirculation* **16,** 265-275.

Clapham DE. (2003). TRP channels as cellular sensors. *Nature* **426,** 517-524.

Cooke JP, Shepherd JT & Vanhoutte PM. (1984). The effect of warming on adrenergic neurotransmission in canine cutaneous vein. *Circulation Research* **54,** 547-553.

Daanen HA. (2003). Finger cold-induced vasodilation: a review. *Eur J Appl Physiol* **89,** 411-426.

Dalsgaard CJ, Haegerstrand A, Theodorssonnorheim E, Brodin E & Hokfelt T. (1985). Neurokinin A-like immunoreactivity in rat primary sensory neurons - coexistence with Substance-P. *Histochemistry* **83,** 37-39.

De Backer D, Ospina-Tascon G, Salgado D, Favory R, Creteur J & Vincent JL. (2010). Monitoring the microcirculation in the critically ill patient: current methods and future approaches. *Intensive Care Med* **36,** 1813-1825.

Del Pozzi AT & Hodges GJ. (2015). To reheat, or to not reheat: that is the question: The efficacy of a local reheating protocol on mechanisms of cutaneous vasodilatation. *Microvascular Research* **97,** 47-54.

Devillier P, Regoli D, Asseraf A, Descours B, Marsac J & Renoux M. (1986). Histamine release and local responses of rat and human skin to Substance-P and other mammalian tachykinins. *Pharmacology* **32,** 340-347.

Drummond PD. (1998). Enhancement of thermal hyperalgesia by alpha-adrenoceptors in capsaicin-treated skin. *J Auton Nerv Syst* **69,** 96-102.

Drummond PD. (2009a). Alpha-1 adrenoceptor stimulation triggers axon-reflex vasodilatation in human skin. *Auton Neurosci-Basic Clin* **151,** 159-163.

Drummond PD. (2009b). alpha(1)-Adrenoceptors augment thermal hyperalgesia in mildly burnt skin. *Eur J Pain* **13,** 273-279.

Durand S, Davis SL, Cui J & Crandall CG. (2005). Exogenous nitric oxide inhibits sympathetically mediated vasoconstriction in human skin. *J Physiol* **562,** 629-634.

Edholm OG, Fox RH & Macpherson RK. (1957). Vasomotor control of the cutaneous blood vessels in the human forearm. *J Physiol-London* **139,** 455-465.

Eisenhardt SU, Schmidt Y, Karaxha G, Iblher N, Penna V, Torio-Padron N, Stark B & Bannasch H. (2012). Monitoring Molecular Changes Induced by Ischemia/Reperfusion in Human Free Muscle Flap Tissue Samples. *Ann Plast Surg* **68,** 202-208.

Eltzschig HK & Collard CD. (2004). Vascular ischaemia and reperfusion injury. *Br Med Bull* **70,** 71-86.

Feletou M & Vanhoutte PM. (2009). EDHF: an update. *Clin Sci* **117,** 139-155.

Flavahan NA. (2015). A vascular mechanistic approach to understanding Raynaud phenomenon. *Nat Rev Rheumatol* **11,** 146-158.

Foreman JC & Jordan CC. (1984). Neurogenic Inflammation. *Trends Pharmacol Sci* **5,** 116-119.

Foreman JC, Jordan CC, Oehme P & Renner H. (1983). Structure activity relationships for some Substance-P related peptides that cause wheal and flare reactions in human skin. *J Physiol-London* **335,** 449-465.

Franco-Cereceda A, Kallner G & Lundberg JM. (1993). Capsazepine-sensitive release of calcitonin gene-related peptide from C-fiber afferents in the guinea pig heart by low pH and lactic acid. *Eur J Pharmacol* **238,** 311-316.

Frantz J, Engelberger RP, Liaudet L, Mazzolai L, Waeber B & Feihl F. (2012). Desensitization of Thermal Hyperemia in the Skin is Reproducible. *Microcirculation* **19,** 78-85.

Fuller RW, Conradson TB, Dixon CMS, Crossman DC & Barnes PJ. (1987). Sensory neuropeptide effects in human skin. *British Journal of Pharmacology* **92,** 781-788.

Garry A, Sigaudo-Roussel D, Merzeau S, Dumont O, Saumet JL & Fromy B. (2005). Cellular mechanisms underlying cutaneous pressure-induced vasodilation: in vivo involvement of potassium channels. *Am J Physiol-Heart Circul Physiol* **289,** H174-H180.

Gaskell P. (1956). Are there sympathetic vasodilator nerves to the vessels of the hands. *J Physiol-London* **131,** 647-656.

Gherardini G, Evans GRD, Theodorsson E, Gurlek A, Milner SM, Palmer B & Lundeberg T. (1996). Calcitonin gene-related peptide in experimental ischemia. Implication of an endogenous anti-ischemic effect. *Ann Plast Surg* **36,** 616-620.

Goedhart PT, Khalilzada M, Bezemer R, Merza J & Ince C. (2007). Sidestream Dark Field (SDF) imaging: a novel stroboscopic LED ring-based imaging modality for clinical assessment of the microcirculation. *Opt Express* **15,** 15101-15114.

Gooding KM, Hannemann MM, Tooke JE, Clough GF & Shore AC. (2006). Maximum skin hyperaemia induced by local heating: Possible mechanisms. *J Vasc Res* **43,** 270-277.

Granger DN. (1988). Role of xanthine-oxidase and granulocytes in ischemia-reperfusion injury. *Am J Physiol* **255,** H1269-H1275.

Granger DN. (1999). Ischemia-reperfusion: Mechanisms of microvascular dysfunction and the influence of risk factors for cardiovascular disease. *Microcirculation* **6,** 167-178.

Granger DN & Kvietys PR. (2015). Reperfusion injury and reactive oxygen species: The evolution of a concept. *Redox Biol* **6,** 524-551.

Granger DN, Rutili G & McCord JM. (1981). Superoxide radicals in feline intestinal ischemia. *Gastroenterology* **81,** 22-29.

Grant RT & Holling HE. (1938). Further observations on the vascular responses of the human limb to body warming, evidence for sympathetic vasodilator nerves in the normal subject. *Clin Sci* **3,** 273-285.

Gray DW & Marshall I. (1992a). Human alpha calcitonin gene-related peptide stimulates adenylate-cyclase and guanylate-cyclase and relaxes rat thoracic aorta by releasing nitric oxide. *British Journal of Pharmacology* **107,** 691-696.

Gray DW & Marshall I. (1992b). Nitric oxide synthesis inhibitors attenuate calcitonin gene-related peptide endothelium-dependent vasorelaxation in rat aorta. *Eur J Pharmacol* **212,** 37-42.

Hales JRS, Jessen C, Fawcett AA & King RB. (1985). Skin AVA and capillary dilatation and constriction induced by local skin heating. *Pflugers Arch* **404,** 203-207.

Hall JM & Brain SD. (1994). Inhibition of SR140333 of NK1 tachykinin receptor-evoked, nitric oxide-dependent vasodilatation in the hamster-cheek pouch microvasculature in-vivo. *British Journal of Pharmacology* **113,** 522-526.

Harada N, Okajima K, Uchiba M & Katsuragi T. (2002). Ischemia/reperfusion-induced increase in the hepatic level of prostacyclin is mainly mediated by activation of capsaicin-sensitive sensory neurons in rats. *J Lab Clin Med* **139,** 218-226.

Hargens AR, Cologne JB, Menninger FJ, Hogan JS, Tucker BJ & Peters RM. (1981). Normal trans-capillary pressures in human skeletal muscle and subcutaneous tissues. *Microvascular Research* **22,** 177-189.

Harris NR. (1997). Opposing effects of L-NAME on capillary filtration rate in the presence or absence of neutrophils. *Am J Physiol-Gastroint Liver Physiol* **273,** G1320-G1325.

Harris NR & Granger DN. (1996). Neutrophil enhancement of reperfusion-induced capillary fluid filtration associated with hypercholesterolemia. *Am J Physiol-Heart Circul Physiol* **271,** H1755-H1761.

Harrison DG. (1997). Cellular and molecular mechanisms of endothelial cell dysfunction. *J Clin Invest* **100,** 2153-2157.

Hashim MA & Tadepalli AS. (1995). Cutaneous vasomotor effects of neuropeptide Y. *Neuropeptides* **29,** 263-271.

Hearse DJ, Humphrey SM & Chain EB. (1973). Abrupt reoxygenation of anoxic potassium-arrested perfused rat heart - study of myocardial enzyme release. *J Mol Cell Cardiol* **5,** 395-407.

Heath ME. (1998). Neuropeptide Y and Y(1)-receptor agonists increase blood flow through arteriovenous anastomoses in rat tail. *Journal of Applied Physiology* **85,** 301-309.

Hirata K, Nagasaka T, Nunomura T & Cabanac M. (1988). Local thermal sensation and finger vasoconstriction in the locally heated hand. *Eur J Appl Physiol Occup Physiol* **58,** 92-96.

Hodges GJ & Del Pozzi AT. (2014). Noninvasive examination of endothelial, sympathetic, and myogenic contributions to regional differences in the human cutaneous microcirculation. *Microvasc Res* **93,** 87-91.

Hodges GJ, Del Pozzi AT, McGarr GW, Mallette MM & Cheung SS. (2015). The contribution of sensory nerves to cutaneous vasodilatation of the forearm and leg to local skin heating. *Eur J Appl Physiol* **115,** 2091-2098.

Hodges GJ, Kosiba WA, Zhao K & Johnson JM. (2008). The involvement of norepinephrine, neuropeptide Y, and nitric oxide in the cutaneous vasodilator response to local heating in humans. *Journal of Applied Physiology* **105,** 233-240.

Hodges GJ, Kosiba WA, Zhao K & Johnson JM. (2009). The involvement of heating rate and vasoconstrictor nerves in the cutaneous vasodilator response to skin warming. *Am J Physiol-Heart Circul Physiol* **296,** H51-H56.

Hodges GJ, McGarr GW, Mallette MM, Del Pozzi AT & Cheung SS. (2016). The contribution of sensory nerves to the onset threshold for cutaneous vasodilatation during gradual local skin heating of the forearm and leg. *Microvasc Res* **105,** 1-6.

Holowatz LA, Jennings JD, Lang JA & Kenney WL. (2009). Ketorolac alters blood flow during normothermia but not during hyperthermia in middle-aged human skin. *J Appl Physiol (1985)* **107,** 1121-1127.

Holowatz LA & Kenney WL. (2007). Local ascorbate administration augments NO- and non-NO-dependent reflex cutaneous vasodilation in hypertensive humans. *Am J Physiol-Heart Circul Physiol* **293,** H1090-H1096.

Holowatz LA & Kenney WL. (2011). Oral atorvastatin therapy increases nitric oxide-dependent cutaneous vasodilation in humans by decreasing ascorbate-sensitive oxidants. *Am J Physiol-Regul Integr Comp Physiol* **301,** R763-R768.

Holowatz LA, Santhanam L, Webb A, Berkowitz DE & Kenney WL. (2011). Oral atorvastatin therapy restores cutaneous microvascular function by decreasing arginase activity in hypercholesterolaemic humans. *J Physiol-London* **589,** 2093-2103.

Holowatz LA, Thompson CS & Kenney WL. (2006). Acute ascorbate supplementation alone or combined with arginase inhibition augments reflex cutaneous vasodilation in aged human skin. *Am J Physiol-Heart Circul Physiol* **291,** H2965-H2970.

Holzer P. (1991). Capsaicin - Cellular targets, mechanisms of action, and selectivity for thin sensory neurons. *Pharmacol Rev* **43,** 143-201.

Horie Y, Wolf R, Flores SC, McCord JM, Epstein CJ & Granger DN. (1998). Transgenic mice with increased copper/zinc superoxide dismutase activity are resistant to hepatic leukostasis and capillary no-reflow after gut ischemia/reperfusion. *Circulation Research* **83,** 691-696.

Houghton BL, Meendering JR, Wong BJ & Minson CT. (2006). Nitric oxide and noradrenaline contribute to the temperature threshold of the axon reflex response to gradual local heating in human skin. *J Physiol-London* **572,** 811-820.

Hughes SR & Brain SD. (1994). Nitric oxide-dependent release of vasodilator quantities of calcitonin gene-related peptide from capsaicin-sensitive nerves in rabbit skin. *British Journal of Pharmacology* **111,** 425-430.

Hurley HJ & Mescon H. (1956). Cholinergic innervation of the digital arteriovenous anastomoses of human skin - A histochemical localization of cholinesterase. *Journal of Applied Physiology* **9,** 82-84.

Ichikawa H, Flores S, Kvietys PR, Wolf RE, Yoshikawa T, Granger DN & Aw TY. (1997). Molecular mechanisms of anoxia/reoxygenation-induced neutrophil adherence to cultured endothelial cells. *Circulation Research* **81,** 922-931.

Jancso N, Jancsoga.A & Szolcsanyi J. (1967). Direct evidence for neurogenic inflammation and its prevention by denervation and by pretreatment with capsaicin. *British Journal of Pharmacology and Chemotherapy* **31,** 138-+.

Jerome SN, Akimitsu T & Korthuis RJ. (1994). Leukocyte adhesion, edema, and development of postischemic capillary no-reflow. *Am J Physiol-Heart Circul Physiol* **267,** H1329-H1336.

Ji P, Jiang T, Wang MH, Wang RR, Zhang LQ & Li Y. (2013). Denervation of capsaicin-sensitive C fibers increases pulmonary inflammation induced by ischemia-reperfusion in rabbits. *J Surg Res* **184,** 782-789.

Johnson JM & Kellogg DL, Jr. (2010). Local thermal control of the human cutaneous circulation. *J Appl Physiol (1985)* **109,** 1229-1238.

Johnson JM, Minson CT & Kellogg DL. (2014). Cutaneous Vasodilator and Vasoconstrictor Mechanisms in Temperature Regulation. *Compr Physiol* **4,** 33-89.

Johnson JM, Taylor WF, Shepherd AP & Park MK. (1984). Laser-Doppler measurement of skin blood flow - comparison with plethysmography. *Journal of Applied Physiology* **56,** 798-803.

Joneschild ES, Chen LE, Seaber AV, Frankel ES & Urbaniak JR. (1999). Effect of a NOS inhibitor, L-NMMA, on the contractile function of reperfused skeletal muscle. *J Reconstr Microsurg* **15,** 55-60.

Kalogeris T, Baines CP, Krenz M & Korthuis RJ. (2012). Cell biology of ischemia/reperfusion injury. In *International Review of Cell and Molecular Biology, Vol 298*, ed. Jeon KW, pp. 229-317. Elsevier Academic Press Inc, San Diego.

Kaminski KA, Bonda TA, Korecki J & Musial WJ. (2002). Oxidative stress and neutrophil activation - the two keystones of ischemia/reperfusion injury. *Int J Cardiol* **86,** 41-59.

Kellogg DL, Johnson JM & Kosiba WA. (1989). Selective abolition of adrenergic vasoconstrictor responses in skin by local iontophoresis of bretylium. *Am J Physiol* **257,** H1599-H1606.

Kellogg DL, Jr., Zhao JL & Wu Y. (2008a). Neuronal nitric oxide synthase control mechanisms in the cutaneous vasculature of humans in vivo. *J Physiol* **586,** 847-857.

Kellogg DL, Liu Y, Kosiba IF & O'Donnell D. (1999). Role of nitric oxide in the vascular effects of local warming of the skin in humans. *Journal of Applied Physiology* **86,** 1185-1190.

Kellogg DL, Zhao JL & Wu Y. (2008b). Endothelial nitric oxide synthase control mechanisms in the cutaneous vasculature of humans in vivo. *Am J Physiol-Heart Circul Physiol* **295,** H123-H129.

Kellogg DL, Zhao JL & Wu YB. (2009). Roles of nitric oxide synthase isoforms in cutaneous vasodilation induced by local warming of the skin and whole body heat stress in humans. *Journal of Applied Physiology* **107,** 1438-1444.

Khan F, Elhadd TA, Greene SA & Belch JJF. (2000). Impaired skin microvascular function in children, adolescents, and young adults with type 1 diabetes. *Diabetes Care* **23,** 215-220.

Kiss M, Kemeny L, Gyulai R, Michel G, Husz S, Kovacs R, Dobozy A & Ruzicka T. (1999). Effects of the neuropeptides substance P, calcitonin gene-related peptide and alpha-melanocyte-stimulating hormone on the IL-8/IL-8 receptor system in a cultured human keratinocyte cell line and dermal fibroblasts. *Inflammation* **23,** 557-567.

Kraemer-Aguiar LG, Laflor CM & Bouskela E. (2008). Skin microcirculatory dysfunction is already present in normoglycemic subjects with metabolic syndrome. *Metabolism* **57,** 1740-1746.

Kramer JH, Phillips TM & Weglicki WB. (1997). Magnesium-deficiency-enhanced post-ischemic myocardial injury is reduced by substance P receptor blockade. *J Mol Cell Cardiol* **29,** 97-110.

Kruger A, Stewart J, Sahityani R, O'Riordan E, Thompson C, Adler S, Garrick R, Vallance P & Goligorsky MS. (2006). Laser Doppler flowmetry detection of endothelial dysfunction in end-stage renal disease patients: correlation with cardiovascular risk. *Kidney Int* **70,** 157-164.

Kubes P & Granger DN. (1996). Leukocyte-endothelial cell interactions evoked by mast cells. *Cardiovasc Res* **32,** 699-708.

Kuo L, Davis MJ & Chilian WM. (1992). Endothelial modulation of arteriolar tone. *News Physiol Sci* **7,** 5-9.

Kurose I, Anderson DC, Miyasaka M, Tamatani T, Paulson JC, Todd RF, Rusche JR & Granger DN. (1994). Molecular determinants of reperfusion-induced leukocyte adhesion and vascular protein leakage. *Circulation Research* **74,** 336-343.

Landis EM. (1930). Micro-injection studies of capillary blood pressure in human skin. *Heart-J Stud Circ* **15,** 209-228.

Lee MCI, Velayutham M, Komatsu T, Hille R & Zweier JL. (2014). Measurement and Characterization of Superoxide Generation from Xanthine Dehydrogenase: A Redox-Regulated Pathway of Radical Generation in Ischemic Tissues. *Biochemistry* **53,** 6615-6623.

Lennertz RC, Medler KA, Bain JL, Wright DE & Stucky CL. (2011). Impaired sensory nerve function and axon morphology in mice with diabetic neuropathy. *J Neurophysiol* **106,** 905-914.

Lewis T. (1927). *The blood vessels of the skin and their responses*. Shaw & Sons, London.

Loerakker S, Manders E, Strijkers GJ, Nicolay K, Baaijens FPT, Bader DL & Oomens CWJ. (2011). The effects of deformation, ischemia, and reperfusion on the development of muscle damage during prolonged loading. *Journal of Applied Physiology* **111,** 1168-1177.

Lorenzo S & Minson CT. (2007). Human cutaneous reactive hyperaemia: role of BKCa channels and sensory nerves. *J Physiol* **585,** 295-303.

Lotti T, Hautmann G & Panconesi E. (1995). Neuropeptides in skin. *J Am Acad Dermatol* **33,** 482-496.

Magerl W & Treede RD. (1996). Heat-evoked vasodilatation in human hairy skin: Axon reflexes due to low-level activity of nociceptive afferents. *J Physiol-London* **497,** 837-848.

Mahmud MS, Cadotte DW, Vuong B, Sun C, Luk TWH, Mariampillai A & Yang VXD. (2013). Review of speckle and phase variance optical coherence tomography to visualize microvascular networks. *J Biomed Opt* **18,** 13.

Mathura KR, Vollebregt KC, Boer K, De Graaff JC, Ubbink DT & Ince C. (2001). Comparison of OPS imaging and conventional capillary microscopy to study the human microcirculation. *Journal of Applied Physiology* **91,** 74-78.

McCord GR, Cracowski JL & Minson CT. (2006). Prostanoids contribute to cutaneous active vasodilation in humans. *Am J Physiol-Regul Integr Comp Physiol* **291,** R596-R602.

McCord JM. (1985). Oxygen-derived free radicals in postischemic tissue injury. *N Engl J Med* **312,** 159-163.

Medow MS, Bamji N, Clarke D, Ocon AJ & Stewart JM. (2011). Reactive oxygen species (ROS) from NADPH and xanthine oxidase modulate the cutaneous local heating response in healthy humans. *J Appl Physiol (1985)* **111,** 20-26.

Mescon H, Hurley HJ & Moretti G. (1956). The anatomy and histochemistry of the arteriovenous anastomosis in human digital skin. *J Invest Dermatol* **27,** 133-145.

Metzler-Wilson K, Kellie LA, Tomc C, Simpson C, Sammons D & Wilson TE. (2012). Differential vasodilatory responses to local heating in facial, glabrous and hairy skin. *Clin Physiol Funct Imaging* **32,** 361-366.

Minson CT, Berry LT & Joyner MJ. (2001). Nitric oxide and neurally mediated regulation of skin blood flow during local heating. *Journal of Applied Physiology* **91,** 1619-1626.

Minson CT, Holowatz LA, Wong BJ, Kenney WL & Wilkins BW. (2002). Decreased nitric oxide- and axon reflex-mediated cutaneous vasodilation with age during local heating. *Journal of Applied Physiology* **93,** 1644-1649.

Miyanohara J, Shirakawa H, Sanpei K, Nakagawa T & Kaneko S. (2015). A pathophysiological role of TRPV1 in ischemic injury after transient focal cerebral ischemia in mice. *Biochem Biophys Res Commun* **467,** 478-483.

Mizutani A, Okajima K, Murakami K, Mizutani S, Kudo K, Uchino T, Kadoi Y & Noguchi T. (2009). Activation of Sensory Neurons Reduces

Ischemia/Reperfusion-induced Acute Renal Injury in Rats. *Anesthesiology* **110,** 361-369.

Montagna W, Yun J & Formisano V. (1964). Histology and cytochemistry of human skin: Cholinesterase-containing nerves in face. *Arch Dermatol* **90,** 526-&.

Munger BL & Ide C. (1988). The structure and function of cutaneous sensory receptors. *Arch Histol Cytol* **51,** 1-34.

Mustoe T. (2004). Understanding chronic wounds: a unifying hypothesis on their pathogenesis and implications for therapy. *Am J Surg* **187,** 65S-70S.

Nagasaka T, Hirata K, Mano T, Iwase S & Rossetti Y. (1990). Heat-induced finger vasoconstriction controlled by skin sympathetic nerve activity. *Journal of Applied Physiology* **68,** 71-75.

Nagasaka T, Hirata K & Nunomura T. (1987a). Contribution of arteriovenous anastomoses to vasoconstriction induced by local heating of the human finger. *Jpn J Physiol* **37,** 425-433.

Nagasaka T, Hirata K, Nunomura T & Cabanac M. (1987b). The effect of local heating on blood flow in the finger and forearm skin. *Can J Physiol Pharmacol* **65,** 1329-1332.

Nawa H, Hirose T, Takashima H, Inayama S & Nakanishi S. (1983). Nucleotide sequences of cloned cDNAs for 2 types of bovine brain Substance-P precursor. *Nature* **306,** 32-36.

Nolano M, Provitera V, Caporaso G, Stancanelli A, Leandri M, Biasiotta A, Cruccu G, Santoro L & Truini A. (2013). Cutaneous innervation of the human face as assessed by skin biopsy. *J Anat* **222,** 161-169.

O'Doherty J, McNamara P, Clancy NT, Enfield JG & Leahy MJ. (2009). Comparison of instruments for investigation of microcirculatory blood flow and red blood cell concentration. *J Biomed Opt* **14,** 13.

Ordy JM, Wengenack TM, Bialobok P, Coleman PD, Rodier P, Baggs RB, Dunlap WP & Kates B. (1993). Selective vulnerability and early progression of Hippocampal-CA1 pyramidal cell degeneration and GFAP-positive astrocyte reactivity in the rat 4-vessel occlusion model of transient global ischemia. *Exp Neurol* **119,** 128-139.

Padilla J, GarciaVillalon AL, Monge L, Garcia JL, Fernandez N, Gomez B & Dieguez G. (1997). Peptidergic modulation of the sympathetic contraction in the rabbit ear artery: Effects of temperature. *British Journal of Pharmacology* **121,** 21-28.

Parks DA & Granger DN. (1986). Contributions of ischemia and reperfusion to mucosal lesion formation. *Am J Physiol* **250,** G749-G753.

Petersen LJ. (1998). Measurement of histamine release in intact human skin by microdialysis technique - Clinical and experimental findings. *Dan Med Bull* **45,** 383-401.

Quayle JM, Bonev AD, Brayden JE & Nelson MT. (1994). Calcitonin gene-related peptide activated ATP-sensitive K+ currents in rabbit arterial smooth muscle via protein kinase A. *J Physiol-London* **475,** 9-13.

Quinlan KL, Naik SM, Cannon G, Armstrong CA, Bunnett NW, Ansel JC & Caughman SW. (1999a). Substance P activates coincident NF-AT- and NF-kappa B-dependent adhesion molecule gene expression in microvascular endothelial cells through intracellular calcium mobilization. *J Immunol* **163,** 5656-5665.

Quinlan KL, Song IS, Bunnett NW, Letran E, Steinhoff M, Harten B, Olerud JE, Armstrong CA, Caughman SW & Ansel JC. (1998). Neuropeptide regulation of human dermal microvascular endothelial cell ICAM-1 expression and function. *Am J Physiol-Cell Physiol* **275,** C1580-C1590.

Quinlan KL, Song IS, Naik SM, Letran EL, Olerud JE, Bunnett NW, Armstrong CA, Caughman SW & Ansel JC. (1999b). VCAM-1 expression on human dermal microvascular endothelial cells is directly and specifically up-regulated by substance P. *J Immunol* **162,** 1656-1661.

Racz IB, Illyes G, Sarkadi L & Hamar J. (1997). The functional and morphological damage of ischemic reperfused skeletal muscle. *European Surgical Research* **29,** 254-263.

Ratych RE, Chuknyiska RS & Bulkley GB. (1987). The primary localization of free radical generation after anoxia reoxygenation in isolated endothelial cells. *Surgery* **102,** 122-131.

Roddie IC, Shepherd JT & Whelan RF. (1957). The contribution of constrictor and dilator nerves to the skin vasodilation during body heating. *J Physiol-London* **136,** 489-497.

Roosterman D, Goerge T, Schneider SW, Bunnett NW & Steinhoff M. (2006). Neuronal control of skin function: the skin as a neuroimmunoendocrine organ. *Physiol Rev* **86,** 1309-1379.

Roustit M, Blaise S, Millet C & Cracowski JL. (2010). Reproducibility and methodological issues of skin post-occlusive and thermal hyperemia

assessed by single-point laser Doppler flowmetry. *Microvascular Research* **79,** 102-108.

Roustit M & Cracowski JL. (2012). Non-invasive assessment of skin microvascular function in humans: an insight into methods. *Microcirculation* **19,** 47-64.

Roustit M & Cracowski JL. (2013). Assessment of endothelial and neurovascular function in human skin microcirculation. *Trends Pharmacol Sci* **34,** 373-384.

Roustit M, Simmons GH, Carpentier P & Cracowski JL. (2008). Abnormal digital neurovascular response to local heating in systemic sclerosis. *Rheumatology (Oxford)* **47,** 860-864.

Rowell LB. (1993). *Human Cardiovascular Control*. Oxford University Press, New York.

Salas A, Panes J, Elizalde JI, Granger DN & Pique JM. (1999). Reperfusion-induced oxidative stress in diabetes: cellular and enzymatic sources. *J Leukoc Biol* **66,** 59-66.

Sangiorgi S, Manelli A, Congiu T, Bini A, Pilato G, Reguzzoni M & Raspanti M. (2004). Microvascularization of the human digit as studied by corrosion casting. *J Anat* **204,** 123-131.

Santicioli P, Giuliani S & Maggi CA. (1993). Failure of L-nitroarginine, a nitric oxide synthase inhibitor, to affect hypotension and plasma protein extravasation produced by tachykinin NK-1 receptor activation in rats. *J Auton Pharmacol* **13,** 193-199.

Sapega AA, Heppenstall RB, Chance B, Park YS & Sokolow D. (1985). Optimizing tourniquet application and release times in extremity surgery - a biochemical and ultrastructural study. *J Bone Joint Surg-Am Vol* **67A,** 303-314.

Sauerstein K, Klede M, Hilliges M & Schmelz M. (2000). Electrically evoked neuropeptide release and neurogenic inflammation differ between rat and human skin. *J Physiol-London* **529,** 803-810.

Saumet JL, Kellogg DL, Taylor WF & Johnson JM. (1988). Cutaneous laser-Doppler flowmetry - Influence of underlying muscle blood flow. *Journal of Applied Physiology* **65,** 478-481.

Schaffer M, Beiter T, Becker HD & Hunt TK. (1998). Neuropeptides - Mediators of inflammation and tissue repair? *Arch Surg* **133,** 1107-1116.

Schlereth T, Schukraft J, Kramer-Best HH, Geber C, Ackerman T & Birklein F. (2016). Interaction of calcitonin gene related peptide (CGRP) and substance P (SP) in human skin. *Neuropeptides* **59,** 57-62.

Schmelz M & Petersen LJ. (2001). Neurogenic inflammation in human and rodent skin. *News Physiol Sci* **16,** 33-37.

Schmidt R, Schmelz M, Forster C, Ringkamp M, Torebjork E & Handwerker H. (1995). Novel classes of responsive and unresponsive C-nociceptors in human skin. *J Neurosci* **15,** 333-341.

Schmidt Y, Bannasch H & Eisenhardt SU. (2012). Ischemia-Reperfusion Injury Leads to Significant Tissue Damage in Free Flap Surgery. *Plast Reconstr Surg* **129,** 174E-175E.

Scholzen TE, Brzoska T, Kalden DH, O'Reilly F, Armstrong CA, Luger TA & Ansel JC. (1999). Effect of ultraviolet light on the release of neuropeptides and neuroendocrine hormones in the skin: Mediators of photodermatitis and cutaneous inflammation. *J Invest Dermatol Symp Proc* **4,** 55-60.

Scholzen TE, Stander S, Riemann H, Brzoska T & Luger TA. (2003). Modulation of cutaneous inflammation by angiotensin-converting enzyme. *J Immunol* **170,** 3866-3873.

Segal SS. (1994). Cell-to-cell communication coordinates blood flow control. *Hypertension* **23,** 1113-1120.

Semenza JC, McCullough JE, Flanders WD, McGeehin MA & Lumpkin JR. (1999). Excess hospital admissions during the July 1995 heat wave in Chicago. *Am J Prev Med* **16,** 269-277.

Shastry S & Joyner MJ. (2002). Geldanamycin attenuates NO-mediated dilation in human skin. *Am J Physiol-Heart Circul Physiol* **282,** H232-H236.

Sherman JL. (1963). Normal arteriovenous anastomoses. *Medicine (Baltimore)* **42,** 247-&.

Shibasaki M, Durand S, Davis SL, Cui J, Low DA, Keller DM & Crandall CG. (2007). Endogenous nitric oxide attenuates neurally mediated cutaneous vasoconstriction. *J Physiol* **585,** 627-634.

Siney L & Brain SD. (1996). Involvement of sensory neuropeptides in the development of plasma extravasation in rat dorsal skin following thermal injury. *British Journal of Pharmacology* **117,** 1065-1070.

Skalak R & Skalak TC. (1995). Flow behavior of leukocytes in small tubes. In *Physiology and Pathophysiology of Leukocyte Adhesion*, ed. Granger DN & Schmid-Shonbein GW, pp. 97-115. Oxford University Press, New York.

Smith CJ & Johnson JM. (2016). Responses to hyperthermia. Optimizing heat dissipation by convection and evaporation: Neural control of skin blood flow and sweating in humans. *Auton Neurosci-Basic Clin* **196,** 25-36.

Smith VA & Johnson T. (2010). Evaluation of an Animal Product-Free Variant of MegaCell (TM) MEM as a Storage Medium for Corneas Destined for Transplantation. *Ophthalmic Res* **43,** 33-42.

Sokolnicki LA, Roberts SK, Wilkins BW, Basu A & Charkoudian N. (2007). Contribution of nitric oxide to cutaneous microvascular dilation in individuals with type 2 diabetes mellitus. *Am J Physiol-Endocrinol Metab* **292,** E314-E318.

Souza DG, Coutinho SF, Silveira MR, Cara DC & Teixeira MM. (2000). Effects of a BLT receptor antagonist on local and remote reperfusion injuries after transient ischemia of the superior mesenteric artery in rats. *Eur J Pharmacol* **403,** 121-128.

Souza DG, Mendonca VA, Castro MSD, Poole S & Teixeira MM. (2002). Role of tachykinin NK receptors on the local and remote injuries following ischaemia and reperfusion of the superior mesenteric artery in the rat. *British Journal of Pharmacology* **135,** 303-312.

Steinhoff M, Stander S, Seeliger S, Ansel JC, Schmelz M & Luger T. (2003). Modern aspects of cutaneous neurogenic inflammation. *Arch Dermatol* **139,** 1479-1488.

Stephens DP, Charkoudian N, Benevento JM, Johnson JM & Saumet JL. (2001). The influence of topical capsaicin on the local thermal control of skin blood flow in humans. *Am J Physiol-Regul Integr Comp Physiol* **281,** R894-R901.

Stewart JM, Medow MS, Minson CT & Taneja I. (2007). Cutaneous neuronal nitric oxide is specifically decreased in postural tachycardia syndrome. *Am J Physiol Heart Circ Physiol* **293,** H2161-2167.

Suzuki H, Poole DC, Zweifach BW & SchmidSchonbein GW. (1995). Temporal correlation between maximum tetanic force and cell death in postischemic rat skeletal muscle. *J Clin Invest* **96,** 2892-2897.

Szolcsanyi J. (1996). Capsaicin-sensitive sensory nerve terminals with local and systemic efferent functions: Facts and scopes of an unorthodox neuroregulatory mechanism. In *Polymodal Receptor - a Gateway to*

Pathological Pain, ed. Kumazawa T, Kruger L & Mizumura K, pp. 343-359. Elsevier Science Bv, Amsterdam.

Taylor NAS, Machado-Moreira CA, van den Heuvel AMJ & Caldwell JN. (2014). Hands and feet: physiological insulators, radiators and evaporators. *European Journal of Applied Physiology* **114,** 2037-2060.

Tenland T, Salerud EG, Nilsson GE & Oberg PA. (1983). Spatial and temporal variations in human skin blood flow. *Int J Microcirc-Clin Exp* **2,** 81-90.

Turchanyi B, Toth B, Racz I, Vendegh Z, Furesz J & Hamar J. (2005). Ischemia Reperfusion injury of the skeletal muscle after selective deafferentation. *Physiol Res* **54,** 25-31.

Ustinova EE, Bergren D & Schultz HD. (1995). Neuropeptide depletion impairs postischemic recovery of the isolated rat heart - Role of Substance-P. *Cardiovasc Res* **30,** 55-63.

Ustinova EE & Schultz HD. (1994a). Activation of cardiac vagal afferents by oxygen-derived free radicals in rats. *Circulation Research* **74,** 895-903.

Ustinova EE & Schultz HD. (1994b). Activation of cardiac vagal afferents in ischemia and reperfusion - Prostaglandins versus oxygen-derived free radicals. *Circulation Research* **74,** 904-911.

Varadarajan R, Golden-Mason L, Young L, McLoughlin P, Nolan N, McEntee G, Traynor O, Geoghegan T, Hegarty JE & O'Farrell C. (2004). Nitric oxide in early ischaemia reperfusion injury during human orthotopic liver transplantation. *Transplantation* **78,** 250-256.

Venturini G, Colasanti M, Fioravanti E, Bianchini A & Ascenzi P. (1999). Direct effect of temperature on the catalytic activity of nitric oxide synthases types I, II, and III. *Nitric Oxide-Biol Chem* **3,** 375-382.

Wallengren J. (1997). *Vasoactive peptides in the skin*. Blackwell Science Inc, Malden.

Wallengren J & Hakanson R. (1987). Effects of Substance-P, Neurokinin-A, and Calcitonin Gene-Related Peptide in human skin and their involvement in sensory nerve mediated responses. *Eur J Pharmacol* **143,** 267-273.

Wallengren J & Wang ZY. (1993). Interactions between tachykinins and CGRP in human skin. *Acta Derm-Venereol* **73,** 259-261.

Wang LH & Wang DH. (2005). TRPV1 gene knockout impairs postischemic recovery in isolated perfused heart in mice. *Circulation* **112,** 3617-3623.

Wang MH, Ji P, Wang RR, Zhao LF & Xia ZY. (2012). TRPV1 Agonist Capsaicin Attenuates Lung Ischemia-Reperfusion Injury in Rabbits. *J Surg Res* **173,** 153-160.

Wang WZ, Baynosa RC & Zamboni WA. (2011). Update on Ischemia-Reperfusion Injury for the Plastic Surgeon: 2011. *Plast Reconstr Surg* **128,** 685E-692E.

Wardell K, Braverman IM, Silverman DG & Nilsson GE. (1994). Spatial heterogeneity in normal skin perfusion recorded with laser-Doppler imaging and flowmetry. *Microvascular Research* **48,** 26-38.

Weber M, Birklein F, Neundorfer B & Schmelz M. (2001). Facilitated neurogenic inflammation in complex regional pain syndrome. *Pain* **91,** 251-257.

Weidner C, Klede M, Rukwied R, Lischetzki G, Neisius U, Skov PS, Petersen LJ & Schmelz M. (2000). Acute effects of substance P and calcitonin gene-related peptide in human skin - A microdialysis study. *J Invest Dermatol* **115,** 1015-1020.

Whittle BJR, Lopezbelmonte J & Rees DD. (1989). Modulation of the vasodepressor actions of acetylcholine, bradykinin, Substance-P, and endothelin in the rat by a specific inhibitor of nitric oxide formation. *British Journal of Pharmacology* **98,** 646-652.

Widgerow AD. (2014). Ischemia-Reperfusion Injury Influencing the Microcirculatory and Cellular Environment. *Ann Plast Surg* **72,** 253-260.

Wingo JE, Low DA, Keller DM, Brothers RM, Shibasaki M & Crandall CG. (2009). Effect of elevated local temperature on cutaneous vasoconstrictor responsiveness in humans. *Journal of Applied Physiology* **106,** 571-575.

Wong BJ. (2013). Sensory nerves and nitric oxide contribute to reflex cutaneous vasodilation in humans. *Am J Physiol-Regul Integr Comp Physiol* **304,** R651-R656.

Wong BJ & Fieger SM. (2010). Transient receptor potential vanilloid type-1 (TRPV-1) channels contribute to cutaneous thermal hyperaemia in humans. *J Physiol* **588,** 4317-4326.

Wong BJ & Minson CT. (2011). Altered thermal hyperaemia in human skin by prior desensitization of neurokinin-1 receptors. *Exp Physiol* **96,** 599-609.

Wong BJ, Tublitz NJ & Minson CT. (2005). Neurokinin-1 receptor desensitization to consecutive microdialysis infusions of substance P in human skin. *J Physiol-London* **568,** 1047-1056.

Wong BJ, Williams SJ & Minson CT. (2006). Minimal role for H1 and H2 histamine receptors in cutaneous thermal hyperemia to local heating in humans. *J Appl Physiol (1985)* **100,** 535-540.

Xu XJ, Dalsgaard CJ, Maggi CA & Wiesenfeldhallin Z. (1992). NK-1, but not NK-2, tachykinin receptors mediate plasma extravasation induced by antidromic C-fiber stimulation in rat hindpaw demonstrated with the NK-1 antagonist CP-96,345 and the NK-2 antagonist MEN-10207. *Neurosci Lett* **139,** 249-252.

Yen A & Braverman IM. (1976). Ultrastructure of human dermal microcirculation - horizontal plexus of papillary dermis. *J Invest Dermatol* **66,** 131-142.

Zegarska B, Lelinska A & Tyrakowski T. (2006). Clinical and experimental aspects of cutaneous neurogenic inflammation. *Pharmacol Rep* **58,** 13-21.

Chapter 3: Objectives and Hypotheses

3.1 Objectives and Hypotheses - Chapter 5

Objective(s): First, to examine the between-day reliability of the cutaneous LTH response in non-glabrous and glabrous skin of the index finger with single-point LDF. Reliability was assessed for the magnitude of each phase as well as the kinetics of the LTH response. Second, to determine the test-retest coefficient of variation (%CV) values for all LTH measures in order to define threshold values for minimally important positive and negative effects for the experiment described in Chapter 6 and to make meaningful inferences about the true (population) effects of I-R injury on each component of the cutaneous LTH response.

Hypothesis-1: Between-day reliability for the magnitude and kinetics of the LTH response will be greater for non-glabrous skin compared to that of glabrous skin.

Hypothesis-2: Between-day reliability in glabrous skin will be greater than prior studies examining reliability with single-point LDF in this skin type.

Hypothesis-3: Normalizing cutaneous vascular conductance to a percentage of maximum will be the most reliable form of data expression in both skin types.

3.2 Objectives and Hypotheses - Chapter 6

Objective(s): To examine the influence of upper limb I-R injury on the responses to local heating in non-glabrous and glabrous skin of the index finger in order to identify potential impairments in neurovascular and/or endothelial function in the cutaneous microcirculation post-ischaemia.

Hypothesis-1: I-R injury will be associated with an attenuation of the initial vasodilatory peak in both non-glabrous and glabrous skin.

Hypothesis-2: I-R injury will be associated with delays in vasodilatory onset time and time to initial peak in both skin types.

Hypothesis-3: I-R injury will be associated with an attenuated vasodilatory response to sustained local heating in non-glabrous skin.

3.3 Objectives and Hypotheses - Chapter 7

Objective(s): First, to examine within- and between-day reliability of the cutaneous LTH response in the forearm using single point LDF. Reliability for the magnitude and the kinetics were assessed for each phase of the LTH response. Second, to determine the test-retest %CV values for all LTH measures to define threshold values for minimally important positive and negative effects for the experiment in Chapter 8 in order to make meaningful inferences about the true (population) effects of I-R injury on each component of the cutaneous LTH response.

Hypothesis-1: Within- and between-day reliability for the magnitude and kinetics of the LTH response will be comparable and consistent with the spatial variation characterizing forearm skin blood flow measurements.

Hypothesis-2: Between-day reliability in the current study will be greater than that seen in previous studies using single-point LDF.

Hypothesis-3: Normalizing cutaneous vascular conductance to a percentage of maximum will be the most reliable form of data expression.

3.4 Objectives and Hypotheses - Chapter 8

Objective(s): First, to examine the influence of upper limb I-R injury on the response to local heating in non-glabrous skin of the forearm. Second, to determine the contribution of sensory nerves in mediating each component of the response. This was accomplished by comparing the effects of I-R injury between untreated sites and skin sites treated with topical anaesthetic.

Hypothesis-1: I-R injury will be associated with an attenuation of the initial vasodilatory peak and delays in the vasodilatory onset time and time to initial peak during local heating in the forearm.

Hypothesis-2: I-R injury will be associated with an attenuated vasodilatory response to sustained local skin heating.

Hypothesis-3: The contribution of sensory nerves in mediating the kinetics and initial peak will be reduced post-ischaemia, indicating sensory nerves as important

mediators of the attenuated early vasodilatory response to local skin heating following I-R injury.

Chapter 4: General Methods

4.1 Ethical approval

Prior to conducting the experiments, ethical approval was obtained from the Bioscience Research Ethics Board at Brock University (BREB 15-077; Appendix-1). Before volunteering, all participants were fully informed of the experimental protocols and associated risks and subsequently provided both verbal and written informed consent. All experimental protocols conformed to the guidelines set forth in the declaration of Helsinki.

4.2 Sample size estimation

The estimated sample sizes required for the experiments in Chapters 6 and 8 were determined based on an expected change in the magnitude of the initial vasodilatory peak following I-R injury for each study. Calculations were based on a two-tailed test with α=0.10 and β=0.10 to obtain a power (1-β) of 90%. The β was set to 0.10 in order to reduce the likelihood of missing a relevant reduction in the sensory nerve response. Sample sizes were calculated according to the following equation (van Belle, 2008):

$$Estimated\ n = \frac{9 \cdot (CV)^2}{\left(ln_{\mu_0} - ln_{\mu_1}\right)^2}$$

The %CV represents the within-subject variation for a test-retest condition, which was derived from the appropriate reliability experiments in Chapters 5 and 7 for each skin type evaluated. The $ln_{\mu_0} - ln_{\mu_1}$ represents the smallest worthwhile difference for detection, expressed as a percentage change in the mean. This value was set to match the CV value in order to detect a change in the mean that is comparable to the CV that defines the normal variation in the response. The sample size calculations for both experiments indicated that nine participants were required to achieve the desired power. To account for possible attrition, ten participants were recruited for each study.

4.3 Participant selection

For each experiment, ten healthy males between the ages of 18 and 35 were recruited from Brock University and the local community. Although only males were recruited for these experiments, females were not excluded *a priori*. General physical health and weekly activity levels for all participants were determined using a modified version of the physical activity readiness questionnaire from the Canadian Society for Exercise Physiology and a weekly physical activity questionnaire, respectively. Participants were excluded if they were smokers or if they reported any cardiovascular, hematologic, metabolic, and/or neurological disease or were currently on any prescription medications.

4.4 Pre-experimental procedures

Participants were asked to refrain from caffeine consumption for 12 h, alcohol and strenuous exercise for 24 h, and exposure to extreme hot or cold temperatures for 48 h prior to the start of experimental sessions. Participants were also asked to avoid consumption of supplements such as multivitamins, as well as over the counter pain and/or anti-inflammatory medications, such as non-steroidal anti-inflammatory drugs for a minimum of two weeks prior to, and throughout the experiments to avoid any potential influence on the responses to ischaemia and reperfusion and to the LTH test.

All experimental sessions took place in the morning. Participants were instructed to have a light breakfast, no later than 1 hour prior to the start of the experiment. However, they were encouraged to drink water *ad libitum*. Upon arrival to the laboratory, each participant was first asked to provide a mid-stream urine sample for hydration assessment, which was assessed by measuring urine specific gravity with a refractometer (Atago, Tokyo). The threshold for euhydration was set to ≤1.02. Any hypohydrated participants were asked to consume 500 mL of water and hydration status was reassessed ~30 min later. If euhydration was confirmed at this point, testing commenced. If participants were still not adequately hydrated at this time, the experimental session was rescheduled for a later date.

After euhydration was confirmed, the participant changed into a standard set of clothing consisting of a cotton t-shirt, underwear, shorts and cotton socks. Height (cm) and body mass (kg) were then recorded, after which the participant was asked to lie supine on a padded table for instrumentation. Assessments of skin blood flow were all performed on the non-dominant upper limb, which was supported on a padded side and positioned at heart level for all experiments. For experiments assessing skin blood flow on the volar surface of the forearm, the limb was placed in the supine position and extended ~90° to the long axis of the body. For experiments assessing skin blood flow on the index finger, the limb was placed in a neutral position and extended ~45° to the long axis of the body. Ambient air temperature (T_{amb}) and relative humidity (%) were maintained at 25.0 ± 0.5°C and ~40-50%, respectively, throughout each experimental session.

4.5 Criteria for test termination

The need for termination of testing was established *a priori* based on the following criteria:

1. The participant reported sharp/intense pain during cuff inflation (when relevant), indicating nerve compression.
2. Heart rate rose to above 95% of maximum (220-age) for 3 minutes.
3. Dizziness or nausea precluded further experimentation
4. The participant decided, for any reason, to end the experiment.
5. The investigators determined that the participant was unable to continue.

During the actual testing, no sessions were terminated based on the preceding criteria.

4.6 Common instrumentation

4.6.1 Temperatures

All temperature measurements were performed using standard T-type thermocouples (PVC-T-24-190, Omega Environmental Inc., Laval, QC, CAN). To assess mean whole-body skin temperature ($\bar{T}_{sk}$), a total of four thermocouples were taped (Transpore™, St. Paul, MN, USA) to the chest, thigh, upper arm, and calf. A

weighted average over the four skin sites was used according to the following equation previously described by Ramanathan (1964):

$$\bar{T}_{sk} = 0.3(thigh) + 0.3(chest) + 0.2(calf) + 0.2(arm)$$

Forearm skin temperature (T_{fa}) was assessed with a single thermocouple placed over the volar surface midway between the elbow and wrist joints. Finger skin temperatures (T_{fi}) were measured on the middle finger of the experimental hand with one thermocouple centered on the dorsal surface of the middle phalanx (non-glabrous) and another centered on the volar surface of the distal phalanx (glabrous).

4.6.2 Heart rate

Heart rate (HR) was calculated from the R-R intervals obtained from an electrocardiogram (ECG) with a standard lead-II configuration. Prior to placement, electrode sites were shaved if necessary, then swabbed with alcohol and allowed to dry. Non-polarized Ag-AgCl electrodes with embedded electrode gel were used to achieve optimal electrical contact with the skin. Electrode leads were subsequently taped (Transpore™, St. Paul, MN, USA) in place to minimize movement artifacts.

4.6.3 Blood pressure

Manual blood pressure recordings were taken every 20 min throughout each experiment. A standard cuff was placed around the brachial artery of the non-experimental arm. MAP was calculated from the measured SBP and DBP according to the following equation:

$$MAP = 0.33(SBP) + 0.67(DBP)$$

Measurements were performed in duplicate at each time point, with a 1 min rest between cuff inflations.

4.6.4 Arterial oxygen saturation

Arterial oxygen saturation (S_aO_2) was determined with a finger pulse oximeter (Nonin, PureSAT, S_pO_2). The pulse oximeter was placed over the third finger on the hand of the experimental arm.

4.6.5 Skin blood flow

Red blood cell flux was assessed using LDF (PeriFlux System 5000, PeriMed, Sweden), which provides an index of skin blood flow (Johnson *et al.*, 1984; Saumet *et al.*, 1988). The resulting LDF signals were recorded in arbitrary perfusion units (APU), where 1 APU = 10 mV. The flowmeter was linked to an external computer with a standard serial interface connecter. The internal smoothing filter of the device was set to 0.2 s in order to capture changes in flux associated with each heart beat. Right-angled probes with integrated heating units were used (P415 probe, PeriMed, Sweden) with an emitter wavelength of 780 nm and a fibre separation between the emitter and receiver of 0.25 mm, were for the assessment of skin blood flow in a tissue volume in the range of 0.5-1.0 mm^3.

For the experiments involving the index finger (Fig 4.1), one probe was centred on the dorsal aspect of the middle phalanx. A second probe was centred on the volar aspect of the distal phalanx (finger pad). For the experiments involving the forearm (Fig 4.2), probes were placed on the volar surface ~5 cm apart from each other over the proximal third portion of the limb. Care was taken to avoid areas with large superficial veins and patches of dry skin. When necessary, overlying hair was gently clipped with scissors during which, care was taken not to scratch the skin surface to avoid an inflammatory response.

At each site, the probes were secured to the skin with double-sided adhesive tape. They were additionally secured with tape (Transpore™, St. Paul, MN, USA) that was gently placed over the top of the probes to ensure they would remain in place throughout testing. Care was taken not to apply any added pressure during this taping procedure that might restrict blood flow and the LDF recordings were examined before and after taping for confirmation.

4.7 Data Processing

All temperature measurements, as well as S_aO_2 and LDF measurements were collected at a sampling rate of 40 Hz. R-R intervals were sampled at 1000 Hz using Powerlab (ADInstruments, Colorado Springs, CO, USA). All data were stored on a personal computer to be analyzed offline using LabChart (ADInstruments, Colorado

Springs, CO, USA). All data were stored and transformed with Excel 2007 (Microsoft Corp., Redmond, WA, USA).

4.8 Local thermal hyperaemia protocol

A schematic of the LTH protocol is presented in Figure 4.3. At baseline, local skin temperature (T_{loc}) was set at 33°C. During the local heating protocol, T_{loc} was increased from 33°C to 42°C at a rate of $3°C \cdot min^{-1}$ (3 min) and held for 30-35 min, until a stable plateau had been reached, as determined by a trained investigator. T_{loc} was subsequently increased from 42°C to 44°C at rate of $1°C \cdot min^{-1}$ (2 min) and held for 20 min to induce maximal vasodilatation. T_{loc} was increased at a slower rate between 42°C and 44°C to avoid any noxious pain stimulus that may be caused by rapid heating at higher skin temperatures.

Measurement regions of the local heating response were defined as follows:

- Baseline - the arithmetic mean of the 3 min period immediately preceding the onset of local heating.
- Initial vasodilatory peak - the arithmetic mean of the highest consecutive 30 s period within the distinct initial hyperaemic response occurring in the first 10 min of local heating.
- Plateau - the arithmetic mean of the highest consecutive 3 min period of heating at 42°C when the response had leveled off (within the 10-30 min range).
- Maximum vasodilatation - the arithmetic mean of the highest consecutive 3 min period of heating at 44°C.

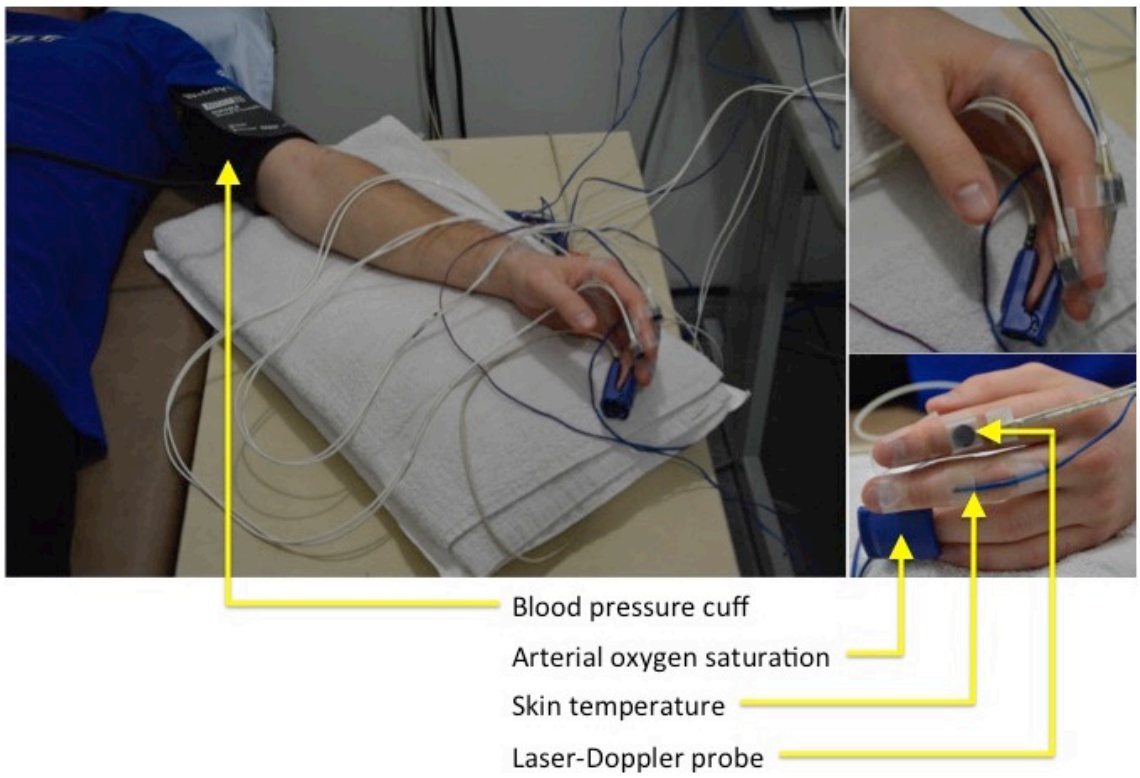

Figure 4.1 Limb configuration for experiments evaluating the index finger

An image of the experimental set-up for the non-dominant upper limb, used for experiments in Chapters 5 and 7. The blood pressure cuff was only inflated for the experiment in Chapter 7 to induce ischaemia. Top right inset depicts the configuration of laser-Doppler probes on the dorsal and volar aspects of the index finger for evaluation of skin blood flow. Bottom right inset shows the configuration across fingers, with laser-Doppler probes attached to the index finger, skin temperature sensors attached to the middle finger, and a pulse oximeter attached to the ring finger for evaluation of arterial oxygen saturation.

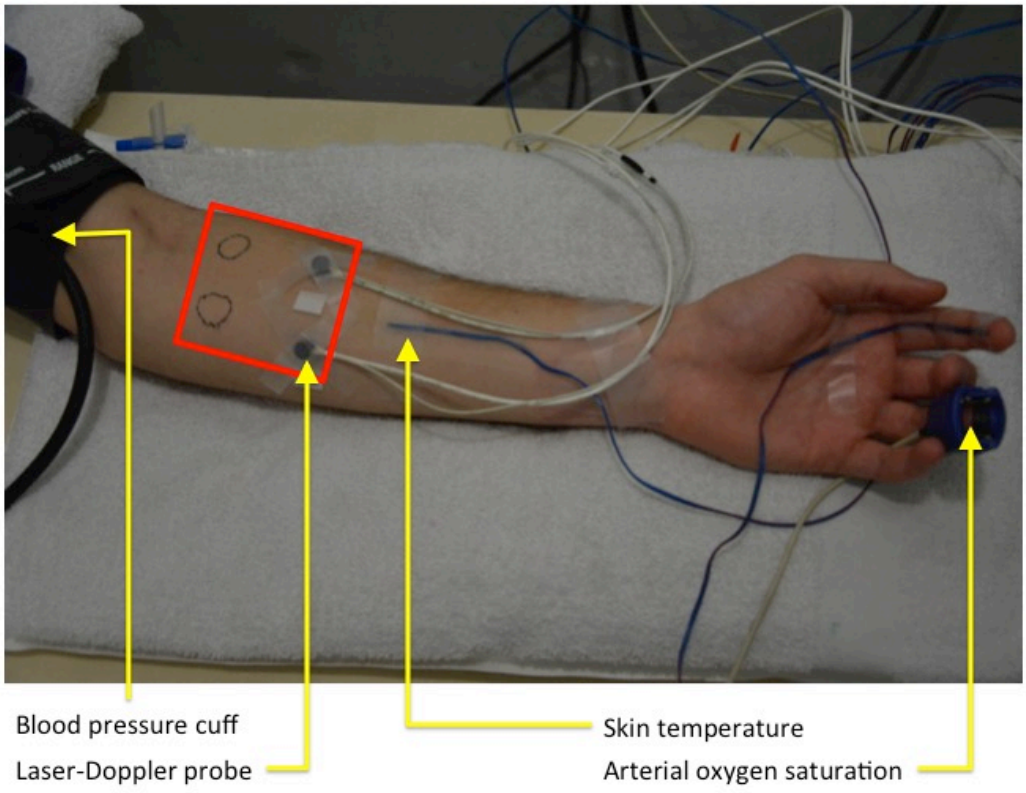

Figure 4.2 Limb configuration for experiments evaluating the forearm

An image of the experimental set-up for the non-dominant upper limb, used for experiments in Chapters 6 and 8. The blood pressure cuff was only inflated for the experiment in Chapter 8 to induce ischaemia. A pulse oximeter was placed on the ring finger to measure arterial oxygen saturation. Skin temperature sensors were placed on the finger pad of the index finger and on the volar forearm, midway between the elbow and wrist joints. Red box indicates the approximate location of the four skin sites that were marked with indelible ink and arranged in a square pattern with laser-Doppler probes placed ~5cm apart to avoid interference.

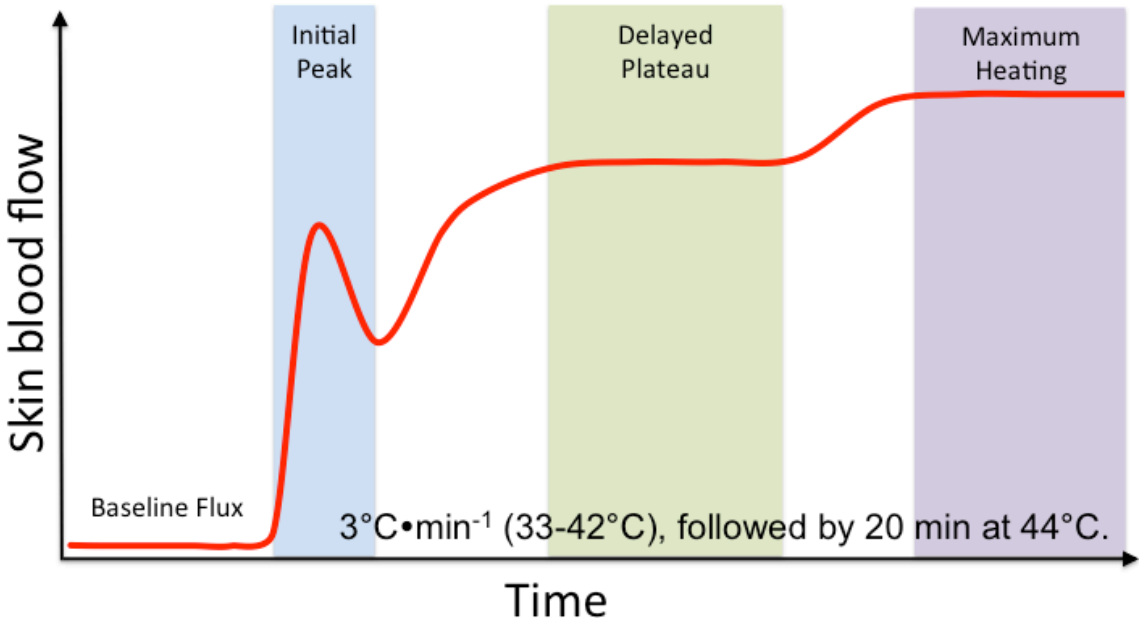

Figure 4.3 Schematic of the cutaneous local heating protocol

Schematic of an idealized local skin heating protocol used for all experiments in Chapters 5-8. The red line represents the skin blood flow response during local heating, obtained by laser-Doppler flowmetry. Starting from a baseline skin temperature of 33°C, the skin is rapidly heated at a rate of $3°C \cdot min^{-1}$ up to 42°C and held at that temperature for 30-35 min. The rapid local heating protocol initiates a biphasic increase in skin blood flow starting with an initial peak, which is highlighted in blue, followed by a brief nadir, and then rising again to form a delayed plateau phase, highlighted in green. This is followed by increasing the skin temperature to 44°C, highlighted in purple, which is held for an additional 20 min.

4.9 References

Johnson JM, Taylor WF, Shepherd AP & Park MK. (1984). Laser-Doppler measurement of skin blood flow - comparison with plethysmography. *Journal of Applied Physiology* **56,** 798-803.

Ramanathan NL. (1964). New weighting system for mean surface temperature of human body. *Journal of Applied Physiology* **19,** 531-&.

Saumet JL, Kellogg DL, Taylor WF & Johnson JM. (1988). Cutaneous laser-Doppler flowmetry - Influence of underlying muscle blood flow. *Journal of Applied Physiology* **65,** 478-481.

van Belle G. (2008). *Statistical rules of thumb*. Wiley, Hoboken, NJ.

Chapter 5: Between-day reliability of cutaneous thermal hyperaemia in non-glabrous and glabrous skin of the index finger using single point laser-Doppler

5.1 Introduction

Laser-Doppler flowmetry (LDF) is a commonly used, non-invasive, optical technique that provides an index of skin blood flow (Johnson *et al.*, 1984; Saumet *et al.*, 1988). When combined with reactivity tests and/or pharmacological interventions, LDF allows for a detailed functional and mechanistic examination of the cutaneous microcirculation in humans (Roustit & Cracowski, 2013). Local heating of the skin generates a biphasic response that allows for an integrative assessment of neurovascular and endothelial function (Johnson *et al.*, 2014). In both non-glabrous and glabrous skin, an initial vasodilatory peak occurs that is primarily mediated by sensory nerves (Minson *et al.*, 2001; Roustit *et al.*, 2008a), with noradrenergic fibres also involved in modulating the response (Wilson *et al.*, 2005; Hodges *et al.*, 2008, 2009). During sustained local heating, a plateau develops in non-glabrous skin that is controlled primarily by NO (Minson *et al.*, 2001). Conversely, in glabrous skin a plateau does not always develop during sustained local heating, which may indicate less of a reliance on NO in this skin type (Roustit *et al.*, 2010a; Metzler-Wilson *et al.*, 2012).

To date, only one study has evaluated the reliability of the local thermal hyperaemia (LTH) response in glabrous skin of the finger pad, demonstrating superior between-day reliability for the initial peak compared to non-glabrous skin of the forearm using single-point LDF (Roustit *et al.*, 2010a). The smaller surface area of the digit may reduce the influence of spatial variation of microvessels relative to that in the forearm, which could be a contributing factor in the superior reliability previously observed. However, glabrous skin blood flow is also known to be highly variable under normothermic conditions, which has been linked to its role in thermoregulation, and is likely due to frequent bursts of efferent sympathetic vasoconstrictor activity regulating the large number of AVAs in this skin type

(Taylor *et al.*, 2014). This observation, combined with specific methodological issues with the LTH protocol in the study by Roustit *et al.* (2010a), suggests that the reliability may not actually be higher in glabrous skin of the finger pad.

In addition, it does not appear that any study has evaluated LTH reliability in the non-glabrous skin covering the dorsal aspect of the hand and fingers. The close proximity on either side of the finger may allow for a more meaningful direct comparison of the axon reflex response between non-glabrous and glabrous skin during LTH under various experimental conditions since the confounding influence of fluctuations in ambient temperature, which typically has a greater effect on blood flow and skin temperature in the digits than the forearm (Roustit *et al.*, 2010a), is likely to have a comparable effect in both skin types on the finger.

As such, the primary objective of the current study was to examine the between-day reliability for the different phases of the cutaneous LTH response in the non-glabrous and glabrous skin of the index finger using single-point LDF for several common forms of LDF data expression in both skin types. It was hypothesized that between-day reliability for the LTH response in the index finger would be better in non-glabrous skin than in glabrous skin. It was further hypothesized that expressing the data as $\%CVC_{44}$ would be the most reliable form of data expression in both skin types, and that expressing the data as raw CVC would produce more accurate results than those previously demonstrated in the forearm.

5.2 Methods

5.2.1 Participants

Ten healthy, recreationally active males (26.2 ± 5.4 y, 178.2 ± 7.4 cm, 81.8 ± 13.2 kg) volunteered for the current study and reported to the laboratory for two experimental sessions.

5.2.2 Experimental Protocol

Following the pre-experimental procedures described in *Section 4.4*, participants rested quietly in the temperature-controlled room for ~30 min prior to the start of data collection while being instrumented, including the placement of one

LDF probe on the volar surface of the distal phalanx (finger pad) of the index finger and another on the middle phalanx on the dorsal side of the finger as previously described in *Section 4.6*. The local heating disc temperature was then set to 33°C for both probes and baseline measurements were recorded for ~20 min to ensure stable LDF and skin temperature values. At this point, the local heating disc temperature on both probes was increased according to the LTH protocol described in *Section 4.8*. The experiment was repeated ~7-14 days later.

5.2.3 Data Processing

Measurement regions of the LTH protocol were defined as previously described in *Section 4.8*. Representative LDF tracings of the LTH protocol for non-glabrous and glabrous skin sites with measurement time points clearly indicated are presented in Figure 5.1. The LDF data were presented in six forms for comparison:

- Raw APU;
- APU normalized to baseline ($\%APU_{BL}$: $[(APU \cdot\ baseline\ APU^{-1}) \cdot 100]$);
- APU normalized to maximum heating at 44°C ($\%APU_{44}$: $[(APU \cdot maximum\ APU^{-1}) \cdot 100]$);
- Raw cutaneous vascular conductance (CVC), whereby the raw LDF output (APU) was divided by MAP to give CVC as $APU \cdot mmHg^{-1}$;
- CVC normalized to baseline ($\%CVC_{BL}$: $[(CVC \cdot\ baseline\ CVC^{-1}) \cdot 100]$);
- CVC normalized to maximum heating at 44°C ($\%CVC_{44}$: $[(CVC \cdot maximum\ CVC^{-1}) \cdot 100]$).

5.2.4 Statistical Analysis

All outcome measures were normally distributed. The data were considered to be normally distributed when visual examination of Q-Q plots and frequency histograms indicated that they followed a Gaussian distribution, combined with skewness values <±3 and kurtosis values <±8 (Kline, 2005). Changes in the mean between conditions were assessed using paired t-tests. Statistical significance was set at $p<0.05$. Data were expressed as mean (SD) unless otherwise stated.

A comprehensive reliability assessment was performed for all paired conditions by examining 1) changes in the mean to identify the presence of systematic error between trials, 2) the coefficient of variation (%CV) to examine within-subject variation (typical error) between trials, and 3) the intraclass correlation coefficient (ICC), to examine the consistency of an individual's relative position (rank) in the group between trials.

Prior to calculating the %CV and ICC values, a natural logarithmic transformation was applied to all data sets in order to correct for heteroscedasticity (Hopkins *et al.*, 2009; Smith & Hopkins, 2011). Subsequently, it was confirmed that all paired differences remained normally distributed following the log transformation.

The %CV values were then calculated using the root mean square method. Specifically, a two-way repeated measures ANOVA was performed, whereby the within-subjects *Trials* and *Error* terms were cast as separate sources of variance in the model. The square root of the mean squared (within-subjects) error term was subsequently calculated. The 95% confidence intervals (CI) for these values were then constructed from the χ^2 distribution. To convert the %CV and 95% CIs from the log transformed values to exact percentages, the antilogs of these values were calculated according to the following equation:

$$Antilog(x) = 100 \cdot \left(e^{\sqrt{x}} - 1\right)$$

%CV values of <10%, 10-25%, and >25% were considered to represent good, moderate, and poor reliability, respectively (Iellamo *et al.*, 1996; Tew *et al.*, 2011).

The ICC values and associated 95% CIs were calculated from the same repeated measures two-way ANOVA used to assess the %CV. Specifically, a two-way mixed (consistency) model was used for the ICC calculation, according to the classification system of McGraw and Wong (1996), which is consistent with the calculation for the ICC (3,1) model described by Shrout and Fleiss (1979). This model was chosen since it represents the observed correlation of measurements between any two real life trials (Hopkins, 2015), and since it is unbiased by sample size, it is also most closely aligned with the mean squared error term from the

ANOVA used to derive the %CV (Weir, 2005). The equation for the ICC (3,1) model is as follows:

$$ICC = \frac{MS_S - MS_E}{MS_S + (k-1)MS_E}$$

where MS_S = subjects mean square; MS_E = error mean square; k = trials

ICC values of <0.40, 0.40-0.75, >0.75 were considered to represent poor, fair-to-good, and excellent reliability, respectively (Landis & Koch, 1977; Tew *et al.*, 2011). All statistics were performed using SPSS Statistics 22.0 (IBM Corp., Armonk, NY, USA).

5.3 Results

There were no significant differences in temperature and haemodynamic indices between trials (Table 5.1). Between-day reliability results for each LTH phase are presented for non-glabrous skin in Table 5.2 and glabrous skin in Table 5.3. Reliability data for the kinetics of the response are presented in Table 5.4.

Mean differences

In non-glabrous skin, systematic changes in the mean were evident at baseline when data were normalized to maximal heating ($\%APU_{44}$, $\%CVC_{44}$), with the mean being significantly higher during the second testing session. Conversely, no systematic changes were evident in non-glabrous skin at baseline when data were expressed as either raw APU or CVC.

For all other measurement regions, systematic changes in the mean were present in non-glabrous skin when data were expressed as either $\%APU_{BL}$ or $\%CVC_{BL}$, with the means being consistently higher during the first testing session. No systematic changes in the mean were present in non-glabrous skin for any other form of data expression. Conversely, in glabrous skin, there were no systematic changes in the mean for any measurement region, regardless of the form of data expression.

When examining the kinetics of the local heating response, there were no systematic changes in the mean for the time to vasodilatory onset, or the time to initial peak in either non-glabrous or glabrous skin sites.

Coefficients of variation

At baseline, %CV values in non-glabrous skin were rated as moderate when data were normalized to maximum heating (CV=22.7% for $\%APU_{44}$ and $\%CVC_{44}$), and poor when expressed as either raw APU or CVC. In glabrous skin, baseline %CV values were rated as poor for all forms of data expression.

At the initial vasodilatory peak, %CV values in non-glabrous skin were rated as good when data were expressed as $\%APU_{44}$ and $\%CVC_{44}$ (%CV=8.1% and 8.0%, respectively), and moderate to poor (%CV=21.8% to 27.5%) for all other forms of data expression. In glabrous skin, %CV values were rated as moderate (%CV=15.2% to 19.6%) for most forms of data expression, with the exception of $\%APU_{BL}$ and $\%CVC_{BL}$, which were both rated as poor.

At the plateau, %CV values in non-glabrous skin were rated as good when data were expressed as $\%APU_{44}$ and $\%CVC_{44}$ (%CV=8.7% for both), and moderate to poor (%CV=24.8% to 31.0%) for all other forms of data expression. Similarly, in glabrous skin, CV values were rated as good when data were expressed as $\%APU_{44}$ and $\%CVC_{44}$ (%CV=8.0% and 10.0%, respectively), and moderate to poor (%CV=23.4% to 32.0%) for all other forms of data expression.

At maximum heating to 44°C, CV values in non-glabrous skin were rated as moderate (%CV=21.8% to 24.2%) for all forms of data expression. Conversely, in glabrous skin, %CV values were primarily rated as poor, with the exception of raw APU (%CV=21.2%), which was rated as moderate.

When examining the kinetics of the local heating response in non-glabrous and glabrous skin, %CV values were rated as moderate for vasodilatory onset time and the time to initial peak.

Intraclass correlation coefficients

In general, ICC values were higher in non-glabrous than in glabrous skin. In non-glabrous skin at baseline, all ICC values were rated as fair-to-good (ICC=0.56 to 0.65). In glabrous skin at baseline, ICC values for $\%APU_{44}$ and $\%CVC_{44}$ were rated as fair-to-good and raw APU, and CVC values were rated as poor.

At the initial vasodilatory peak, in non-glabrous skin, ICC values were primarily rated as excellent (ICC=0.75-0.81), with the exception of $\%APU_{BL}$ and

$\%CVC_{BL}$, which were both rated as fair-to-good. In glabrous skin, ICC values were primarily rated as fair-to-good (ICC=0.40-0.54), with the exception of APU and CVC, which were both rated as poor.

At the plateau, in non-glabrous skin, ICC values were rated as excellent for APU (ICC=0.76) and CVC (ICC=0.77), and fair-to-good to poor (ICC=0.37 to 0.45) for all other forms of data expression. In glabrous skin at the plateau, ICC values were primarily rated as moderate (ICC=0.48 to 0.60), with the exception of raw APU and CVC, which were both rated as poor.

At maximum heating to 44°C in non-glabrous skin, ICC values were generally rated as excellent (ICC=0.71 to 0.75) for all forms of data expression. In contrast, at maximum heating in glabrous skin, ICC values were only rated as fair-to-good for $\%APU_{BL}$ (ICC=0.58) and $\%CVC_{BL}$ (ICC=0.56), and poor for APU and CVC.

When examining the kinetics of the local heating response in non-glabrous skin, the ICC value for the vasodilatory onset time was rated as fair-to-good (ICC=0.53), while all other ICC values for both skin types were rated as poor for the vasodilatory onset time and the time to initial peak.

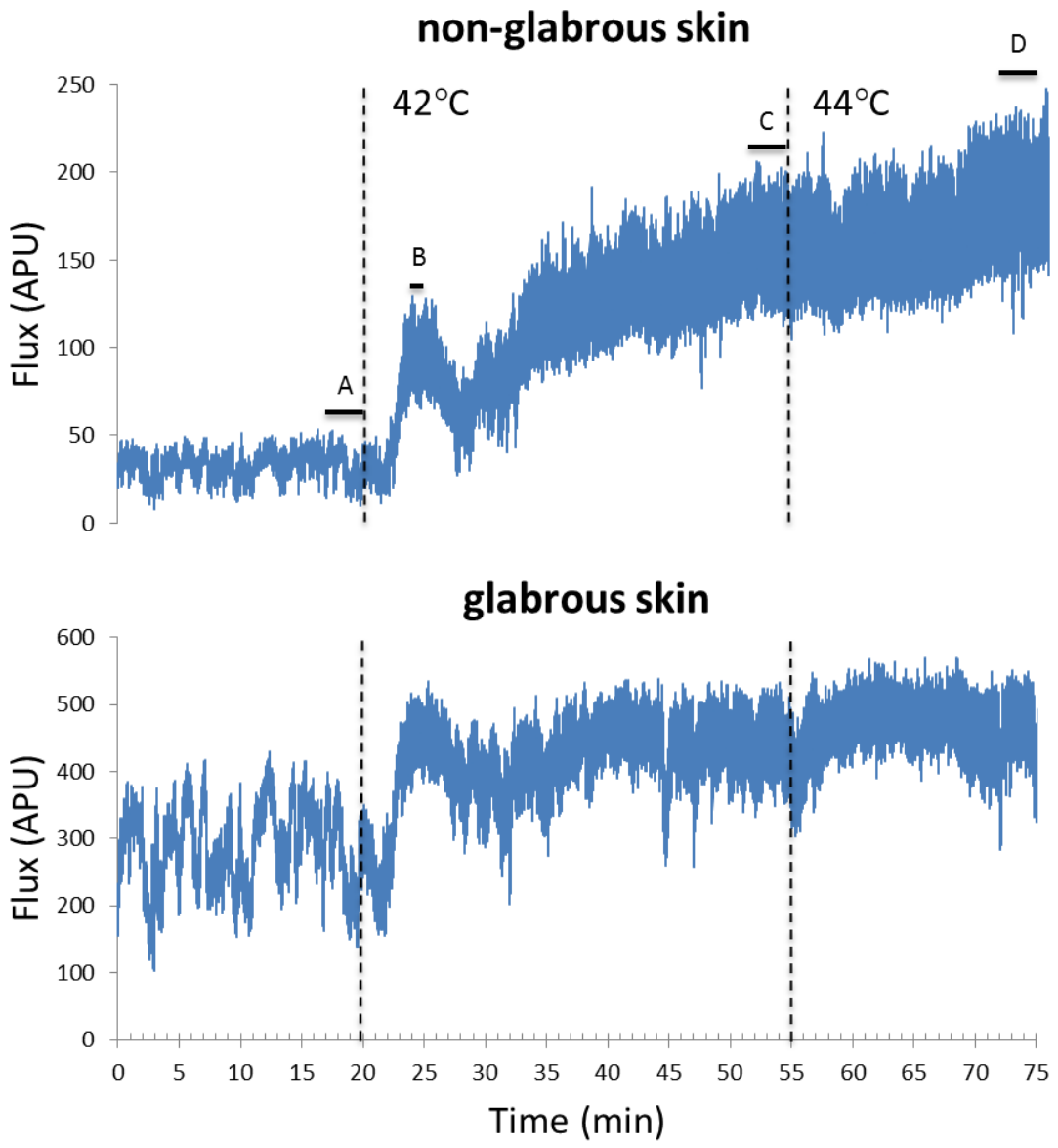

Figure 5.1 Representative cutaneous thermal hyperaemia response during local heating in non glabrous and glabrous skin

Dashed vertical lines represent a change in local LDF probe temperature. A, baseline; B, initial vasodilatory peak; C, plateau; D, maximum heating.

Table 5.1 Between-day temperature and haemodynamic conditions at the start of LTH

	Day-1	**Day-2**	**(Day-2 – Day-1)**
	Mean (SD)	Mean (SD)	$Mean_{diff}$ [95%CI]
Temperatures			
T_{amb} (°C)	25.15 (0.13)	25.18 (0.16)	0.03 [-0.07, 0.13], p=0.49
T_f: glabrous (°C)	32.4 (3.8)	33.1 (3.8)	0.7 [-1.4, 2.8], p=0.48
T_f: non-glabrous (°C)	31.5 (3.3)	32.5 (2.9)	1.0 [-0.6, 2.6], p=0.20
$\bar{T}_{sk}$ (°C)	32.7 (0.5)	33.1 (0.6)	0.4 [-0.2, 0.9], p=0.16
Haemodynamics			
HR (bpm)	55.3 (5.4)	56.9 (8.5)	1.6 [-2.8, 6.0], p=0.43
MAP (mmHg)	88.7 (9.7)	88.1 (10.8)	-0.6 [-7.2, 6.0], p=0.84
S_aO_2 (%)	97.1 (1.3)	96.6 (1.2)	-0.5 [-1.5, 0.5], p=0.27

*Significance was set to p<0.05. SD, standard deviation; CI, confidence interval; $Mean_{diff}$, mean difference between trials; T_{amb}, ambient air temperature; T_f, finger skin temperature; $\bar{T}_{sk}$, mean skin temperature; HR, heart rate; MAP, mean arterial pressure; S_aO_2, arterial oxygen saturation. NOTE: For mean skin temperature, n=8 due to broken wiring; For S_aO_2 Saturation, n=9

Table 5.2 Between-day reliability of the local heating response in non-glabrous skin

		Mean$_{diff}$	**CV (%)**	**ICC**
Baseline	APU	8.2 (-7.0, 23.3)	33.6 (22.1, 69.9)	0.64 (0.06, 0.90)
	APU$_{\%BL}$	---	---	---
	APU$_{\%44}$	5.8 (0.4, 11.2)*	22.7 (15.0, 44.8)	0.56 (-0.06, 0.87)
	CVC	0.1 (-0.1, 0.3)	33.4 (22.1, 69.9)	0.65 (0.08, 0.90)
	CVC$_{\%BL}$	---	---	---
	CVC$_{\%44}$	6.9 (0.9, 12.9)*	22.7 (15.0, 44.8)	0.57 (-0.49, 0.87)
Initial Peak	APU	-34.0 (-89.6, 21.6)	27.5 (18.5, 55.3)	0.75 (0.27, 0.93)
	APU$_{\%BL}$	-95.5 (-176.3, -14.6)*	21.8 (15.0, 43.3)	0.44 (-0.22, 0.83)
	APU$_{\%44}$	-0.3 (-6.2, 5.6)	8.1 (5.4, 15.0)	0.78 (0.337, 0.94)
	CVC	-0.4 (-1.1, 0.3)	25.6 (17.4, 52.2)	0.78 (0.34, 0.94)
	CVC$_{\%BL}$	-95.5 (-176.3, -14.6)*	21.8 (15.0, 43.3)	0.44 (-0.22, 0.83)
	CVC$_{\%44}$	2.8 (-3.8, 9.4)	8.0 (5.4, 15.0)	0.81 (0.42, 0.95)
Plateau	APU	-37.2 (-94.0, 19.7)	24.8 (16.2, 49.2)	0.76 (0.29, 0.94)
	APU$_{\%BL}$	-113.3 (-212.7, -13.8)*	29.3 (19.7, 60.0)	0.45 (-0.21, 0.83)
	APU$_{\%44}$	-2.5 (-9.1, 4.1)	8.7 (6.0, 16.2)	0.43 (-0.24, 0.82)
	CVC	-0.5 (-1.2, 0.3)	25.3 (17.4, 50.7)	0.77 (0.31, 0.94)
	CVC$_{\%BL}$	-117.8 (-224.9, -10.8)*	31.0 (20.9, 63.2)	0.38 (-0.29, 0.80)
	CVC$_{\%44}$	-1.4 (-8.6, 5.9)	8.7 (6.0, 16.2)	0.37 (-0.30, 0.79)
Heat-44	APU	-35.4 (-93.1, 22.3)	21.8 (15.0, 43.3)	0.75 (0.26, 0.93)
	APU$_{\%BL}$	-124.4 (-216.2, -32.6)*	22.7 (15.0, 44.8)	0.71 (0.19, 0.92)
	APU$_{\%44}$	---	---	---
	CVC	-0.5 (-1.3, 0.4)	24.2 (16.2, 49.2)	0.74 (0.26, 0.93)
	CVC$_{\%BL}$	-139.8 (-225.8, -53.9)*	22.7 (15.0, 44.8)	0.74 (0.24, 0.93)
	CVC$_{\%44}$	---	---	---

*Significance set at $p<0.05$. Brackets represent 95% confidence limits. Mean$_{diff}$, mean difference between trials; CV, coefficient of variation; ICC, intraclass correlation coefficient; APU, arbitrary perfusion units; APU$_{\%BL}$, APU normalized to baseline; APU$_{\%44}$, APU normalized to maximum heating; CVC, cutaneous vascular conductance; CVC$_{\%BL}$, CVC normalized to baseline; CVC$_{\%44}$, CVC normalized to maximum heating. For %CV, dark-gray shading represents good reliability (%CV: <10%) and light-gray shading represents moderate reliability (%CV: 10-25%). For ICC, dark-gray shading represents excellent reliability (ICC: >0.75) and light-gray shading represents fair-to-good reliability (ICC: 0.40-0.75).

Table 5.3 Between-day reliability of the local heating response in glabrous skin

		$Mean_{diff}$	CV (%)	ICC
	APU	14.9 (-64.4, 94.2)	44.2 (28.4, 95.4)	0.36 (-0.31, 0.79)
	$APU_{\%BL}$	---	---	---
	$APU_{\%44}$	2.6 (-16.8, 22.0)	34.3 (22.1, 71.6)	0.58 (-0.04, 0.88)
	CVC	0.3 (-0.6, 1.2)	44.9 (29.7, 97.4)	0.39 (-0.28, 0.80)
	$CVC_{\%BL}$	---	---	---
	$CVC_{\%44}$	5.3 (-16.2, 26.9)	36.5 (23.4, 76.8)	0.56 (-0.06, 0.87)
Initial Peak	APU	-49.6 (-115.3, 16.2)	16.4 (10.5, 32.3)	0.06 (-0.56, 0.64)
	$APU_{\%BL}$	-23.4 (-98.1, 51.3)	30.5 (19.7, 63.2)	0.51 (-0.14, 0.85)
	$APU_{\%44}$	-14.7 (-32.8, 3.3)	15.2 (10.2, 29.7)	0.46 (-0.19, 0.83)
	CVC	-0.4 (-1.3, 0.5)	19.6 (12.7, 39.1)	0.01 (-0.60, 0.61)
	$CVC_{\%BL}$	-23.4 (-98.1, 51.3)	30.5 (19.7, 60.0)	0.54 (-0.10, 0.86)
	$CVC_{\%44}$	-11.1 (-32.1, 9.8)	17.9 (11.6, 35.0)	0.40 (-0.27, 0.81)
Plateau	APU	-22.5 (-103.6, 58.6)	23.4 (15.0, 46.2)	-0.03 (-0.62, 0.58)
	$APU_{\%BL}$	-7.5 (-65.1, 50.1)	28.8 (18.5, 58.4)	0.54 (-0.10, 0.86)
	$APU_{\%44}$	-4.6 (-12.5, 3.3)	8.0 (5.4, 15.0)	0.60 (-0.002, 0.88)
	CVC	-0.2 (-1.2, 0.7)	24.2 (16.2, 49.2)	-0.01 (-0.61, 0.59)
	$CVC_{\%BL}$	-9.7 (-70.3, 51.0)	32.0 (20.9, 66.5)	0.48 (-0.17, 0.84)
	$CVC_{\%44}$	-3.4 (-12.8, 6.0)	10.0 (6.7, 18.5)	0.56 (-0.06, 0.87)
Heat-44	APU	-9.6 (-90.4, 71.2)	21.2 (13.9, 41.9)	0.09 (-0.54, 0.65)
	$APU_{\%BL}$	-0.1 (-65.6, 65.5)	34.3 (22.1, 71.6)	0.58 (-0.04, 0.88)
	$APU_{\%44}$	---	---	---
	CVC	-0.2 (-1.4, 1.0)	27.5 (18.5, 55.3)	0.07 (-0.55, 0.65)
	$CVC_{\%BL}$	-7.2 (-69.8, 55.4)	36.5 (23.4, 76.8)	0.56 (-0.06, 0.87)
	$CVC_{\%44}$	---	---	---

*Significance set at $p<0.05$. Brackets represent 95% confidence limits. $Mean_{diff}$, mean difference between trials; CV, coefficient of variation; ICC, intraclass correlation coefficient; APU, arbitrary perfusion units; $APU_{\%BL}$, APU normalized to baseline; $APU_{\%44}$, APU normalized to maximum heating; CVC, cutaneous vascular conductance; $CVC_{\%BL}$, CVC normalized to baseline; $CVC_{\%44}$, CVC normalized to maximum heating. For %CV, dark-gray shading represents good reliability (%CV: <10%) and light-gray shading represents moderate reliability (%CV: 10-25%). For ICC, dark-gray shading represents excellent reliability (ICC: >0.75) and light-gray shading represents fair-to-good reliability (ICC: 0.40-0.75).

Table 5.4 Between-day reliability of local heating kinetics in non-glabrous and glabrous skin

	Mean$_{diff}$	**CV (%)**	**ICC**
Vasodilatory onset (s)			
Non-glabrous	-3.01 (-14.6, 8.15)	10.5 (7.1, 19.7)	0.53 (-0.11, 0.86)
Glabrous	14.73 (-12.34, 41.79)	23.3 (15.0, 46.2)	0.35 (-0.32, 0.78)
Time to initial peak (s)			
Non-glabrous	19.06 (-13.42, 51.54)	13.0 (8.8, 24.6)	-0.18 (-0.71, 0.47)
Glabrous	9.55 (-21.68, 40.78)	13.0 (8.8, 24.6)	0.28 (-0.38, 0.76)

*Significance set at $p<0.05$. Brackets represent 95% confidence limits. Mean$_{diff}$, mean difference between trials; CV, coefficient of variation; ICC, intraclass correlation coefficient. For %CV, dark-gray shading represents good reliability (%CV: <10%) and light-gray shading represents moderate reliability (%CV: 10-25%). For ICC, dark-gray shading represents excellent reliability (ICC: >0.75) and light-gray shading represents fair-to-good reliability (ICC: 0.40-0.75).

5.4 Discussion

In the present study, reliability assessments demonstrated equivalent results between LDF data in original units (APU) and when corrected for blood pressure (CVC), with data presented as raw values or when normalized to either baseline or maximum heating. For clarity and consistency with previous reliability studies, only the results from CVC data will be discussed further below.

The cutaneous LTH response for both skin types demonstrated good to moderate between-day reliability for the initial vasodilatory peak and plateau phases when data were expressed as a percentage of maximum, moderate reliability when data were expressed as raw CVC, and poor reliability when data were expressed as a percentage of baseline when using single-point LDF in a group of young, healthy males. In addition, vasodilatory onset time and the time to initial peak both demonstrated moderate between-day reliability in both skin types.

Basal skin blood flow is known to exhibit significant spatial and temporal variability in the forearm (Braverman, 1997), which contributes to poor reliability of baseline measurements (Roustit *et al.*, 2010a; Roustit *et al.*, 2010b). Variation in basal flow appears to be even greater on the finger pad (Roustit *et al.*, 2010a), likely due to the presence of AVAs, which are heavily influenced by tonic bursts of sympathetic vasoconstrictor activity, a characteristic that is consistent with their role in thermoregulatory vasoconstriction and blood pressure control (Daanen, 2003; Taylor *et al.*, 2014). In support of this, Roustit *et al.* (2010a) demonstrated that room temperature had a significant influence on baseline skin blood flow on the finger pad of the index finger. However, since local skin temperature was not controlled at baseline, the authors speculated that this lack of control may have also contributed to poor baseline reliability using single-point LDF in the finger. To address these concerns, both local skin temperature (33°C) and room temperature (25°C) were tightly controlled at baseline in the current study in an attempt to minimize fluctuations in basal perfusion. Despite these steps, baseline reliability remained poor in the glabrous skin for all forms of data expression, and poor in the non-glabrous skin when data were expressed as raw values. Conversely, baseline

perfusion did demonstrate moderate reliability in non-glabrous skin of the index finger when data were expressed as a percentage of maximum.

The influence of spatial variation on LTH reliability has not previously been examined when using single-point LDF on the finger pad since probe positioning is less variable here due to the smaller surface area of the digit (Roustit *et al.*, 2010a). Other techniques that address spatial variability, such as integrating-probe LDF, have not been used on the finger to examine the LTH response since these laser-Doppler probes are too large for these sites. Furthermore, full-field techniques, such as laser speckle contrast imaging (LSCI) and laser-Doppler imaging (LDI), are also problematic for examining cutaneous LTH on the finger since the heating units for these imagers are generally too large for the digit.

Roustit *et al.* (2010a) attributed the superior reliability they observed on the finger pad relative to that in the forearm to lower capillary heterogeneity at this location, in contrast to the well-documented spatial variation previously observed in the forearm skin (Braverman & Schechner, 1991; Braverman *et al.*, 1992; Wardell *et al.*, 1994). In support of this assertion, corrosion casting of the cutaneous vasculature from a cadaver finger has revealed that cutaneous microvessels in the papillary layer are uniformly distributed on the finger pad with two parallel rows of vessels that follow the patterning of the fingerprint (Sangiorgi *et al.*, 2004).

Unlike the glabrous skin found on the palm and volar aspect of the fingers, skin on the dorsal aspect of the hand and fingers is more consistent in both form and function with the non-glabrous skin of the forearm. Indeed, Johnson *et al.* (1995) demonstrated that skin here possesses an active cutaneous vasodilator system, like that seen in the non-glabrous skin of the forearm and most other body regions (Braverman, 1997; Johnson *et al.*, 2014). The dorsal skin covering the middle phalanges is also largely devoid of AVAs, which is in contrast to the dorsal skin of the distal phalanx (nail bed), and volar skin of the finger pad, where AVAs are abundant (Taylor *et al.*, 2014). The microvascular organization on the dorsal side of the finger is also characterized by greater spatial heterogeneity, similar to that observed in the forearm (Sangiorgi *et al.*, 2004). Despite the problem with spatial heterogeneity in non-glabrous skin of the forearm and finger, the lack of influence

from cyclical AVA vasoconstriction (Taylor *et al.*, 2014) and the relative complexity of neural and metabolic control over microvascular function in this skin type (Johnson *et al.*, 2014) may have contributed to more consistent responses to heating-induced vasodilatation, resulting in greater reliability over that of glabrous skin.

Overall, normalizing the data to a percentage of maximum CVC produced the most reliable results. The rationale for using this approach is that when maximal vasodilatation is produced, resistance vessels will be completely relaxed. As such, all measurement sites will theoretically have the same vasomotor tone under these conditions so changes relative to the maximum CVC can be meaningfully compared among different sites (Johnson *et al.*, 2014). Although this approach is commonly used to avoid the issue of spatial heterogeneity in the non-glabrous skin of the forearm, it is not necessarily appropriate to normalize data to maximum when comparing groups that may have different maximal heating responses, such as healthy controls versus diabetic or hypertensive patients with microvascular impairments. This approach is also not appropriate in longitudinal studies where functional and/or structural changes may be expected over time, such as during exercise training or following tissue injury.

Normalizing to maximum heating at 44°C has been used previously when examining glabrous skin (Roustit *et al.*, 2008b). However, it has since been demonstrated that this approach does not necessarily induce maximum vasodilatation in this skin type (Roustit *et al.*, 2010a; Metzler-Wilson *et al.*, 2012). Indeed, in the current study, local skin heating to 44°C for 20 minutes failed to produce maximum CVC values in 13 out of the 20 cutaneous LTH tests performed on the finger pad. As such, even though normalizing to maximum heating at 44°C provided similar reliability results with raw CVC values, the current findings, combined with those from previous work mentioned above, call into question the validity of using this form of data expression in glabrous skin.

In the current study, ICC values were generally rated as excellent or fair-to-good for non-glabrous skin of the index finger at all measurement points when data were expressed as either raw CVC or $\%CVC_{44}$. This is in contrast to the glabrous skin

of the finger pad, where ICC values were generally rated as either fair-to-good or poor. The smaller %CV values reported for the non-glabrous skin relative to those in glabrous skin indicate that the higher ICC values may be due to smaller within-subject variation in this skin type (Weir, 2005).

Conclusion

Examining the cutaneous response to local heating is reliable in both the non-glabrous and glabrous skin of the index finger when using single-point LDF. The present study demonstrated that between-day reliability for non-glabrous skin was generally greater than that of glabrous skin in the index finger. In both skin types reliability was typically moderate when data were expressed as raw CVC. Expressing data as a percentage of maximum demonstrated good reliability for non-glabrous skin and good to moderate reliability for glabrous skin. However, the validity of this approach for glabrous skin is questionable. In addition, examining the kinetics of the response demonstrated moderate between-day reliability for both skin types.

5.5 References

Braverman IM. (1997). The cutaneous microcirculation: Ultrastructure and microanatomical organization. *Microcirculation-London* **4,** 329-340.

Braverman IM & Schechner JS. (1991). Contour mapping of the cutaneous microvasculature by computerized laser doppler velocimetry. *J Invest Dermatol* **97,** 1013-1018.

Braverman IM, Schechner JS, Silverman DG & Kehyen A. (1992). Topographic mapping of the cutaneous microcirculation using 2 outputs of laser-Doppler flowmetry - flux and the concentration of moving blood cells. *Microvascular Research* **44,** 33-48.

Daanen HA. (2003). Finger cold-induced vasodilation: a review. *Eur J Appl Physiol* **89,** 411-426.

Hodges GJ, Kosiba WA, Zhao K & Johnson JM. (2008). The involvement of norepinephrine, neuropeptide Y, and nitric oxide in the cutaneous vasodilator response to local heating in humans. *Journal of Applied Physiology* **105,** 233-240.

Hodges GJ, Kosiba WA, Zhao K & Johnson JM. (2009). The involvement of heating rate and vasoconstrictor nerves in the cutaneous vasodilator response to skin warming. *Am J Physiol-Heart Circul Physiol* **296,** H51-H56.

Hopkins WG. (2015). Spreadsheets for Analysis of Validity and Reliability. *Sportscience* **19,** 36-44.

Hopkins WG, Marshall SW, Batterham AM & Hanin J. (2009). Progressive Statistics for Studies in Sports Medicine and Exercise Science. *Med Sci Sports Exerc* **41,** 3-12.

Iellamo F, Legramante JM, Raimondi G, Castrucci F, Massaro M & Peruzzi G. (1996). Evaluation of reproducibility of spontaneous baroreflex sensitivity at rest and during laboratory tests. *J Hypertens* **14,** 1099-1104.

Johnson JM, Minson CT & Kellogg DL. (2014). Cutaneous Vasodilator and Vasoconstrictor Mechanisms in Temperature Regulation. *Compr Physiol* **4,** 33-89.

Johnson JM, Pergola PE, Liao FK, Kellogg DL & Crandall CG. (1995). Skin of the dorsal aspect of human hands and fingers possesses an active vasodilator system. *Journal of Applied Physiology* **78,** 948-954.

Johnson JM, Taylor WF, Shepherd AP & Park MK. (1984). Laser-Doppler measurement of skin blood flow - comparison with plethysmography. *Journal of Applied Physiology* **56,** 798-803.

Kline RB. (2005). *Principles and Practice of Structural Equation Modeling*. The Guilford Press, New York.

Landis JR & Koch GG. (1977). Measurement of observer agreement for categorical data. *Biometrics* **33,** 159-174.

McGraw KO & Wong SP. (1996). Forming inferences about some intraclass correlation coefficients. *Psychol Methods* **1,** 30-46.

Metzler-Wilson K, Kellie LA, Tomc C, Simpson C, Sammons D & Wilson TE. (2012). Differential vasodilatory responses to local heating in facial, glabrous and hairy skin. *Clin Physiol Funct Imaging* **32,** 361-366.

Minson CT, Berry LT & Joyner MJ. (2001). Nitric oxide and neurally mediated regulation of skin blood flow during local heating. *Journal of Applied Physiology* **91,** 1619-1626.

Roustit M, Blaise S, Millet C & Cracowski JL. (2010a). Reproducibility and methodological issues of skin post-occlusive and thermal hyperemia

assessed by single-point laser Doppler flowmetry. *Microvascular Research* **79,** 102-108.

Roustit M & Cracowski JL. (2013). Assessment of endothelial and neurovascular function in human skin microcirculation. *Trends Pharmacol Sci* **34,** 373-384.

Roustit M, Millet C, Blaise S, Dufournet B & Cracowski JL. (2010b). Excellent reproducibility of laser speckle contrast imaging to assess skin microvascular reactivity. *Microvasc Res* **80,** 505-511.

Roustit M, Simmons G, Carpentier P & Cracowski JL. (2008a). Abnormal digital neurovascular response to local heating in systemic sclerosis. *Fundam Clin Pharmacol* **22,** 90-90.

Roustit M, Simmons GH, Carpentier P & Cracowski JL. (2008b). Abnormal digital neurovascular response to local heating in systemic sclerosis. *Rheumatology (Oxford)* **47,** 860-864.

Sangiorgi S, Manelli A, Congiu T, Bini A, Pilato G, Reguzzoni M & Raspanti M. (2004). Microvascularization of the human digit as studied by corrosion casting. *J Anat* **204,** 123-131.

Saumet JL, Kellogg DL, Taylor WF & Johnson JM. (1988). Cutaneous laser-Doppler flowmetry - Influence of underlying muscle blood flow. *Journal of Applied Physiology* **65,** 478-481.

Shrout PE & Fleiss JL. (1979). Intraclass correlations - Uses in assessing rater reliability. *Psychol Bull* **86,** 420-428.

Smith TB & Hopkins WG. (2011). Variability and Predictability of Finals Times of Elite Rowers. *Med Sci Sports Exerc* **43,** 2155-2160.

Taylor NAS, Machado-Moreira CA, van den Heuvel AMJ & Caldwell JN. (2014). Hands and feet: physiological insulators, radiators and evaporators. *European Journal of Applied Physiology* **114,** 2037-2060.

Tew GA, Klonizakis M, Moss J, Ruddock AD, Saxton JM & Hodges GJ. (2011). Reproducibility of cutaneous thermal hyperaemia assessed by laser Doppler flowmetry in young and older adults. *Microvasc Res* **81,** 177-182.

Wardell K, Braverman IM, Silverman DG & Nilsson GE. (1994). Spatial heterogeneity in normal skin perfusion recorded with laser-Doppler imaging and flowmetry. *Microvascular Research* **48,** 26-38.

Weir JP. (2005). Quantifying test-retest reliability using the intraclass correlation coefficient and the SEM. *J Strength Cond Res* **19,** 231-240.

Wilson TE, Zhang R, Levine BD & Crandall CG. (2005). Dynamic autoregulation of cutaneous circulation: differential control in glabrous versus nonglabrous skin. *Am J Physiol Heart Circ Physiol* **289,** H385-391.

Chapter 6: Influence of upper limb ischaemia-reperfusion on sensory nerve responses to local skin heating in glabrous and non-glabrous skin of the index finger

6.1 Introduction

A hallmark of ischaemia-reperfusion (I-R) injury is acute endothelial damage and microcirculatory dysfunction due to the rapid production of reactive oxygen species (ROS) at the onset of reperfusion, which reduces nitric oxide (NO) bioavailability and ultimately impairs microvascular dilatory capacity (Harrison, 1997; Granger, 1999; Carden & Granger, 2000). In addition, sensory nerves have been shown to play an important role in mediating blood flow and inflammation during reperfusion in a variety of animal models of I-R (Harada *et al.*, 2002; Turchanyi *et al.*, 2005; Wang & Wang, 2005; Mizutani *et al.*, 2009; Wang *et al.*, 2012; Ji *et al.*, 2013). Although sensory afferents promote blood flow through the consequent release of vasodilatory neuropeptides, including substance P (SP) and calcitonin gene-related peptide (CGRP) from their nerve endings (Ustinova *et al.*, 1995; Gherardini *et al.*, 1996; Harada *et al.*, 2002; Mizutani *et al.*, 2009), reperfusion is also associated with hyperpolarization of these nerves, resulting in elevated firing thresholds (Lin *et al.*, 2002). Furthermore, stimulation of neuropeptide receptors is known to render them desensitized to subsequent stimulation (Wong *et al.*, 2005; Wong & Minson, 2006, 2011), which in addition to the impaired NO bioavailability, can inhibit the response to a subsequent vasodilatory stimulus following I-R injury.

Local heating of the skin generates a biphasic response that allows for an integrative assessment of neurovascular and endothelial function (Johnson *et al.*, 2014). In both non-glabrous and glabrous skin, an initial vasodilatory peak occurs that is primarily mediated by sensory nerves (Minson *et al.*, 2001; Roustit *et al.*, 2008), with noradrenergic fibres also involved in modulating the response (Wilson *et al.*, 2005; Hodges *et al.*, 2008, 2009). During sustained local heating, a plateau develops in non-glabrous skin that is controlled primarily by NO (Kellogg *et al.*, 1999). Conversely, in glabrous skin, a plateau does not always develop during

sustained local heating, which may indicate less of a reliance on NO in this skin type (Roustit *et al.*, 2010; Metzler-Wilson *et al.*, 2012).

In humans, important differences in the morphology and neural input of the cutaneous microcirculation exist between non-glabrous and glabrous skin. Importantly, glabrous skin contains a higher density of sensory afferents than non-glabrous skin. In addition, resting blood flow is also greater due to the large number of AVAs, which are primarily under noradrenergic vasoconstrictor control (Wilson *et al.*, 2005; Taylor *et al.*, 2014). Conversely, non-glabrous skin is largely devoid of AVAs, and perfusion through nutritional capillary loops represents a greater proportion of total blood flow (Braverman, 1997). This skin type is also under dual sympathetic control, consisting of an adrenergic vasoconstrictor system as well as an active cholinergic vasodilator system (Johnson *et al.*, 2014).

Due to their close proximity to one another on the hand, non-glabrous and glabrous skin will both be influenced by exposure to a period of upper limb I-R, which may result in an impaired capacity for vasodilatation during subsequent local skin heating, although this has yet to be evaluated. The distinct anatomical and functional differences that are present between skin types also indicates that they may not be negatively affected by upper limb I-R to the same extent. As such, the purpose of the current study was to examine the influence of upper limb I-R injury on the response to local heating in non-glabrous and glabrous skin of the index finger. It was hypothesized that I-R injury would impair the initial vasodilatory peak, and therefore also the kinetics of the response in both skin types and the plateau phase in non-glabrous skin.

6.2 Methods

6.2.1 Participants

The same ten healthy, active males previously described in *Section 5.2.1* volunteered for this study.

6.2.2 Familiarization

Prior to the experiment, all participants completed a familiarization session. First, informed consent was obtained by the primary researcher as previously described in *Section 4.1*. Next, height (cm) and body mass (kg) were measured, after which each participant underwent a full 20 min forearm cuff occlusion and reperfusion. This was done to give all participants the opportunity to experience the discomfort associated with the procedure so they could decide if they were unable or unwilling to go through with the rest of the experiment. This was also done to minimize participant anxiety during the actual experiment to avoid the influence of undue psychological strain on physiological measurements. The procedure for cuff occlusion and reperfusion is described further in the following section.

6.2.3 Experimental Protocol

Following the familiarization session, participants took part in two counterbalanced experimental trials separated by ~7 days. One trial included a bout of upper limb I-R (ISCH) and the other was a time matched, non-ischaemia (SHAM) trial. All participants followed the pre-experimental procedures previously described in *Section 4.*4. Following this, each participant rested quietly in the temperature-controlled room for ~30 min prior to the start of data collection while being instrumented, including the placement of one LDF probe on the volar surface of the distal phalanx (finger pad) and another on the middle phalanx on the dorsal side of the index finger as previously described in *Section 4.6*. The local heating disc temperature was then set to 33°C for both probes and baseline measurements were recorded for ~20 min to ensure stable LDF and skin temperature values. During the ischaemia trial, a standard blood pressure cuff, which was placed around the upper arm, was quickly (<10 s) inflated to a pressure of 220 mmHg and held at that pressure for 20 min. The cuff was then rapidly deflated and the arm was allowed to reperfuse for 20 min, at which point the LTH protocol began as previously described in *Section 4.8*. The protocol for the SHAM trial was identical to that for the I-R trial, except for the fact that the cuff was not inflated.

6.2.4 Data processing and statistical analysis

All outcome measures were normally distributed. The data were considered to be normally distributed when visual examination of Q-Q plots and frequency histograms indicated that they followed a Gaussian distribution, with skewness values <±3 and kurtosis values <±8 (Kline, 2005). All data were analyzed using paired t-tests.

A natural logarithmic transformation was applied to all individual variables of the LTH response prior to analysis in order to reduce non-uniformity of error. Mean differences between trials (ISCH – SHAM) were assessed with paired t-tests. To make inferences about the true (population) value for the effects of I-R on individual variables, the uncertainty of each observed effect was expressed as 90% confidence limits and as likelihoods that the true value for the effect of I-R represented a substantial percentage change, in either the negative or positive direction, relative to the SHAM trial (Hopkins, 2002; Batterham & Hopkins, 2006). For the purpose of the current study, a positive change represents either an increase in the magnitude of skin blood flow (CVC or $\%CVC_{44}$) or a delay in the kinetics of the response, where relevant. An effect was deemed *UNCLEAR* if its 90% CI substantially overlapped the thresholds for both positive and negative such that the effect had both a >5% chance of being positive and a >5% chance of being negative. The threshold value for the smallest important positive effect for each LTH variable was defined by its between-day %CV derived from Chapter 5 for the same group of participants. The region defined by ±%CV was considered to represent a trivial effect. For each effect that was identified as *CLEAR*, the chances of it being negative(%), trivial(%), or positive(%) were subsequently calculated according to the technique described by Hopkins (2007). Using this approach, chances were calculated based on the p-value of the pairwise comparison, its uncertainty (90% confidence limits), the magnitude of the observed effect (%Change from SHAM), and the threshold value for the smallest important positive effect (%CV). Qualitative probability descriptors for the chances of each effect were defined by the following default ranges (Hopkins, 2002):

- <1%, almost certainly not;

- 1-5%, very unlikely;
- 5-25%, unlikely;
- 25-75%, possibly;
- 75-95%, likely;
- 95-99%, very likely;
- >99%, almost certainly

Grouped data for temperature and haemodynamic variables are presented as Mean (SD). Grouped data for components of the LTH response are presented as Mean (CV), where CV represents a factor change from the mean. Pairwise differences are presented as the mean difference ($Mean_{diff}$) [90% CI]. Statistical significance was assumed at p<0.10, unless stated otherwise. All statistics were performed using GraphPad Prism 6 (GraphPad Software Inc., La Jolla, CA, USA).

6.3 Results

A representative tracing of the LTH response for both non-glabrous and glabrous skin is presented in Figure 5.1. No significant differences were observed for any temperature or haemodynamic variable at the start of LTH between trials (Table 6.1).

6.3.1 Baseline

At baseline, the CVC in non-glabrous skin was 0.48 $APU \cdot mmHg^{-1}$ (CV 1.67) in the SHAM trial and 0.44 $APU \cdot mmHg^{-1}$ (CV 1.59) in the ISCH trial, which were not significantly different (-9.5% [-33.1 to 22.5%], p=0.56) (Fig. 6.1.A). The true effect of I-R on baseline CVC was *likely trivial* (14.1%/83.7%/2.2%) in non-glabrous skin (Fig. 6.2). In glabrous skin, the baseline CVC was 2.56 APU•mmHg^{-1} (CV 1.50) in the SHAM trial and 1.95 APU•mmHg^{-1} (CV 1.90) in the ISCH trial, which were not significantly different (-23.9% [-53.9 to 25.5%], p=0.34). The true effect of I-R on baseline CVC was *possibly trivial* (36.3%/61.6%/2.1%) in glabrous skin (Fig. 6.2).

6.3.2 Initial vasodilatory peak

At the initial vasodilatory peak, the CVC in non-glabrous skin was 2.03 $APU \cdot mmHg^{-1}$ (CV 1.81) in the SHAM trial and 1.70 $APU \cdot mmHg^{-1}$ (CV 1.32) in

the ISCH trial, which were not significantly different (-16.3% [-38.4 to 13.7%], p=0.32) (Fig. 6.1.B). The true effect of I-R on CVC at the initial vasodilatory peak was *possibly trivial* (38.7%/59.3%/2.0%) in non-glabrous skin (Fig. 6.3). In glabrous skin, the CVC at the initial peak was 5.32 $APU \cdot mmHg^{-1}$ (CV 1.17) in the SHAM trial and 4.76 $APU \cdot mmHg^{-1}$ (CV 1.30) in the ISCH trial, which were not significantly different (-10.5% [-26.6 to 9.1%], p=0.33). The true effect of I-R on CVC at the initial vasodilatory peak was *possibly trivial* (27.2%/71.6%/1.2%) for glabrous skin (Fig 6.3).

6.3.3 Plateau

At the plateau, the CVC in non-glabrous skin was 2.21 $APU \cdot mmHg^{-1}$ (CV 1.75) in the SHAM trial and 1.96 $APU \cdot mmHg^{-1}$ (CV 1.37) in the ISCH trial, which were not significantly different (-11.1% [-34.8 to 21.3%], p=0.51) (Fig. 6.1.C). The true effect of I-R on the plateau was *possibly trivial* (27.2%/68.9%/3.8%) in non-glabrous skin (Fig. 6.4). In glabrous skin, the CVC at the plateau was 4.31 $APU \cdot mmHg^{-1}$ (CV 1.29) in the SHAM trial and 4.81 $APU \cdot mmHg^{-1}$ (CV 1.21) in the ISCH trial, which were also not significantly different (11.6% [-0.4 to 25.1%], p=0.11). The true effect of I-R on the plateau was *likely trivial* (0.0%/94.1%/5.9%) in glabrous skin (Fig. 6.4).

6.3.4 Maximum heating

During maximum heating to 44°C, the CVC in non-glabrous skin was 2.77 $APU \cdot mmHg^{-1}$ (CV 1.68) in the SHAM trial and 2.54 $APU \cdot mmHg^{-1}$ (CV 1.22) in the ISCH trial, which were not significantly different (-8.3% [-28.7 to 17.8%], p=0.54) (Fig. 6.1.D). The true effect of I-R at maximum heating was *likely trivial* (18.2%/79.2%/2.6%) in non-glabrous skin (Fig. 6.5). In glabrous skin, the CVC was 4.62 $APU \cdot mmHg^{-1}$ (CV 1.37) in the SHAM trial and 5.22 $APU \cdot mmHg^{-1}$ (CV 1.21) in the ISCH trial, demonstrating a significant increase in CVC during maximum heating with I-R (13.1% [0.5 to 27.2%], p=0.09). However, the true effect of I-R at maximum heating was *very likely trivial* (0.0%/95.1%/4.9%) in glabrous skin (Fig. 6.5).

6.3.5 Vasodilatory onset time

The vasodilatory onset time in non-glabrous skin was 113.1 s (CV 1.09) in the SHAM trial and 138.9 s (CV 1.19) in the ISCH trial, demonstrating a significant delay in the onset time with I-R injury (22.9% [11.8 to 35.0%], p=0.003) (Fig 6.6.A). The true effect of I-R on vasodilatory onset time was *very likely positive* (0.0%/4.8%/95.2%) in non-glabrous skin (Fig. 6.7). In glabrous skin, vasodilatory onset time was 138.5 s (CV 1.14) in the SHAM trial and 161.7 s (CV 1.21) in the ISCH trial, also demonstrating a significant delay in onset time with I-R (16.8% [3.8 to 31.3%], p=0.04). However, the true effect of I-R on vasodilatory onset time was *likely trivial* (0.0%/93.8%/6.2%) in glabrous skin (Fig 6.7).

6.3.6 Time to initial peak

The time to initial peak in non-glabrous skin was 244.2 s (CV 1.10) in the SHAM trial and 283.7 s (CV 1.11) in the ISCH trial, demonstrating a significant delay in the time to initial peak with I-R injury (16.2% [7.1 to 26.2%], p=0.008) (Fig. 6.6.B). The true effect of I-R on the time to initial peak was *possibly positive* (0.0%/40.6%/59.4%) for non-glabrous skin (Fig. 6.8). In glabrous skin, the time to initial peak was 268.3 s (CV 1.14) in the SHAM trial and 291.8 s (CV 1.16) in the ISCH trial, which were not significantly different (8.8% [-3.4 to 22.5%], p=0.22). The true effect of I-R on the time to initial peak was *likely trivial* (0.3%/79.0%/20.6%) for glabrous skin (Fig. 6.8).

6.3.7 CVC normalized to maximum heating at 44°C

Results for $\%CVC_{44}$ at baseline, the initial vasodilatory peak, and plateau for both non-glabrous and glabrous skin are presented in Table 6.2.

Table 6.1 Temperature and Haemodynamic Conditions at the start of local skin heating

	SHAM	**ISCH**	**(ISCH-SHAM)**
	Mean (SD)	Mean (SD)	$Mean_{diff}$ [95%CI]
Temperatures			
T_{amb} (°C)	25.14 (0.14)	25.15 (0.06)	0.01 [-0.10, 0.13], p=0.83
T_f: glabrous (°C)	32.3 (3.8)	31.3 (3.9)	-1.0 [-3.2, 1.3], p=0.35
T_f: non-glabrous (°C)	31.4 (3.3)	30.9 (3.0)	-0.5 [-2.3, 1.2], p=0.50
$\bar{T}_{sk}$ (°C)	32.8 (0.7)	32.7 (0.6)	-0.1 [-0.4, 0.2], p=0.40
Haemodynamics			
HR (bpm)	57.0 (6.8)	55.9 (7.9)	-1.1 [-4.4, 2.2], p=0.46
MAP (mmHg)	87.6 (8.5)	91.3 (9.0)	3.7 [-0.4, 7.9], p=0.07
S_aO_2 (%)	97.3 (1.3)	96.9 (1.5)	-0.4 [-1.2, 0.4], p=0.24

*Significance was set to p<0.05. SD, standard deviation; CI, confidence interval; $Mean_{diff}$, mean difference between trials; T_{amb}, ambient air temperature; T_f, finger skin temperature; $\bar{T}_{sk}$, mean skin temperature; HR, heart rate; MAP, mean arterial pressure; S_aO_2, arterial oxygen saturation. NOTE: Mean skin temperature is n=9, due to broken wiring.

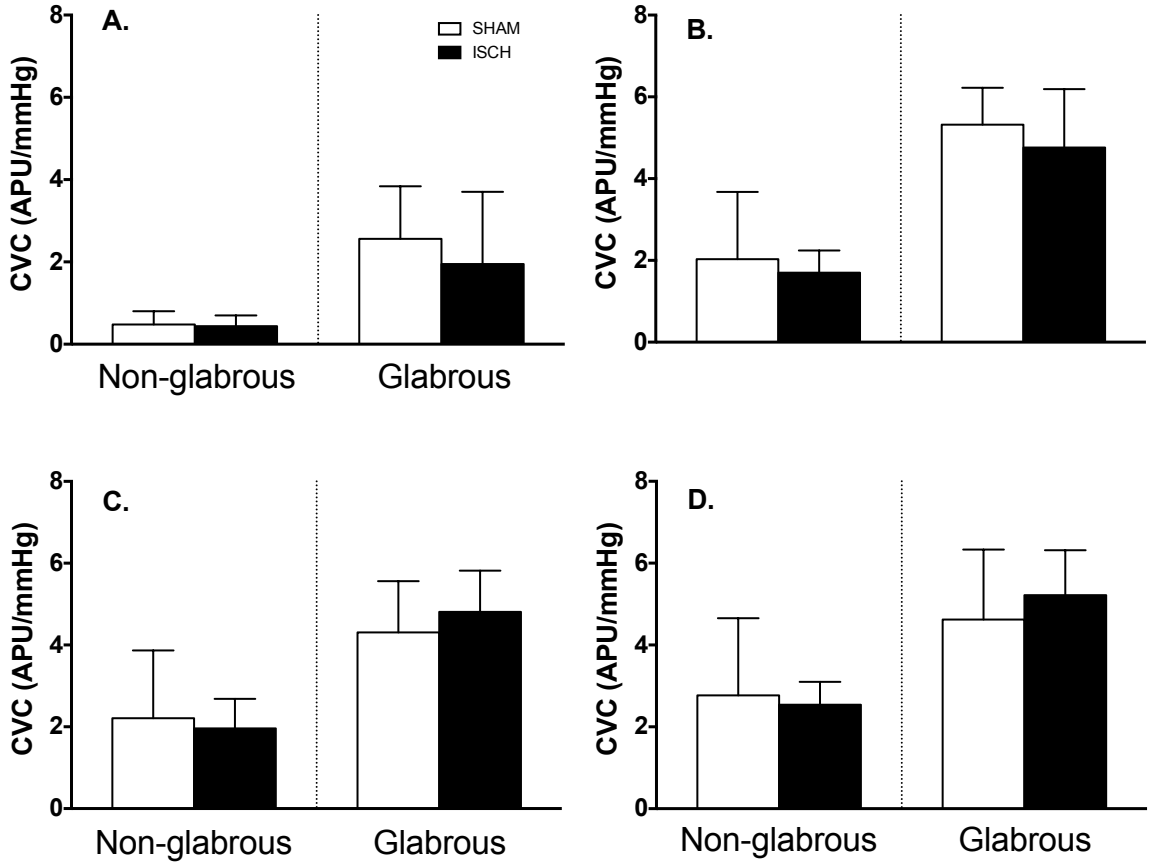

Figure 6.1 Cutaneous vascular conductance during local skin heating in the SHAM and ISCH trials for non-glabrous and glabrous skin.

*Significance set at $p<0.10$. A. Baseline; B. Initial peak; C. Plateau; D Maximum skin heating to 44°C. APU, arbitrary perfusion units; CVC, cutaneous vascular conductance; ISCH, ischaemia-reperfusion trial; SHAM, control trial.

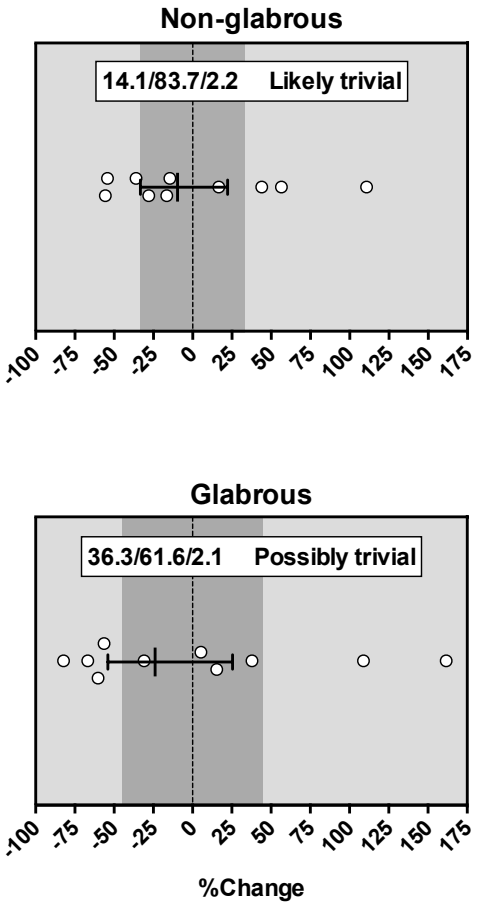

Figure 6.2 Baseline: Percent change (ISCH-SHAM) for non-glabrous and glabrous skin

Dark shaded area represents the within-subject coefficient of variation (%CV) derived from Chapter 5 for each skin type. ISCH, ischaemia-reperfusion trial; SHAM, control trial. Black bar represents mean percentage difference with 90% confidence limits. White circles represent individual responses. Qualitative inferences are based on the presence or absence of a substantial effect, defined as Mean difference being outside of the test-retest %CV determined for each variable in Chapter 5. If the chance of being substantially positive and negative were both >5%, true effect was assessed as UNCLEAR (could be positive or negative). Otherwise, chances of being positive or negative were assessed as follows: <1%, almost certainly not; 1-5%, very unlikely; 5-25%, unlikely; 25-75%, possibly; 75-95%, likely; 95-99%, very unlikely; >99%, almost certainly.

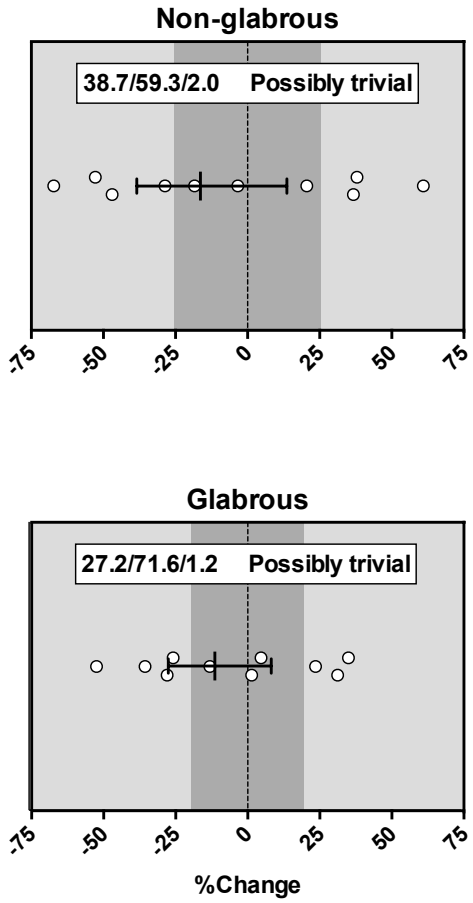

Figure 6.3 Initial vasodilatory peak: Percent change (ISCH-SHAM) for non-glabrous and glabrous skin

Dark shaded area represents the within-subject coefficient of variation (%CV) derived from Chapter 5 for each skin type. ISCH, ischaemia-reperfusion trial; SHAM, control trial. Black bar represents mean percentage difference with 90% confidence limits. White circles represent individual responses. Qualitative inferences are based on the presence or absence of a substantial effect, defined as Mean difference being outside of the test-retest %CV determined for each variable in Chapter 5. If the chance of being substantially positive and negative were both >5%, true effect was assessed as UNCLEAR (could be positive or negative). Otherwise, chances of being positive or negative were assessed as follows: <1%, almost certainly not; 1-5%, very unlikely; 5-25%, unlikely; 25-75%, possibly; 75-95%, likely; 95-99%, very unlikely; >99%, almost certainly.

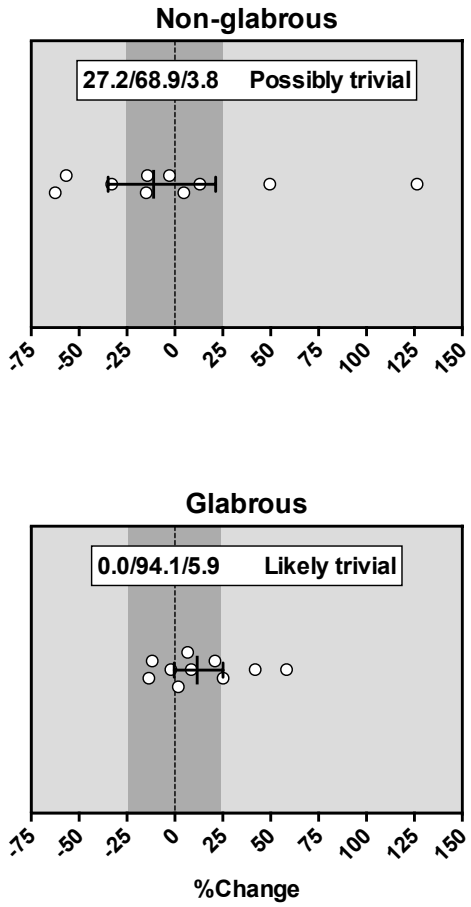

Figure 6.4 Plateau: Percent change (ISCH-SHAM) for non-glabrous and glabrous skin

Dark shaded area represents the within-subject coefficient of variation (%CV) derived from Chapter 5 for each skin type. ISCH, ischaemia-reperfusion trial; SHAM, control trial. Black bar represents mean percentage difference with 90% confidence limits. White circles represent individual responses. Qualitative inferences are based on the presence or absence of a substantial effect, defined as Mean difference being outside of the test-retest %CV determined for each variable in Chapter 5. If the chance of being substantially positive and negative were both >5%, true effect was assessed as UNCLEAR (could be positive or negative). Otherwise, chances of being positive or negative were assessed as follows: <1%, almost certainly not; 1-5%, very unlikely; 5-25%, unlikely; 25-75%, possibly; 75-95%, likely; 95-99%, very unlikely; >99%, almost certainly.

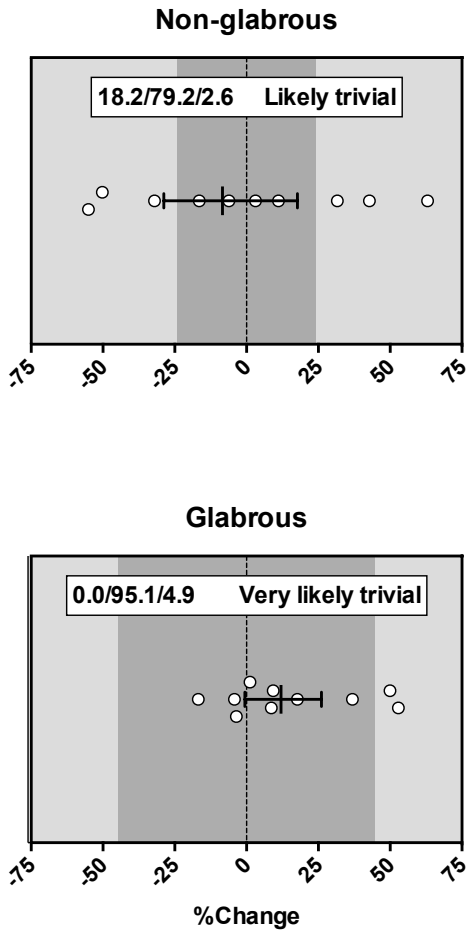

Figure 6.5 Maximum heating: Percent change (ISCH-SHAM) for non-glabrous and glabrous skin

Dark shaded area represents the within-subject coefficient of variation (%CV) derived from Chapter 5 for each skin type. ISCH, ischaemia-reperfusion trial; SHAM, control trial. Black bar represents mean percentage difference with 90% confidence limits. White circles represent individual responses. Qualitative inferences are based on the presence or absence of a substantial effect, defined as Mean difference being outside of the test-retest %CV determined for each variable in Chapter 5. If the chance of being substantially positive and negative were both >5%, true effect was assessed as UNCLEAR (could be positive or negative). Otherwise, chances of being positive or negative were assessed as follows: <1%, almost certainly not; 1-5%, very unlikely; 5-25%, unlikely; 25-75%, possibly; 75-95%, likely; 95-99%, very unlikely; >99%, almost certainly.

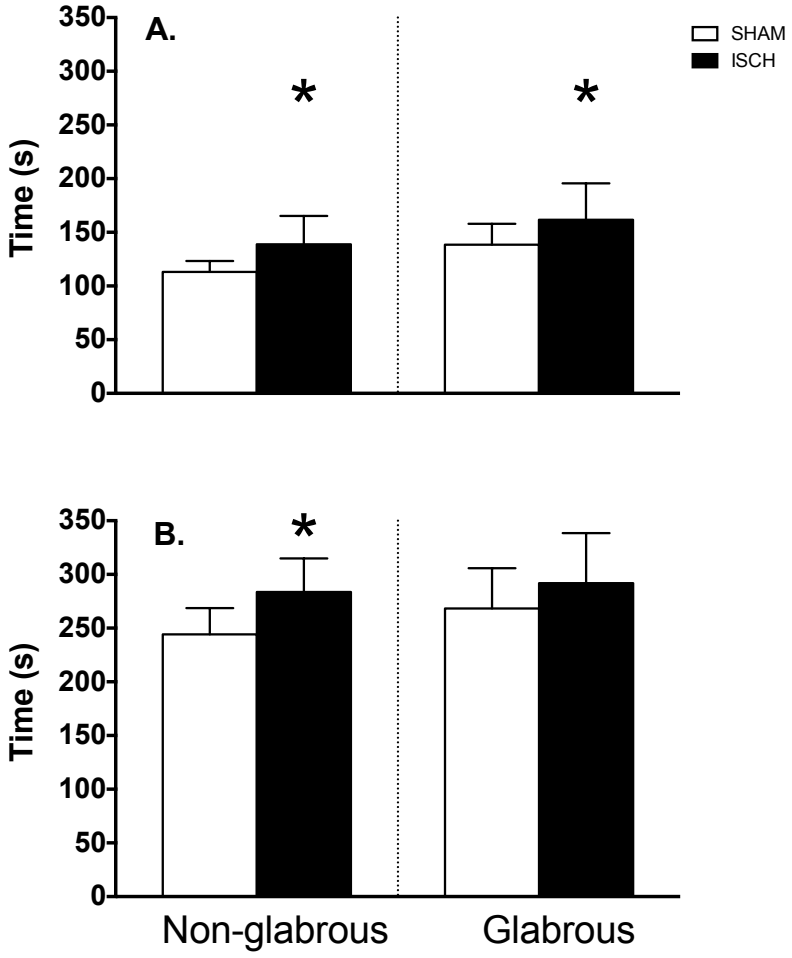

Figure 6.6 Kinetics of the vasodilatory response to local heating in the SHAM and ISCH trials in non-glabrous and glabrous skin.

*Significance set at $p<0.10$. A. Vasodilatory onset time; B. Time to initial peak. ISCH, ischaemia-reperfusion trial; SHAM, control trial.

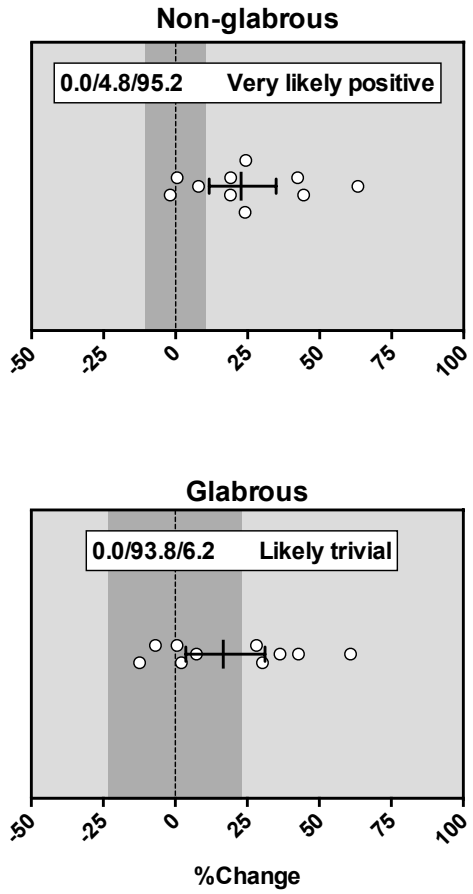

Figure 6.7 Vasodilatory onset time: Percent change (ISCH-SHAM) for non-glabrous and glabrous skin

Dark shaded area represents the within-subject coefficient of variation (%CV) derived from Chapter 5 for each skin type. ISCH, ischaemia-reperfusion trial; SHAM, control trial. Black bar represents mean percentage difference with 90% confidence limits. White circles represent individual responses. Qualitative inferences are based on the presence or absence of a substantial effect, defined as Mean difference being outside of the test-retest %CV determined for each variable in Chapter 5. If the chance of being substantially positive and negative were both >5%, true effect was assessed as UNCLEAR (could be positive or negative). Otherwise, chances of being positive or negative were assessed as follows: <1%, almost certainly not; 1-5%, very unlikely; 5-25%, unlikely; 25-75%, possibly; 75-95%, likely; 95-99%, very unlikely; >99%, almost certainly.

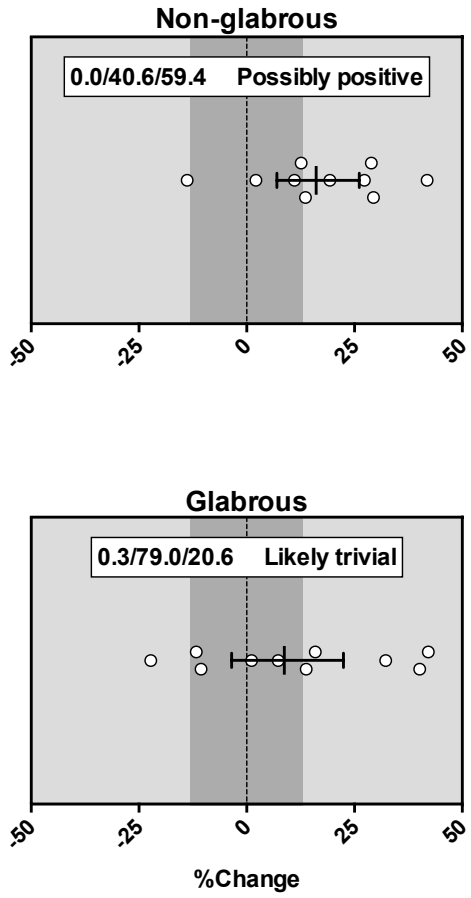

Figure 6.8 Time to initial peak: Percent change (ISCH-SHAM) for non-glabrous and glabrous skin

Dark shaded area represents the within-subject coefficient of variation (%CV) derived from Chapter 5 for each skin type. ISCH, ischaemia-reperfusion trial; SHAM, control trial. Black bar represents mean percentage difference with 90% confidence limits. White circles represent individual responses. Qualitative inferences are based on the presence or absence of a substantial effect, defined as Mean difference being outside of the test-retest %CV determined for each variable in Chapter 5. If the chance of being substantially positive and negative were both >5%, true effect was assessed as UNCLEAR (could be positive or negative). Otherwise, chances of being positive or negative were assessed as follows: <1%, almost certainly not; 1-5%, very unlikely; 5-25%, unlikely; 25-75%, possibly; 75-95%, likely; 95-99%, very unlikely; >99%, almost certainly.

Table 6.2 Local skin heating responses with data normalized to maximum

	SHAM	**ISCH**	**%Difference**	**Qualitative Inference***
	Mean (CV)	Mean (CV)	Mean [90% CI]	(%Negative/%Trivial/%Positive)
Baseline				
non-glabrous	17.4% (1.4)	17.2% (1.5)	-1.3% [-19.3 to 20,9%], p=0.91	Likely Trivial (6.2%/89.6%/4.3%)
glabrous	55.5% (1.6)	37.4% (2.0)	-32.7% [-59.7 to 12.4%], p=0.19	Possibly Negative (61.6%/36.8%/1.6%)
Initial Peak				
non-glabrous	73.5% (1.2)	67.2% (1.2)	-8.6% [-20.4 to 4.9%], p=0.26	Possibly Negative (56.7%/40.7%/2.6%)
glabrous	115.2% (1.3)	91.2% (1.3)	-20.9% [-36.7 to -1.0%], p=0.09	Possibly Negative (70.7%/28.8%/0.5%)
Plateau				
non-glabrous	79.8% (1.1)	77.4% (1.2)	-3.0% [-15.7 to 11.6%], p=0.70	UNCLEAR (25.3%/66.1%/8.6%)
glabrous	93.3% (1.2)	92.1% (1.1)	-1.3% [-8.6 to 6.6%], p=0.77	Likely Trivial (4.5%/93.8%/1.7%)

Significance set at p<0.10. CV, coefficient of variation; CI, confidence interval; ISCH, ischaemia reperfusion trial; SHAM, control trial. NOTE: CV is presented as a factor. To calculate upper and lower limits, ×/÷ the mean by this value. *Substantial effect defined as Mean difference being outside of the test-retest CV determined for each variable in Chapter 5. If the chance of being substantially positive and negative were both >5%, true effect was assessed as UNCLEAR (could be positive or negative). Otherwise, chances of being positive or negative were assessed as follows: <1%, almost certainly not; 1-5%, very unlikely; 5-25%, unlikely; 25-75%, possibly; 75-95%, likely; 95-99%, very unlikely; >99%, almost certainly.

6.4 Discussion

In the current study, the influence of upper limb I-R injury on the subsequent response to local heating in the non-glabrous and glabrous skin of the index finger was examined. The main findings were (i) I-R was associated with an impaired cutaneous LTH response in non-glabrous skin, but not in glabrous skin, and (ii) the vasodilatory onset time and the time to initial peak were also delayed following I-R in non-glabrous skin. For the present investigation, final conclusions for differences between the ISCH and SHAM trials were based on the use of inferential statistics emphasizing precision of estimation over null-hypothesis testing. Specifically, a systematic approach was taken to interpret the practical importance of confidence limits, which describe the uncertainty in the true (population) value of an effect. Along this line, a set of previously described rules were used for determining whether an effect was clear or unclear, and for making quantitative assertions about the likelihood of the effect being substantially negative or positive (Hopkins, 2002; Batterham & Hopkins, 2006).

Contrary to expectations, there was no attenuation of the initial vasodilatory peak following I-R in either skin type. However, in non-glabrous skin, there were delays in vasodilatory onset time and the time to initial peak post-ischaemia. In prior studies, cutaneous sensory nerve blockade with topical application of EMLA cream has been shown to reduce and delay the initial vasodilatory peak in the non-glabrous skin of the forearm (Minson *et al.*, 2001; Hodges *et al.*, 2015), and to reduce the initial peak in glabrous skin of the index finger (Roustit *et al.*, 2008). Interestingly, Metzler-Wilson *et al.* (2012) previously identified that EMLA treatment in the cheek and forehead skin was effective in delaying the timing of the initial peak, but failed to alter its magnitude, suggesting that the standard anaesthetic protocol used in that study was not strong enough to completely abolish the response. The current findings are consistent with this response and suggest that 20 minutes of ischaemia followed by reperfusion was sufficient to partially inhibit sensory nerve function, which affected the timing, but ultimately not the magnitude of the initial peak during local skin heating.

Alternatively, the results could indicate that mechanisms other than sensory nerves contributed to the observed delay in the formation of the initial vasodilatory peak following I-R. A hallmark of I-R injury is the rapid production of ROS at the onset of reperfusion that reduces NO bioavailability, resulting in an elevation of sympathetic vasoconstrictor tone (Harrison, 1997; Carden & Granger, 2000). Such an effect could delay the vasodilatory response to local heating. In support of this notion, Wingo *et al.* (2009) demonstrated that NO release is directly responsible for inhibiting the vasoconstrictor response to exogenous norepinephrine administration in the non-glabrous skin of the forearm during local heating. Furthermore, although the initial vasodilatory peak is mediated primarily by sensory nerves, NO also contributes to the response and NOS inhibition with L-NAME modestly attenuates or delays the initial peak during local heating in the non-glabrous skin of the forearm (Minson *et al.*, 2001; Houghton *et al.*, 2006; Hodges *et al.*, 2008). In previous studies utilizing the same I-R model as that used in the current experiment, acute reductions in conduit and resistance artery NO-dependent endothelial function (Kharbanda *et al.*, 2001) and an elevation in muscle sympathetic nerve activity were observed throughout ischaemia and early reperfusion (Lambert *et al.*, 2016). Thus, if NO-bioavailability is reduced as a result of scavenging by ROS during reperfusion, an increase in sympathetic tone will delay the vasodilatory response to local heating in this model.

In response to a sustained local heating stimulus, I-R injury had no effect on the magnitude of the increase in CVC in either skin type. Since the plateau phase is primarily mediated by NO release (Kellogg *et al.*, 1999), this finding indicates that the model of I-R used in the current study was not strong enough to impair the full expression of endothelium-dependent vasodilatation in the skin of the finger in response to local heating. This is consistent with the findings of Gori *et al.* (2006) who failed to demonstrate any change in acetylcholine-mediated vasodilatation in the non-glabrous skin of the forearm with 15 minutes of ischaemia followed by reperfusion. In contrast to these findings in the cutaneous microcirculation, NO-mediated vasodilatation in conduit arteries is impaired with this model of I-R (Kharbanda *et al.*, 2001; Gori *et al.*, 2006). Since the microcirculation is typically

considered to be more susceptible to the deleterious effect of I-R (Carden & Granger, 2000), the discrepancy in these findings remains unclear.

There are several potential reasons why I-R injury appeared to have a greater influence on the local heating response in non-glabrous skin compared to the glabrous skin of the index finger. Glabrous skin on the volar surface of the hand contains a higher density of sensory afferents (Greenfield, 1963) and this skin type is typically considered to possess greater thermosensitivity, possibly due to habitual hand use (Taylor *et al.*, 2014). Thus, it could be that the greater density of sensory afferents was sufficient to compensate for any modest impairments in sensory nerve function that may have been incurred with the current level of I-R injury. Additionally, thermoregulatory blood flow dominates perfusion in glabrous skin due to the presence of a large number of wide diameter AVAs, and total flow is much higher than that of non-glabrous skin (Taylor *et al.*, 2014). This greater blood flow through these shunt vessels can potentially mask the negative effects of I-R injury on nutritional blood flow through capillary loops, which contributes to a greater proportion of total blood flow in non-glabrous skin (Braverman, 1997; Taylor *et al.*, 2014). The higher blood flow through these wide diameter shunt vessels in glabrous skin may also be more effective at rapidly flushing out the metabolic byproducts of ischaemia and reperfusion. Furthermore, leukocytes are less likely to firmly adhere to the microvascular endothelium in glabrous skin during reperfusion due to the greater flow rate as a result of bypassing the small diameter nutritive capillaries, minimizing the direct cell-to-cell contact that is necessary for adhesion to occur (Eltzschig & Collard, 2004).

Limitations

The effects of sensory nerve blockade with EMLA treatment on the LTH response were not directly examined in the current study. This additional control was not included due to the limited surface area of the finger sites for probe placement, which would have necessitated two ischaemia trials. Increasing the number of trials would have placed an unnecessary burden on the participants since it is well-established that the initial peak phase of the cutaneous LTH response is predominantly mediated by intact sensory nerves in both non-glabrous (Minson *et*

al., 2001; Metzler-Wilson *et al.*, 2012; Hodges *et al.*, 2015) and glabrous skin (Roustit *et al.*, 2008; Metzler-Wilson *et al.*, 2012). Thus, examination of changes in the magnitude and timing of this phase of the LTH response can be reasonably considered to predominantly reflect alterations in sensory nerve function.

In the current study, core body temperature was not assessed, which may have had an influence on the observed skin blood flow responses. However, the ambient temperature was tightly controlled between trials, the participants were examined at the same time of day, and each experimental session was time-matched with the same acclimation period prior to baseline data collection. Furthermore, mean whole-body skin temperature, as well as non-glabrous and glabrous skin temperatures from the middle finger of the experimental limb, did not differ between trials, indicating that marked changes in core temperature were unlikely.

Conclusions

The current data indicate that I-R injury of the upper limb has detrimental effects on the initial vasodilatory response to a subsequent local heating stimulus in the non-glabrous skin of the index finger. In contrast, the response to sustained local heating was unaltered. Unlike non-glabrous skin, the current model of I-R injury did not influence the response to local heating in glabrous skin. These findings suggest that in non-glabrous skin of the index finger, cutaneous afferent sensory nerve function and/or early NO release may be impaired following 20 minutes of upper limb ischaemia. In contrast, the magnitude of the injury was not sufficient to impair NO-mediated vasodilatation during sustained local heating.

6.5 References

Batterham AM & Hopkins WG. (2006). Making Meaningful Inferences About Magnitudes. *Int J Sport Physiol Perform* **1,** 50-57.

Braverman IM. (1997). The cutaneous microcirculation: Ultrastructure and microanatomical organization. *Microcirculation-London* **4,** 329-340.

Carden DL & Granger DN. (2000). Pathophysiology of ischaemia-reperfusion injury. *J Pathol* **190,** 255-266.

Eltzschig HK & Collard CD. (2004). Vascular ischaemia and reperfusion injury. *Br Med Bull* **70,** 71-86.

Gherardini G, Evans GRD, Theodorsson E, Gurlek A, Milner SM, Palmer B & Lundeberg T. (1996). Calcitonin gene-related peptide in experimental ischemia. Implication of an endogenous anti-ischemic effect. *Ann Plast Surg* **36,** 616-620.

Gori T, Di Stolfo G, Sicuro S, Dragoni S, Parker JD & Forconi S. (2006). The effect of ischemia and reperfusion on microvascular function: A human in vivo comparative study with conduit arteries. *Clin Hemorheol Microcirc* **35,** 169-173.

Granger DN. (1999). Ischemia-reperfusion: Mechanisms of microvascular dysfunction and the influence of risk factors for cardiovascular disease. *Microcirculation* **6,** 167-178.

Greenfield ADM. (1963). *The circulation through the skin. In: Handbook of Physiology: Circulation*, vol. II. American Physiological Society, Washington, D.C.

Harada N, Okajima K, Uchiba M & Katsuragi T. (2002). Ischemia/reperfusion-induced increase in the hepatic level of prostacyclin is mainly mediated by activation of capsaicin-sensitive sensory neurons in rats. *J Lab Clin Med* **139,** 218-226.

Harrison DG. (1997). Cellular and molecular mechanisms of endothelial cell dysfunction. *J Clin Invest* **100,** 2153-2157.

Hodges GJ, Del Pozzi AT, McGarr GW, Mallette MM & Cheung SS. (2015). The contribution of sensory nerves to cutaneous vasodilatation of the forearm and leg to local skin heating. *Eur J Appl Physiol* **115,** 2091-2098.

Hodges GJ, Kosiba WA, Zhao K & Johnson JM. (2008). The involvement of norepinephrine, neuropeptide Y, and nitric oxide in the cutaneous vasodilator response to local heating in humans. *Journal of Applied Physiology* **105,** 233-240.

Hodges GJ, Kosiba WA, Zhao K & Johnson JM. (2009). The involvement of heating rate and vasoconstrictor nerves in the cutaneous vasodilator response to skin warming. *Am J Physiol-Heart Circul Physiol* **296,** H51-H56.

Hopkins WG. (2002). Probabiliites of Clinical or Practical Significance. *Sportscience* **6**.

Hopkins WG. (2007). A Spreadsheet for Deriving a Confidence Interval, Mechanistic Inference and Clinical Inference from a P value. *Sportscience* **11,** 16-20.

Houghton BL, Meendering JR, Wong BJ & Minson CT. (2006). Nitric oxide and noradrenaline contribute to the temperature threshold of the axon reflex response to gradual local heating in human skin. *J Physiol-London* **572,** 811-820.

Ji P, Jiang T, Wang MH, Wang RR, Zhang LQ & Li Y. (2013). Denervation of capsaicin-sensitive C fibers increases pulmonary inflammation induced by ischemia-reperfusion in rabbits. *J Surg Res* **184,** 782-789.

Johnson JM, Minson CT & Kellogg DL. (2014). Cutaneous Vasodilator and Vasoconstrictor Mechanisms in Temperature Regulation. *Compr Physiol* **4,** 33-89.

Kellogg DL, Liu Y, Kosiba IF & O'Donnell D. (1999). Role of nitric oxide in the vascular effects of local warming of the skin in humans. *Journal of Applied Physiology* **86,** 1185-1190.

Kharbanda RK, Peters M, Walton B, Kattenhorn M, Mullen M, Klein N, Vallance P, Deanfield J & MacAllister R. (2001). Ischemic preconditioning prevents endothelial injury and systemic neutrophil activation during ischemia-reperfusion in humans in vivo. *Circulation* **103,** 1624-1630.

Kline RB. (2005). *Principles and Practice of Structural Equation Modeling*. The Guilford Press, New York.

Lambert EA, Thomas CJ, Hemmes R, Eikelis N, Pathak A, Schlaich MP & Lambert GW. (2016). Sympathetic nervous response to ischemia-reperfusion injury in humans is altered with remote ischemic preconditioning. *Am J Physiol-Heart Circul Physiol* **311,** H364-H370.

Lin CSY, Kuwabara S, Cappelen-Smith C & Burke D. (2002). Responses of human sensory and motor axons to the release of ischaemia and to hyperpolarizing currents. *J Physiol-London* **541,** 1025-1039.

Metzler-Wilson K, Kellie LA, Tomc C, Simpson C, Sammons D & Wilson TE. (2012). Differential vasodilatory responses to local heating in facial, glabrous and hairy skin. *Clin Physiol Funct Imaging* **32,** 361-366.

Minson CT, Berry LT & Joyner MJ. (2001). Nitric oxide and neurally mediated regulation of skin blood flow during local heating. *Journal of Applied Physiology* **91,** 1619-1626.

Mizutani A, Okajima K, Murakami K, Mizutani S, Kudo K, Uchino T, Kadoi Y & Noguchi T. (2009). Activation of Sensory Neurons Reduces

Ischemia/Reperfusion-induced Acute Renal Injury in Rats. *Anesthesiology* **110,** 361-369.

Roustit M, Blaise S, Millet C & Cracowski JL. (2010). Reproducibility and methodological issues of skin post-occlusive and thermal hyperemia assessed by single-point laser Doppler flowmetry. *Microvascular Research* **79,** 102-108.

Roustit M, Simmons G, Carpentier P & Cracowski JL. (2008). Abnormal digital neurovascular response to local heating in systemic sclerosis. *Fundam Clin Pharmacol* **22,** 90-90.

Taylor NAS, Machado-Moreira CA, van den Heuvel AMJ & Caldwell JN. (2014). Hands and feet: physiological insulators, radiators and evaporators. *European Journal of Applied Physiology* **114,** 2037-2060.

Turchanyi B, Toth B, Racz I, Vendegh Z, Furesz J & Hamar J. (2005). Ischemia Reperfusion injury of the skeletal muscle after selective deafferentation. *Physiol Res* **54,** 25-31.

Ustinova EE, Bergren D & Schultz HD. (1995). Neuropeptide depletion impairs postischemic recovery of the isolated rat heart - Role of Substance-P. *Cardiovasc Res* **30,** 55-63.

Wang LH & Wang DH. (2005). TRPV1 gene knockout impairs postischemic recovery in isolated perfused heart in mice. *Circulation* **112,** 3617-3623.

Wang MH, Ji P, Wang RR, Zhao LF & Xia ZY. (2012). TRPV1 Agonist Capsaicin Attenuates Lung Ischemia-Reperfusion Injury in Rabbits. *J Surg Res* **173,** 153-160.

Wilson TE, Zhang R, Levine BD & Crandall CG. (2005). Dynamic autoregulation of cutaneous circulation: differential control in glabrous versus nonglabrous skin. *Am J Physiol Heart Circ Physiol* **289,** H385-391.

Wingo JE, Low DA, Keller DM, Brothers RM, Shibasaki M & Crandall CG. (2009). Effect of elevated local temperature on cutaneous vasoconstrictor responsiveness in humans. *Journal of Applied Physiology* **106,** 571-575.

Wong BJ & Minson CT. (2006). Neurokinin-1 receptor desensitization attenuates cutaneous active vasodilatation in humans. *J Physiol-London* **577,** 1043-1051.

Wong BJ & Minson CT. (2011). Altered thermal hyperaemia in human skin by prior desensitization of neurokinin-1 receptors. *Exp Physiol* **96,** 599-609.

Wong BJ, Tublitz NJ & Minson CT. (2005). Neurokinin-1 receptor desensitization to consecutive microdialysis infusions of substance P in human skin. *J Physiol-London* **568,** 1047-1056.

Chapter 7: Between- and Within-day reliability of cutaneous thermal hyperaemia in the forearm using single point laser-Doppler

7.1 Introduction

Laser-Doppler flowmetry (LDF) is a commonly used, non-invasive, optical technique that provides an index of skin blood flow (Johnson *et al.*, 1984; Saumet *et al.*, 1988). When combined with reactivity tests and/or pharmacological interventions, LDF allows for a detailed functional and mechanistic examination of the cutaneous microcirculation in humans (Roustit & Cracowski, 2013). Examining the cutaneous response to local thermal hyperaemia (LTH) is a common test of microvascular reactivity that has been widely used in a variety of healthy and clinical populations (Minson, 2010; Johnson *et al.*, 2014). The skin responds to a rapid, non-painful local heating stimulus with a biphasic increase in blood flow that begins with an initial vasodilatory peak, predominantly mediated by sensory nerves, followed by a sustained plateau that is mediated primarily by nitric oxide (Kellogg *et al.*, 1999) and other endothelium-derived mediators (Brunt & Minson, 2012). As such, this test allows for a combined assessment of neurovascular and endothelial function.

Several studies have focused on examination of inter-site and between-day reliability of the cutaneous LTH response with different groups reporting widely varying results (Agarwal *et al.*, 2010; Roustit *et al.*, 2010a; Roustit *et al.*, 2010b; Tew *et al.*, 2011). Poor inter-site reliability has previously been reported when using single-point LDF (Roustit *et al.*, 2010a), which has been attributed to the heterogeneous nature of the cutaneous microcirculation in the forearm (Braverman, 1997). This is also consistent with poor between-day reliability previously reported when using single-point LDF (Roustit *et al.*, 2010a; Roustit *et al.*, 2010b). In contrast, studies utilizing integrating-probe LDF, which compensates for spatial variation by averaging the LDF signal from several evenly spaced lasers, have demonstrated superior between-day reliability of the cutaneous LTH response compared to studies using single-point LDF (Agarwal *et al.*, 2010; Tew *et al.*, 2011). Beyond

spatial variability, other differences between studies, such as the rate and duration of the local heating protocol and the extent of environmental controls, were also likely contributors to these inconsistent findings.

Another important concern when examining the reliability of the cutaneous LTH response is that several forms of data expression are commonly used to describe the results. For example, the data can be expressed in raw form as arbitrary perfusion units (APU), or standardized by mean arterial pressure to provide a measure of cutaneous vascular conductance (CVC). Other common approaches involve normalizing the raw values to either baseline or maximum perfusion at each measurement site. Therefore, identifying the most reliable form of data expression will contribute to greater consistency in reporting of LDF results, which should allow for easier comparison between studies.

Interestingly, while several studies have examined the cutaneous LTH response under test-retest conditions on the same day, it does not appear that the reliability of the test has been adequately investigated with this experimental design. Using such an approach is appealing since it allows for direct comparison of the skin's response to local heating before and after an acute experimental or clinical intervention in the same individual. It remains to be seen, however, exactly how test-retest reliability compares to inter-site reliability on the same day, or to between-day reliability, which is often less than desirable (Agarwal *et al.*, 2010; Roustit *et al.*, 2010a; Roustit *et al.*, 2010b; Tew *et al.*, 2011).

As such, the primary objective of the current study was to examine the within-day and between-day reliability for the magnitude and kinetics of the different phases of a rapid, non-painful cutaneous LTH response on the volar surface of the forearm using single-point LDF in young, healthy males. A secondary aim was to determine the most reliable form of data expression. It was hypothesized that within-day and between-day reliability of the LTH response will be equivalent and consistent with variations in the response due to inter-site differences in microvessel density in the forearm. It was further hypothesized that expressing the data as CVC, normalized to maximum, will be the most reliable form of data expression.

7.2 Methods

7.2.1 Participants

Ten healthy, recreationally active males (26.8 ± 5.8 y, 178.3 ± 7.5 cm, 80.7 ± 12.6 kg) volunteered for the current study and reported to the laboratory for two experimental sessions. Nine of these individuals also participated in the experiments previously described in Chapters 5 and 6.

7.2.2 Experimental Protocol

Following the pre-experimental procedures previously described in *Section 4.4*, participants rested quietly in the temperature-controlled room for ~30 min prior to the start of data collection while being instrumented as described in *Section 4.6*. A total of four skin sites were selected on the volar forearm for LDF probe placement and were marked with indelible ink. The four selected sites formed a square pattern over the skin surface and all were ~5 cm apart to avoid interference. Initially, LDF probes were placed on two skin sites, after which, the local heating disk temperature was set to 33°C for both probes. Baseline measurements were recorded for ~20 min to ensure stable LDF and skin temperature values. At this point, the local heating disk temperature on both probes was increased according to the LTH protocol described in *Section 4.8*. Following the first LTH protocol, the LDF probes were removed and participants were allowed to void their bladders and stretch. Subsequently, the LDF probes were placed on two new skin sites. Participants continued resting quietly for another 60 min, at which point a second LTH protocol was performed. This procedure allowed for two inter-site reliability assessments of the cutaneous LTH protocol, one during the first skin heating period and another during the second. These will subsequently be referred to as within-day (inter-site) reliability for the *Heat-1* and *Heat-2* conditions. It also allowed for two simultaneous test-retest reliability assessments of the LTH protocol, one for each LDF probe, that were separated by 60 min. These will subsequently be referred to as within-day (test-retest) reliability for *Probe-1* and *Probe-2*. During a second testing session, separated by ~7-14 days, the identical procedure for the participant set-up

and running of the first LTH protocol for *Probe-2* was performed to assess between-day reliability.

7.2.3 Data Processing

Measurement regions of the LTH protocol were defined as previously described in *Section 4.8*. A representative laser-Doppler tracing of the LTH protocol on the volar surface of the forearm with measurement time points clearly indicated is presented in Figure 7.1. The LDF data were presented in six forms as previously described in *Section 5.2.3*.

7.2.4 Statistical Analysis

All statistical analyses were conducted according to the same procedures previously described in *Section 5.2.4*. All outcome measures in the current study were normally distributed.

7.3 Results

Results for baseline temperature and haemodynamic variables are presented in Table 7.1. For the within-day (inter-site) and within-day (test-retest) conditions, results were generally equivalent between *Heat-1* and *Heat-2* and between *Probe-1* and *Probe-2*, respectively. For clarity, only data for *Heat-1* and *Probe-1* will be presented in the corresponding sections below. Results for within-day (inter-site) and within-day (test-retest) reliability are presented in Table 7.2 and Table 7.3, respectively. Between-day reliability data are presented in Table 7.4 and reliability data for the kinetics of the response under all test-retest conditions are presented in Table 7.5.

<u>Within-day (inter-site) reliability</u>

Mean differences

No systematic changes in the mean were evident at baseline for the within-day (inter-site) condition for any form of LDF data expression. When examining the kinetics of the response, no systematic changes in the mean were observed for the vasodilatory onset time or the time to initial peak.

Coefficients of variation

At baseline, %CV values were rated as poor for all forms of data expression. When normalized to maximum heating, %CV values were rated as moderate for the initial vasodilatory peak (%CV both 13.5%) and good for the plateau (%CV both 4.6%) for $\%APU_{44}$ and $\%CVC_{44}$, respectively. In contrast, %CV values were rated as poor for all other forms of data expression in each phase. When examining the kinetics of the response, %CV values for vasodilatory onset time (%CV=7.3%) and the time to initial peak (%CV=4.6%) were both rated as good.

Intraclass correlation coefficients

Expressing the data as $\%CVC_{44}$ produced the strongest overall correlation coefficients for some LTH phases. However, ICC values for these forms of data expression still varied widely across phases, with ratings ranging from fair-to-good and poor. When data were expressed as APU and CVC or as $\%APU_{BL}$ and $\%CVC_{BL}$, ICC values primarily rated as poor, although in some measurement regions they rated as fair-to-good. When examining the kinetics of the response, the ICC values were rated as excellent for vasodilatory onset time, and poor for time to initial peak.

Within-day (test-retest) reliability

Mean differences

Systematic changes in the mean were typically absent for the within-day (test-retest) condition. The one exception to this was in the plateau phase when data were expressed as $\%APU_{44}$, for which the mean was larger during the second heating protocol. When examining the kinetics of the response, a systematic change in the mean was evident for the time to initial peak, for which the mean response was reduced during the second LTH protocol.

Coefficients of variation

At baseline, %CV values were rated as poor for all forms of data expression. For the initial vasodilatory peak and plateau phases, normalization to maximum heating, either as $\%APU_{44}$ or $\%CVC_{44}$, produced %CV values ranging between good to moderate (%CV=4.6% to 10.5%). For all other forms of data expression, %CV values were typically rated as poor. The exception to this was at maximum heating to 44°C, where %CV values (%CV=24.8% and 21.8%) were rated as moderate when data were expressed as APU or CVC, respectively. When examining the kinetics of

the response, the %CV values were rated as moderate for vasodilatory onset time (%CV=19.6%) and good for the time to initial peak (%CV=5.6%).

Intraclass correlation coefficients

Expressing data as either $\%APU_{44}$ or $\%CVC_{44}$ produced the strongest overall correlation coefficients for most LTH phases. However, ICC values for these forms of data expression still ranged widely across phases, with ratings between excellent and poor. When data were expressed as APU and CVC, ICC values rated as fair-to-good and when data were expressed as $\%APU_{BL}$ and $\%CVC_{BL}$, ICC values were rated as poor for all phases. When examining the kinetics of the response, ICC values were rated as poor for vasodilatory onset time and the time to initial peak.

Between-day reliability

Mean differences

Systematic changes in the mean were typically absent for the between-day condition. The one exception to this was for the plateau phase when data were expressed as APU, for which the mean was larger during the second heating protocol. This was, however, not evident for the plateau region with any other form of data expression. When examining the kinetics of the response, no systematic changes in the mean were present for vasodilatory onset time or time to initial peak.

Coefficients of variation

At baseline, %CV values were rated as poor for all forms of data expression. For the initial vasodilatory peak and plateau phases, normalization to maximum heating, either as $\%APU_{44}$ or $\%CVC_{44}$, produced %CV values ranging between good to moderate (%CV=5.6% to 12.6%). Expressing the data as raw APU or CVC produced moderate to poor ratings (%CV=19.3% to 25.6%) for the initial peak and plateau phases, and normalizing to baseline ($\%APU_{BL}$, $\%CVC_{BL}$) produced %CV values that were consistently rated as poor across all of these phases. When examining the kinetics of the response, the %CV value was rated as moderate for vasodilatory onset time (%CV=13.0%) and good for time to initial peak (%CV=5.6%).

Intraclass correlation coefficients

At baseline, the ICC value for $\%APU_{44}$ was rated as fair-to-good (ICC=0.41), while ICC values were rated as poor for all other forms of data expression. At the initial peak, ICC values were primarily rated as fair-to-good (ICC=0.40 to 0.69), except when normalized to baseline, which were rated as poor for $\%APU_{BL}$ and $\%CVC_{BL}$. For the plateau, ICC values were primarily rated as fair-to-good (ICC=0.49 to 0.67), except when normalized to baseline, which were rated as poor for $\%APU_{BL}$ and $\%CVC_{BL}$. At maximum heating, ICC values were mainly rated as fair-to-good (ICC=0.41 to 0.64), except for $\%CVC_{BL}$, which was rated as poor. When examining the kinetics of the local heating response, ICC values were rated as fair-to-good for vasodilatory onset time and time to initial peak (ICC=0.56 and 0.51, respectively).

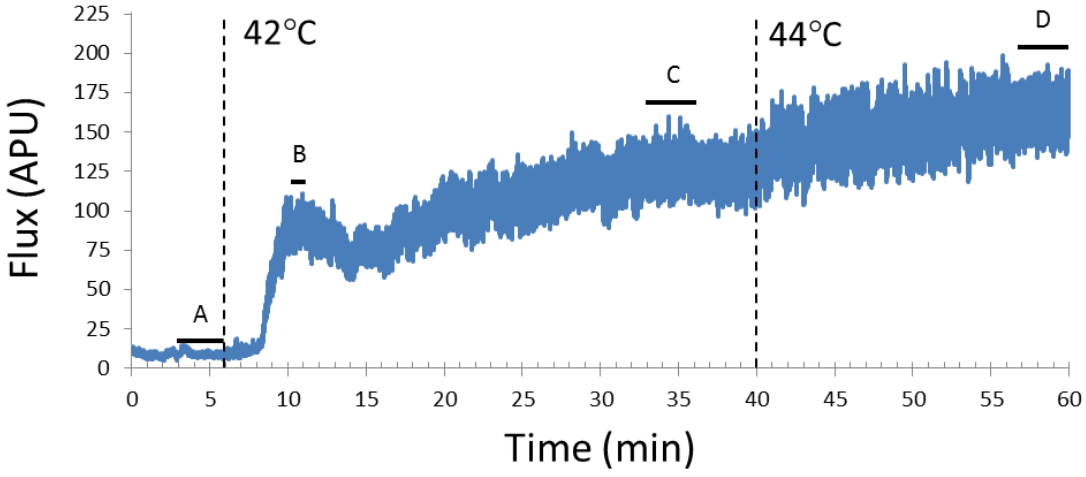

Figure 7.1 Representative cutaneous thermal hyperaemia response during local heating in non-glabrous forearm skin

Dashed vertical lines represent a change in local laser-Doppler probe temperature. A, baseline; B, initial vasodilatory peak; C, plateau; D, maximum local skin heating at 44°C.

Table 7.1 Temperature and haemodynamic conditions at the start of local thermal hyperaemia

	Within-day		
	Heat-1 (Day-1)	**Heat-2**	**Within-day *(Heat-2 – Heat-1*)**
	Mean (SD)	Mean (SD)	$Mean_{diff}$ [95%CI]
Temperatures			
T_{amb} (°C)	25.11 (0.18)	25.11 (0.14)	0.005 [-0.16, 0.17], p=0.95
T_{fa} (°C)	32.7 (0.6)	32.2 (1.0)	-0.5 [-1.0 -0.005], p=0.048*
$\bar{T}_{sk}$ (°C)	32.8 (0.6)	32.5 (0.6)	-0.3 [-0.5, -0.1], p=0.007*
Haemodynamics			
HR (bpm)	56.3 (6.2)	57.0 (8.0)	0.7 [-3.0, 4.4], p=0.67
MAP (mmHg)	85.1 (8.4)	88.9 (10.2)	3.8 [0.7, 6.9], p=0.02*
S_aO_2 (%)	97.0 (1.2)	97.6 (1.3)	0.6 [-0.2, 1.4], p=0.12

	Between-day		
	Day-1 (Heat-1)	**Day-2**	**Between-day (*Day-2* – Day-*1*)**
	Mean (SD)	Mean (SD)	$Mean_{diff}$ [95%CI]
Temperatures			
T_{amb} (°C)	25.1 (0.2)	25.2 (0.3)	0.1 [-0.2, 0.4], p=0.31
T_{fa} (°C)	32.7 (0.6)	31.6 (1.1)	-1.1 [-1.7, -0.6], p=0.001*
$\bar{T}_{sk}$ (°C)	32.8 (0.6)	32.7 (0.6)	-0.1 [-0.5, 0.3], p=0.46
Haemodynamics			
HR (bpm)	56.34 (6.22)	56.31 (9.64)	-0.03 [-3.81, 3.75], p=0.99
MAP (mmHg)	85.1 (8.4)	88.1 (5.8)	3.0 [-3.6, 9.6], p=0.33
S_aO_2 (%)	97.0 (1.2)	97.5 (1.3)	0.5 [0.04, 1.0], p=0.04*

*Significance was set to p<0.05. SD, standard deviation; CI, confidence interval; $Mean_{diff}$, mean difference between trials; T_{amb}, ambient air temperature; T_{fa}, forearm skin temperature; $\bar{T}_{sk}$, mean skin temperature; HR, heart rate; MAP, mean arterial pressure; S_aO_2, arterial oxygen saturation.

Table 7.2 Within-day (inter-site) reliability assessment of the local heating protocol for Heat-1

		$Mean_{diff}$	CV (%)	ICC
Baseline	APU	1.1 (-3.1, 5.3)	59.0 (37.7, 134.0)	-0.23 (-0.73, 0.44)
	$APU_{\%BL}$	---	---	---
	$APU_{\%44}$	1.0 (-2.2, 4.2)	58.1 (37.7, 131.6)	0.07 (-0.56, 0.64)
	CVC	0.01 (-0.03, 0.06)	59.0 (37.7, 134.0)	-0.04 (-0.63, 0.58)
	$CVC_{\%BL}$	---	---	---
	$CVC_{\%44}$	1.1 (-2.1, 4.2)	58.1 (37.7, 131.6)	0.04 (-0.58, 0.63)
Initial Peak	APU	-15.8 (-53.2, 21.5)	38.1 (24.6, 80.4)	0.16 (-0.49, 0.70)
	$APU_{\%BL}$	-411.6 (-896.8, 73.6)	46.7 (29.7, 101.3)	0.23 (-0.44, 0.73)
	$APU_{\%44}$	-0.7 (-8.2, 6.9)	13.5 (9.1, 25.9)	0.33 (-0.34, 0.78)
	CVC	-0.2 (-0.6, 0.3)	38.1 (24.6, 80.4)	0.28 (-0.39, 0.76)
	$CVC_{\%BL}$	-411.6 (-896.8, 73.6)	46.7 (29.7, 101.4)	0.23 (-0.44, 0.73)
	$CVC_{\%44}$	-0.6 (-8.1, 6.9)	13.5 (9.1, 25.9)	0.43 (-0.23, 0.82)
Plateau	APU	-13.7 (-58.0, 30.5)	33.6 (22.1, 69.9)	0.28 (-0.39, 0.76)
	$APU_{\%BL}$	-484.5 (-1136.2, 167.2)	55.2 (35.0, 122.6)	0.19 (-0.47, 0.71)
	$APU_{\%44}$	1.4 (-2.3, 5.2)	4.6 (3.1, 8.5)	0.63 (0.05, 0.89)
	CVC	-0.1 (-0.7, 0.4)	33.6 (22.1, 69.9)	0.39 (-0.28, 0.80)
	$CVC_{\%BL}$	-475.5 (-1125.6, 174.6)	55.2 (35.0, 122.6)	0.21 (-0.45, 0.72)
	$CVC_{\%44}$	1.5 (-2.3, 5.3)	4.6 (3.1, 8.5)	0.74 (0.24, 0.93)
Heat-44	APU	-18.6 (-74.2, 37.0)	35.4 (23.4, 73.3)	0.12 (-0.52, 0.67)
	$APU_{\%BL}$	-602.0 (-1444.9, 240.9)	58.1 (37.7, 85.2)	0.07 (-0.56, 0.64)
	$APU_{\%44}$	---	---	---
	CVC	-0.2 (-0.9, 0.4)	35.4 (23.4, 73.3)	0.17 (-0.48, 0.70)
	$CVC_{\%BL}$	-567.0 (-1406.9, 272.9)	58.1 (37.7, 131.6)	0.04 (-0.58, 0.63)
	$CVC_{\%44}$	---	---	---

*Significance set at $p<0.05$. Brackets represent 95% confidence limits. CV, coefficient of variation; ICC, intraclass correlation coefficient; $Mean_{diff}$, mean difference between trials; APU, arbitrary perfusion units; $APU_{\%BL}$, APU normalized to baseline; $APU_{\%44}$, APU normalized to maximum heating; CVC, cutaneous vascular conductance; $CVC_{\%BL}$, CVC normalized to baseline; $CVC_{\%44}$, CVC normalized to maximum heating. For CV, dark-gray shading represents good reliability (CV: <10%) and light-gray shading represents moderate reliability (CV: 10-25%). For ICC, dark-gray shading represents excellent reliability (ICC: >0.75) and light-gray shading represents fair-to-good reliability (ICC: 0.40-0.75).

Table 7.3 Within-day (test-retest) reliability assessment of the local heating protocol for Probe-1

		$Mean_{diff}$	**CV (%)**	**ICC**
Baseline	APU	0.5 (-2.5, 3.5)	31.5 (20.9, 64.9)	0.58 (-0.04, 0.88)
	$APU_{\%BL}$	---	---	---
	$APU_{\%44}$	0.7 (-1.4, 2.8)	36.1 (23.4, 75.1)	0.24 (-0.43, 0.73)
	CVC	0.001 (-0.03, 0.03)	30.5 (19.7, 63.2)	0.67 (0.12, 0.91)
	$CVC_{\%BL}$	---	---	---
	$CVC_{\%44}$	0.8 (-1.1, 2.7)	32.7 (20.9, 68.2)	0.36 (-0.31, 0.79)
Initial Peak	APU	1.8 (-15.2, 18.8)	25.1 (16.2, 50.7)	0.65 (0.07, 0.90)
	$APU_{\%BL}$	-17.9 (-324.6, 288.8)	32.7 (20.9, 68.2)	0.04 (-0.58, 0.63)
	$APU_{\%44}$	1.1 (-4.3, 6.4)	9.4 (6.4, 17.4)	0.78 (0.34, 0.94)
	CVC	-0.02 (-0.2, 0.2)	26.2 (17.4, 52.2)	0.75 (0.28, 0.93)
	$CVC_{\%BL}$	-17.9 (-324.6, 288.8)	32.7 (20.9, 68.2)	0.04 (-0.58, 0.63)
	$CVC_{\%44}$	2.1 (-4.3, 8.6)	10.5 (7.3, 19.7)	0.76 (0.28, 0.93)
Plateau	APU	8.3 (-19.8, 36.5)	25.6 (17.4, 52.2)	0.51 (-0.13, 0.85)
	$APU_{\%BL}$	49.2 (-448.2, 547.3)	38.5 (24.6, 80.4)	0.22 (-0.44, 0.73)
	$APU_{\%44}$	4.3 (0.3, 8.3)*	4.6 (3.1, 8.5)	0.67 (0.11, 0.91)
	CVC	0.01 (-0.3, 0.3)	25.1 (16.2, 50.7)	0.61 (0.01, 0.89)
	$CVC_{\%BL}$	34.8 (-439.9, 509.6)	37.8 (24.6, 80.4)	0.27 (-0.39, 0.75)
	$CVC_{\%44}$	4.9 (-0.3, 10.1)	6.5 (4.5, 12.7)	0.61 (0.01, 0.89)
Heat-44	APU	1.7 (-30.7, 34.2)	24.8 (16.2, 49.2)	0.56 (-0.06, 0.87)
	$APU_{\%BL}$	-41.5 (-589.7, 506.8)	36.1 (23.4, 75.1)	0.29 (-0.38, 0.76)
	$APU_{\%44}$	---	---	---
	CVC	-0.1 (-0.4, 0.2)	21.8 (15.0, 43.3)	0.64 (0.06, 0.90)
	$CVC_{\%BL}$	-69.1 (-583.4, 445.1)	32.7 (20.9, 68.2)	0.38 (-0.29, 0.80)
	$CVC_{\%44}$	---	---	---

*Significance set at $p<0.05$. Brackets represent 95% confidence limits. CV, coefficient of variation; ICC, intraclass correlation coefficient; $Mean_{diff}$, mean difference between trials; APU, arbitrary perfusion units; $APU_{\%BL}$, APU normalized to baseline; $APU_{\%44}$, APU normalized to maximum heating; CVC, cutaneous vascular conductance; $CVC_{\%BL}$, CVC normalized to baseline; $CVC_{\%44}$, CVC normalized to maximum heating. For CV, dark-gray shading represents good reliability (CV: <10%) and light-gray shading represents moderate reliability (CV: 10-25%). For ICC, dark-gray shading represents excellent reliability (ICC: >0.75) and light-gray shading represents fair-to-good reliability (ICC: 0.40-0.75).

Table 7.4 Between-day reliability assessment of the local heating protocol

		$Mean_{diff}$	CV (%)	ICC
Baseline	APU	0.2 (-4.0, 4.3)	45.0 (29.7, 97.4)	0.09 (-0.54, 0.66)
	$APU_{\%BL}$	---	---	---
	$APU_{\%44}$	-0.5 (-2.2, 1.3)	30.0 (19.7, 61.6)	0.41(-0.26, 0.81)
	CVC	-0.003 (-0.05, 0.05)	45.2 (29.7, 97.4)	0.23 (-0.44, 0.73)
	$CVC_{\%BL}$	---	---	---
	$CVC_{\%44}$	-0.6 (-2.5, 1.2)	33.2 (22.1, 68.2)	0.31 (-0.36, 0.77)
Initial Peak	APU	12.2 (-11.9, 36.2)	24.5 (16.2, 49.2)	0.40 (-0.26, 0.81)
	$APU_{\%BL}$	151.7 (-129.8, 433.1)	28.3 (18.5, 56.8)	0.28 (-0.39, 0.75)
	$APU_{\%44}$	-3.0 (-8.9, 2.9)	10.0 (6.7, 18.5)	0.69 (0.14, 0.91)
	CVC	0.1 (-0.2, 0.4)	25.3 (17.4, 50.7)	0.50 (-0.15, 0.85)
	$CVC_{\%BL}$	151.7 (-129.8, 433.1)	28.3, (18.5, 56.8)	0.28 (-0.39, 0.75)
	$CVC_{\%44}$	-5.4 (-12.7, 2.0)	12.6 (8.4, 24.6)	0.60 (-0.01, 0.88)
Plateau	APU	31.1 (0.1, 62.1)*	19.3 (12.7, 37.7)	0.67 (0.12, 0.91)
	$APU_{\%BL}$	369.2 (-141.3, 879.7)	35.0 (23.4, 73.3)	0.27 (-0.40, 0.75)
	$APU_{\%44}$	2.4 (-2.4, 7.2)	5.6 (3.9, 10.5)	0.49 (-0.15, 0.84)
	CVC	0.4 (-0.1, 0.8)	21.8 (15.0, 43.3)	0.64 (0.06, 0.90)
	$CVC_{\%BL}$	431.3 (-91.5, 954.1)	36.8 (24.6, 76.8)	0.18 (-0.47, 0.71)
	$CVC_{\%44}$	2.0 (-3.3, 7.3)	6.5 (4.5, 12.7)	0.54 (-0.10, 0.86)
Heat-44	APU	33.2 (-6.3, 72.7)	19.6 (12.7, 39.1)	0.64 (0.07, 0.90)
	$APU_{\%BL}$	384.5 (-127.6, 896.7)	30.0 (19.7, 61.6)	0.41 (-0.26, 0.81)
	$APU_{\%44}$	---	---	---
	CVC	0.4 (-0.1, 0.9)	22.4 (15.0, 44.8)	0.64 (0.05, 0.90)
	$CVC_{\%BL}$	497.6 (-74.0, 1069.2)	33.2 (22.1, 68.2)	0.31 (-0.36, 0.77)
	$CVC_{\%44}$	---	---	---

*Significance set at $p<0.05$. Brackets represent 95% confidence limits. CV, coefficient of variation; ICC, intraclass correlation coefficient; $Mean_{diff}$, mean difference between trials; APU, arbitrary perfusion units; $APU_{\%BL}$, APU normalized to baseline; $APU_{\%44}$, APU normalized to maximum heating; CVC, cutaneous vascular conductance; $CVC_{\%BL}$, CVC normalized to baseline; $CVC_{\%44}$, CVC normalized to maximum heating. For CV, dark-gray shading represents good reliability (CV: <10%) and light-gray shading represents moderate reliability (CV: 10-25%). For ICC, dark-gray shading represents excellent reliability (ICC: >0.75) and light-gray shading represents fair-to-good reliability (ICC: 0.40-0.75).

Table 7.5 Reliability assessment for the kinetics of the local heating protocol

	Within-day (inter-site)		
	Heat-1		
	$Mean_{diff}$	CV (%)	ICC
Vasodilatory onset (s)	0.4 (-7.4, 8.2)	7.3 (5.0, 13.9)	0.86 (0.54, 0.96)
Time to initial peak (s)	-10.9 (-23.6, 1.8)	4.6 (3.1, 8.5)	0.37 (-0.30, 0.80)
	Within-day (test-retest)		
	Probe-1		
	$Mean_{diff}$	CV (%)	ICC
Vasodilatory onset (s)	-8.0 (-26.5, 10.5)	19.6 (12.7, 39.1)	0.16 (-0.49, 0.70)
Time to initial peak (s)	-16.3 (-32.1, -0.5)*	5.6 (3.9, 10.5)	0.17 (-0.48, 0.70)
	Between-day		
	$Mean_{diff}$	CV (%)	ICC
Vasodilatory onset (s)	-7.0 (-21.0, 6.9)	13.0 (8.8, 24.6)	0.56 (-0.06, 0.87)
Time to initial peak (s)	-1.3 (-17.7, 15.2)	5.6 (3.9, 10.5)	0.51 (-0.13, 0.85)

*Significance set at $p<0.05$. Brackets represent 95% confidence limits. CV, coefficient of variation; $Mean_{diff}$, mean difference between trials; ICC, intraclass correlation coefficient; APU, arbitrary perfusion units; $APU_{\%BL}$, APU normalized to baseline; $APU_{\%44}$, APU normalized to maximum heating; CVC, cutaneous vascular conductance; $CVC_{\%BL}$, CVC normalized to baseline; $CVC_{\%44}$, CVC normalized to maximum heating. For CV, dark-gray shading represents good reliability (CV: <10%) and light-gray shading represents moderate reliability (CV: 10-25%). For ICC, dark-gray shading represents excellent reliability (ICC: >0.75) and light-gray shading represents fair-to-good reliability (ICC: 0.40-0.75).

7.4 Discussion

In the present study, reliability assessments demonstrated comparable results between LDF data in original units (APU) and when corrected for blood pressure (CVC), with data presented as raw values and when normalized to either baseline or maximum heating. For clarity and consistency with previous reliability studies, only the results from CVC data will be discussed further. The initial vasodilatory peak and plateau phases of the cutaneous LTH protocol in the forearm demonstrated good to moderate reliability when data were expressed as a percentage of maximum, and moderate to poor reliability when data were expressed either as raw CVC or as a percentage of baseline using single-point LDF in a group of young, healthy males. These results were equivalent for within-day (inter-site), within-day (test-retest), and between-day reliability assessments, which is consistent with the notion that reliability of skin blood flow measurements in the forearm is largely influenced by the spatial heterogeneity of the cutaneous microcirculation here (Braverman, 1997). When examining the kinetics of the response, both the vasodilatory onset time and the time to initial peak both demonstrated good to moderate reliability.

In the current study, the poor reliability observed at baseline and when data were normalized to a percentage of baseline is consistent with the significant spatial and temporal heterogeneity of cutaneous perfusion in the forearm under normothermic conditions (Braverman, 1997), as well as with reports of poor reliability at baseline in similar studies (Roustit *et al.*, 2010a; Roustit *et al.*, 2010b; Tew *et al.*, 2011). Roustit *et al.* (2010a) previously demonstrated that room temperature had a significant effect on baseline skin blood flow when using single-point LDF, although this influence was much larger in the glabrous skin of the index finger than in the non-glabrous skin of the forearm. In that study, local skin temperature was not controlled at baseline, which the authors noted as a possible reason for the poor reliability observed. In a separate study, the same group used an identical LTH protocol while clamping local baseline skin temperature at 33°C, and failed to demonstrate any improvement (Roustit *et al.*, 2010b). Likewise, baseline reliability remained poor in the current study despite efforts to minimize the

influence of temperature fluctuations on LDF measurements by tightly controlling both local skin (33°C) and room temperature (25°C).

In order to address the well-known issue of spatial heterogeneity in the cutaneous microcirculation of the forearm (Braverman, 1997), techniques such as laser speckle contrast imaging (LSCI), laser-Doppler imaging (LDI), and integrating-probe LDF have been developed, which all provide indices of skin blood flow over larger surface areas than single-point LDF (Roustit & Cracowski, 2012). Using LSCI, Roustit *et al.* (2010b) demonstrated moderate between-day reliability for both the initial vasodilatory peak (%CV=21%) and plateau (%CV=24%) phases of the LTH protocol when data were normalized to baseline. Conversely, LDI demonstrated poor within-day (inter-site) and between-day reliability when normalizing to baseline, which was attributed to the slow processing time of the instrument (Roustit *et al.*, 2010b). Using integrating-probe LDF, Tew *et al.* (2011) demonstrated poor baseline reliability when data were expressed as either a percentage of maximum or raw CVC. In the same study, normalizing to baseline also consistently demonstrated poor reliability. As such, the current data support previous claims that baseline values vary considerably in the forearm skin, and that normalization to baseline is generally not an appropriate form of data expression when examining cutaneous LTH.

Two previous studies examined the initial vasodilatory peak using single-point LDF and demonstrated generally poor within-day (inter-site) and between-day reliability for this phase of the response with all forms of data expression (Roustit *et al.*, 2010a; Roustit *et al.*, 2010b). In contrast, the current study demonstrated moderate to good between-day reliability for the initial vasodilatory peak when data were normalized to maximum, consistent with results previously reported using integrating-probe LDF (Tew *et al.*, 2011). Distinct differences between the current and previous LTH protocols using single-point LDF may explain this discrepancy. The first difference is the much slower heating rate used in the current study ($3°C \cdot min^{-1}$) compared to that used previously ($1°C \cdot s^{-1}$) (Roustit *et al.*, 2010a; Roustit *et al.*, 2010b). This slower heating rate is far less likely to induce pain in participants, and allowed for a more controlled development of the initial

peak during LTH compared to the very rapid heating method used previously. In the studies by Roustit *et al.* (2010a) and Roustit *et al.* (2010b), the initial vasodilatory peak was also evaluated using a 60 sec average, compared to the 30 sec average used in the current study. Since the initial peak typically develops rapidly within the first 5 minutes of local heating, with its rise and decay occurring within a ~1-2 min span, a 60 sec average was probably too broad to specifically capture the peak point itself and would have been more heavily influenced by differences in the rates of onset and decline in the peak between measurements. When data were normalized to maximum skin temperature, the most important difference between the current and prior studies that influenced reliability is likely the duration of local skin heating at 44°C. In the previous studies, heating at 44°C was only performed for 5 min to induce maximum vasodilatation (Roustit *et al.*, 2010a; Roustit *et al.*, 2010b), while in the current study, heating at 44°C was sustained for 20 min. Although it is certainly possible to obtain a maximum, steady state perfusion within the first 5 min of the response at 44°C, this is typically insufficient to achieve the desired result. Indeed, in the current study this response only occurred in 1 of the 50 LTH protocols evaluated, while in the other 49 protocols maximum steady state perfusion occurred between 10-20 min into the heating at 44°C. As such, it is argued that an inadequate duration of maximum heating is likely responsible for the relatively poor reliability reported in previous studies when normalizing to maximum perfusion (Roustit *et al.*, 2010a; Roustit *et al.*, 2010b). Roustit *et al.* (2010b) previously demonstrated superior between-day reliability for the initial vasodilatory peak with LSCI (%CV=9%) compared to single-point LDF (%CV=25%), while LDI (%CV=42%) demonstrated very poor reliability due to the slow recording speed of the instrument. This is in contrast to the current study, which demonstrated moderate between-day reliability for the initial vasodilatory peak (%CV=12.6%) using single-point LDF when data were expressed as a percentage of maximum CVC.

Two studies have examined the between-day reliability of the cutaneous LTH response during the plateau phase using integrating-probe LDF. Agarwal *et al.* (2010) demonstrated a CV of 9% when data were expressed as the absolute

increase in skin blood flow above baseline. However, in that study, a topical anaesthetic was used to inhibit the axon reflex, and local heating was only done at 41°C, which makes direct comparisons between studies difficult. Tew *et al.* (2011) examined between-day reliability of the LTH protocol in both young and older healthy males using a heating protocol that is more consistent with the one used in the current study. In the young group, these authors demonstrated moderate reliability (%CV=19%) when data were expressed as raw CVC and good reliability (%CV=4%) when data were expressed as a percentage of maximum, results which are almost identical to those reported in the current study.

At maximum heating, both LSCI (%CV=15%), and LDI (%CV=17%) previously demonstrated superior between-day reliability compared to single-point LDF (%CV=42%) when data were expressed as raw CVC (Roustit *et al.*, 2010b). Importantly, in the current study, when data were expressed as raw CVC, between-day reliability for single-point LDF at maximum heating (%CV=22.4%) was almost half that reported by Roustit *et al.* (2010b), and closer to the values reported by that group for LSCI and LDI, although the current results still demonstrate reduced reliability compared to those full-field techniques. It is important to note here that the heating protocol used for LSCI and LDI in the previous study was different than that used for single-point LDF. For the imaging devices, the temperature was set to 43°C and the heating controller used was a water perfused unit that worked at a much slower ($4°C \cdot min^{-1}$) rate (Roustit *et al.*, 2010b). As such, the heating rate used for LSCI and LDI were more similar to the one used in the current study, and therefore, likely allowed for the development of a stable plateau at maximum heating.

When examining within-day (test-retest) reliability, different skin sites were selected for the two LTH protocols in the current study. This approach is in contrast to some studies that have utilized a heat-reheat protocol on the same skin site of the calf to avoid the well-known issue of inter-site variability in non-glabrous skin when examining the cutaneous microcirculation (Stewart *et al.*, 2007; Medow *et al.*, 2008). Although those authors have claimed this approach to be reliable, the validity of a heat-reheat protocol has since been questioned, since the forearm skin is known to

be desensitized (lower maximal heating response) for up to 2 hours following the first heating period (Ciplak *et al.*, 2009; Frantz *et al.*, 2012). In addition, this approach also influences the involvement of adrenergic nerves in both limbs during the second bout of local heating (Del Pozzi & Hodges, 2015).

To overcome the issue of desensitization that is known to occur in the same skin site with longer duration local heating, Huang *et al.* (2012) evaluated the reliability of a shorter (5 min) protocol. These authors demonstrated moderate reliability (%CV=16.02% left arm; 17.31% right arm) for the peak when data were expressed as raw CVC, which contrasts with the poor reliability demonstrated in the current study. The time to peak for this protocol also demonstrated moderate reliability (%CV= 21.38% for right arm; 17.51% for left arm), compared to the good reliability demonstrated in the current study (%CV=5.6%). Importantly, although proven reliable, the validity of using a short duration heat-reheat protocol on the same skin site has not been evaluated, and the adrenergic response may be influenced to the same extent during the second heating bout as it is with longer duration local heating on the same skin site (Del Pozzi & Hodges, 2015).

Evaluating reliability using ICCs resulted in widely varying and inconsistent results. This is in agreement with previous studies using this approach for evaluating reliability of cutaneous LTH in the face (Svalestad *et al.*, 2010) and forearm (Roustit *et al.*, 2010a; Roustit *et al.*, 2010b; Tew *et al.*, 2011). The ICC is appropriately viewed as a measure of relative reliability, which indicates how consistent an individual's ranking in a group will be compared to others in that group during repeated testing (Weir, 2005). This is in contrast to the %CV, which can be considered a measure of absolute reliability, and indicates how consistent each individual's score will be with repeated testing (Weir, 2005). As such, it is not surprising that variation between-subjects has a major influence on the magnitude of the ICC, which underscores the relative nature of this measure. In essence, if participants have very similar scores on a test, the ICC values will be small even if the trial-to-trial variation is small for each participant. Conversely, if participants have very different scores from each other, an ICC will be large, even when individual variation is large between tests (Hopkins, 2000; Weir, 2005). As such,

homogeneous responses between individuals, coupled with relatively large within-subject variation (%CV) with some forms of data expression contributed to the inconsistency and generally poor reliability when evaluated using ICCs in the current study.

Overall, normalizing the data to a percentage of maximum CVC produced the most reliable results in the non-glabrous skin of the forearm. The rationale for using this approach is that when maximum vasodilatation is produced, resistance vessels will be completely relaxed. As such, all measurement sites will theoretically have the same vasomotor tone under these conditions, so changes relative to maximum CVC can be meaningfully compared among different sites (Johnson *et al.*, 2014). Although this approach is commonly used in forearm skin to avoid the issue of spatial heterogeneity, it is not necessarily appropriate to normalize data to maximum when comparing groups that may have different maximal heating responses, such as healthy controls versus diabetic or hypertensive patients with microvascular impairments, or during longitudinal studies where significant functional and/or structural changes are expected to occur over time.

In conclusion, data were presented for within-day (inter-site), within-day (test-retest), and between-day reliability of cutaneous LTH on the volar forearm using single-point LDF, in a group of young, healthy males. All three assessments demonstrated comparable reliability. Good to moderate reliability was demonstrated for the initial vasodilatory peak and for the plateau phase when data were expressed as a percentage of maximum; on the other hand, expressing the data as raw values or as a percentage of baseline, generally demonstrated moderate to poor reliability. In addition to these findings, good to moderate reliability was also obtained when examining the kinetics of the response, which has not been previously reported. In contrast to previous studies (Roustit *et al.*, 2010a; Roustit *et al.*, 2010b), it was demonstrated here that single-point LDF is comparable to both integrating-probe LDF (Tew *et al.*, 2011) and LSCI (Roustit *et al.*, 2010b) for assessing the initial vasodilatory peak and plateau phases of the cutaneous LTH response on the forearm when data are presented as a percentage of maximum and local skin heating at 44°C is sustained for ~20 min.

7.5 References

Agarwal SC, Allen J, Murray A & Purcell IF. (2010). Comparative reproducibility of dermal microvascular blood flow changes in response to acetylcholine iontophoresis, hyperthermia and reactive hyperaemia. *Physiol Meas* **31,** 1-11.

Braverman IM. (1997). The cutaneous microcirculation: Ultrastructure and microanatomical organization. *Microcirculation-London* **4,** 329-340.

Brunt VE & Minson CT. (2012). KCa channels and epoxyeicosatrienoic acids: major contributors to thermal hyperaemia in human skin. *J Physiol-London* **590,** 3523-3534.

Ciplak M, Pasche A, Heim A, Haeberli C, Waeber B, Liaudet L, Feihl F & Engelberger R. (2009). The Vasodilatory Response of Skin Microcirculation to Local Heating is Subject to Desensitization. *Microcirculation* **16,** 265-275.

Del Pozzi AT & Hodges GJ. (2015). To reheat, or to not reheat: that is the question: The efficacy of a local reheating protocol on mechanisms of cutaneous vasodilatation. *Microvascular Research* **97,** 47-54.

Frantz J, Engelberger RP, Liaudet L, Mazzolai L, Waeber B & Feihl F. (2012). Desensitization of Thermal Hyperemia in the Skin is Reproducible. *Microcirculation* **19,** 78-85.

Hopkins WG. (2000). Measures of reliability in sports medicine and science. *Sports Med* **30,** 1-15.

Huang CS, Wang SF & Tsai YF. (2012). Axon reflex-related hyperemia induced by short local heating is reproducible. *Microvasc Res* **84,** 351-355.

Johnson JM, Minson CT & Kellogg DL. (2014). Cutaneous Vasodilator and Vasoconstrictor Mechanisms in Temperature Regulation. *Compr Physiol* **4,** 33-89.

Johnson JM, Taylor WF, Shepherd AP & Park MK. (1984). Laser-Doppler measurement of skin blood flow - comparison with plethysmography. *Journal of Applied Physiology* **56,** 798-803.

Kellogg DL, Liu Y, Kosiba IF & O'Donnell D. (1999). Role of nitric oxide in the vascular effects of local warming of the skin in humans. *Journal of Applied Physiology* **86,** 1185-1190.

Medow MS, Glover JL & Stewart JM. (2008). Nitric oxide and prostaglandin inhibition during acetylcholine-mediated cutaneous vasodilation in humans. *Microcirculation* **15,** 569-579.

Minson CT. (2010). Thermal provocation to evaluate microvascular reactivity in human skin. *J Appl Physiol (1985)* **109,** 1239-1246.

Roustit M, Blaise S, Millet C & Cracowski JL. (2010a). Reproducibility and methodological issues of skin post-occlusive and thermal hyperemia assessed by single-point laser Doppler flowmetry. *Microvascular Research* **79,** 102-108.

Roustit M & Cracowski JL. (2012). Non-invasive assessment of skin microvascular function in humans: an insight into methods. *Microcirculation* **19,** 47-64.

Roustit M & Cracowski JL. (2013). Assessment of endothelial and neurovascular function in human skin microcirculation. *Trends Pharmacol Sci* **34,** 373-384.

Roustit M, Millet C, Blaise S, Dufournet B & Cracowski JL. (2010b). Excellent reproducibility of laser speckle contrast imaging to assess skin microvascular reactivity. *Microvasc Res* **80,** 505-511.

Saumet JL, Kellogg DL, Taylor WF & Johnson JM. (1988). Cutaneous laser-Doppler flowmetry - Influence of underlying muscle blood flow. *Journal of Applied Physiology* **65,** 478-481.

Stewart JM, Medow MS, Minson CT & Taneja I. (2007). Cutaneous neuronal nitric oxide is specifically decreased in postural tachycardia syndrome. *Am J Physiol Heart Circ Physiol* **293,** H2161-2167.

Svalestad J, Hellem S, Vaagbo G, Irgens A & Thorsen E. (2010). Reproducibility of transcutaneous oximetry and laser Doppler flowmetry in facial skin and gingival tissue. *Microvascular Research* **79,** 29-33.

Tew GA, Klonizakis M, Moss J, Ruddock AD, Saxton JM & Hodges GJ. (2011). Reproducibility of cutaneous thermal hyperaemia assessed by laser Doppler flowmetry in young and older adults. *Microvasc Res* **81,** 177-182.

Weir JP. (2005). Quantifying test-retest reliability using the intraclass correlation coefficient and the SEM. *J Strength Cond Res* **19,** 231-240.

Chapter 8: Influence of upper limb ischaemia-reperfusion injury on the sensory nerve response to local skin heating

8.1 Introduction

A hallmark of I-R injury is acute endothelial damage and microcirculatory dysfunction due to the rapid production of reactive oxygen species (ROS) at the onset of reperfusion, which reduces nitric oxide (NO) bioavailability and ultimately impairs microvascular vasodilator capacity (Harrison, 1997; Granger, 1999; Carden & Granger, 2000). Sensory afferent function may also be impaired due to hyperpolarization of these nerves during reperfusion (Lin *et al.*, 2002). In addition, stimulation of neuropeptide receptors throughout ischaemia and reperfusion may render them desensitized to a subsequent vasodilatory challenge (Wong *et al.*, 2005; Wong & Minson, 2006, 2011).

In the non-glabrous skin of the forearm, local heating generates a biphasic response that provides an integrative assessment of neurovascular and endothelial function (Johnson *et al.*, 2014). An initial vasodilatory peak occurs that is primarily mediated by sensory nerves (Minson *et al.*, 2001). In addition, noradrenergic fibres are also involved in modulating the response (Hodges *et al.*, 2009). During sustained local heating, a plateau develops in that is controlled primarily by NO (Kellogg *et al.*, 1999).

In Chapter 6, it was demonstrated that upper limb I-R injury impaired the vasodilatory response to a subsequent local heating stimulus in non-glabrous skin of the index finger by causing delays in the vasodilatory onset time and time to initial peak. Conversely, the vasodilatory response during sustained local heating was not altered by I-R injury. These previous findings suggest that acute I-R attenuates the cutaneous vasodilatory response to a subsequent local heating stimulus in non-glabrous skin via an impairment of sensory nerve function that influences the development of the initial vasodilatory peak. However, the influence of upper limb I-R on sensory nerve control of the cutaneous LTH response has not been directly evaluated.

Therefore, the current study sought to determine whether previously observed impairments of the initial vasodilatory peak during local heating of non-glabrous skin following I-R were due to sensory nerve involvement. As such, in the current study, the effects of I-R injury on the response to local skin heating in the non-glabrous skin of the forearm was compared with those of sensory nerve blockade using topical application of EMLA cream. It was hypothesized that I-R will be associated with an attenuation of the initial vasodilatory peak and delays in both the vasodilatory onset time and time to peak during local heating in the forearm, while the response to sustained local heating will remain unchanged. It was further hypothesized that the contribution of sensory nerves will be reduced post-ischaemia. Such a finding will further implicate sensory nerve impairment as a key mediator in the attenuated vasodilatory response to local skin heating following I-R.

8.2 Methods

8.2.1 Participants

The same ten healthy, active males as previously described in *Section 7.2.1* volunteered for this study.

8.2.2 Familiarization

Prior to the experiment, all participants completed a familiarization session. First, informed consent was obtained by the primary researcher as previously described in *Section 4.1*. Next, height (cm) and body mass (kg) were measured, after which, each participant underwent a full 20 min forearm cuff occlusion and reperfusion. This was done to give all participants the opportunity to experience the discomfort associated with the procedure so they could decide if they were unable or unwilling to go through with the rest of the experiment. This was also done to minimize participant anxiety during the actual experiment to avoid the influence of undue psychological strain on physiological measurements. The procedure for cuff occlusion and reperfusion is described further in the following section.

8.2.3 Experimental Protocol

Following the familiarization session, the participants took part in two, counterbalanced, experimental trials separated by ~7-14 days. One trial included forearm ischaemia-reperfusion and the other was a time-matched sham trial. This time-matched sham trial was the same experimental session as the within-day reliability trial described in Chapter 7. All participants followed the pre-experimental procedures previously described in *Section 4.4.* For the ischaemia trial, a total of four skin sites were selected on the volar forearm for LDF probe placement and were marked with indelible ink. The four selected sites formed a square pattern over the skin surface and all were at least 5 cm apart from each other to avoid interference. Initially, two sites that were equidistant from the cuff were selected and one was randomly chosen as an untreated (UNTR) control site and the other was chosen to receive topical anaesthetic (EMLA) cream treatment (EMLA® 2.5% lidocaine and 2.5% prilocaine, AstraZeneca, Wilmington, DE, USA). Approximately 2.5 g of the cream was applied to the forearm over an area of skin roughly equivalent to 4 cm^2. An occlusive dressing (Tegaderm™, 3M, London, ON, Canada) was placed over the applied cream, which remained in place for 1 h. The EMLA cream was then wiped clear and a second application was applied for an additional hour. Prior work using this approach has demonstrated that sensory nerve blockade with two, 1 h applications of EMLA cream typically blocks sensory nerve function for >3.5 h (Hodges *et al.*, 2015; Hodges *et al.*, 2016). Approximately 15 min following the second application of EMLA cream at the first site, a new application was started at a separate skin site, following the same procedure described above. Staggering of the anaesthetic cream applications on the two EMLA sites by ~60 min allowed for separate comparisons between UNTR and EMLA skin sites before and after the period of ischaemia and reperfusion. At each EMLA site, immediately following removal of the second application of cream and again after the LTH protocol for that site, sensory nerve blockade over the area of interest was verified using a common approach, whereby the primary investigator alternated between gently brushing, pricking, and pinching the skin on and around the EMLA site with a set of tweezers (Hodges *et al.*, 2015; Hodges *et al.*, 2016).

Following the procedures described above, the participants rested quietly in the temperature-controlled room for the final 30 min of anaesthetic application for the first site, while being instrumented as described in *Section 4.6*. Baseline measurements were recorded for ~20 min to ensure stable LDF and skin temperature values. At this point, the local heating disc temperature on the first set of UNTR and EMLA sites was increased according to the LTH protocol described in *Section 4.8*. Following the first LTH protocol, the LDF probes were removed and the participants were allowed to void their bladders and stretch. Subsequently, the LDF probes were placed on the second set of UNTR and EMLA sites. Following establishment of a new baseline, a standard blood pressure cuff, which was placed around the upper arm, was manually inflated to a pressure of 220 mmHg as fast as possible and held for 20 min. The cuff was then rapidly deflated and the arm was allowed to reperfuse for 20 min, at which point the second LTH protocol began. The protocol for the sham trial was identical to that for the ischaemia trial, except for the fact that the cuff was not inflated and only UNTR skin sites were evaluated.

8.2.4 Data processing and statistical analysis

A natural logarithmic transformation was applied to all individual variables of the LTH response prior to analysis in order to reduce non-uniformity of error. The percent contribution of sensory nerve function pre- and post-ischaemia were determined by calculating the mean difference between the UNTR and EMLA skin sites of the log-transformed data and subsequently the antilog of each value was calculated to convert it to an exact percentage as previously described in *Section 5.2.4*. This approach is equivalent to the technique previously described by Wong (2013) for determining the percent contribution in the natural scale.

All outcome measures were normally distributed. The data were considered to be normally distributed when visual examination of Q-Q plots and frequency histograms indicated that they followed a Gaussian distribution, combined with skewness values $<\pm 3$ and kurtosis values $<\pm 8$ (Kline, 2005).

Paired t-tests were used to compare temperature and haemodynamic data at the beginning of each LTH protocol before and after ischaemia. Comparisons

between the four skin sites for each phase of the LTH protocol were examined using a repeated-measures, one-way ANOVA. When the assumption of sphericity was violated, the degrees of freedom were adjusted using the Greenhouse-Geisser correction. Significant main effects were followed up using the uncorrected Fisher's least significant difference test to evaluate pairwise multiple comparisons (Perneger, 1998).

Inferences were made about the true (population) value for the effects of I-R injury alone (UN-PST – UN-PRE) and the combined I-R injury and EMLA treatment (EM-PST – UN-PRE). Additionally, inferences were made about the true effect for sensory nerve contribution pre-ischaemia (UN-PRE – EM-PRE) and post-ischaemia (UN-PST – EM-PST). The uncertainty of each observed effect was expressed as 90% confidence limits and as likelihoods that the true value of the effect represents a substantial percentage change, in either the negative or positive direction (Hopkins, 2002; Batterham & Hopkins, 2006). For the purpose of the current study, a positive change represents either an increase in skin blood flow or a delay in the kinetics of the response, where relevant. An effect was deemed unclear if its 90% CI overlapped the thresholds for substantially positive and substantially negative, which corresponds to an unclear effect having both a >5% chance of being positive and a >5% chance of being negative. The threshold value for the smallest important positive effect for each LTH parameter was defined by the relevant within-day (test-retest) %CV derived from Chapter 5 for the same group of participants. The region defined by +/- values for the %CV was considered to represent a trivial effect. For each effect that was identified as clear, the %Chance of it being negative, trivial, or positive were subsequently calculated according to the approach developed by Hopkins (2007), based on the unadjusted p-value of the pairwise comparison, its uncertainty (90% confidence limits), the magnitude of the observed effect (Mean %Change), and the threshold value for the smallest important positive effect (%CV). Qualitative probability terms describing the chances for each effect were defined by the following default ranges (Hopkins, 2002):

- <1%, almost certainly not;

- 1-5%, very unlikely;
- 5-25%, unlikely;
- 25-75%, possibly;
- 75-95%, likely;
- 95-99%, very likely;
- >99%, almost certainly

Grouped data for temperature and haemodynamic variables are presented as Mean (SD). Grouped data for components of the LTH response are presented as Mean (CV), where CV represents a factor change from the mean. Pairwise differences are presented as the $Mean_{diff}$ [90% CI]. Statistical significance was assumed at $p<0.10$, unless stated otherwise. All statistics were performed using GraphPad Prism 6 (GraphPad Software Inc., La Jolla, CA, USA).

8.3 Results

A representative tracing of the LTH response in the forearm is presented in Figure 7.1. Grouped temperature and haemodynamic variables at the start of LTH before and after ischaemia are presented in Table 8.1. No significant differences were observed for any temperature or haemodynamic variable at the start of the LTH protocol before and after ischaemia and reperfusion.

8.3.1 Baseline

At baseline, the CVC values for untreated skin sites were 0.09 $APU \cdot mmHg^{-1}$ (CV 1.49) pre I-R and 0.11 $APU \cdot mmHg^{-1}$ (CV 1.50) post I-R, demonstrating a significant increase in baseline perfusion following I-R (23.7% [3.6 to 47.6%], p=0.06) (Fig. 8.1.A). Baseline CVC values for the EMLA-treated skin sites were 0.09 $APU \cdot mmHg^{-1}$ (CV 1.68) pre I-R and 0.12 $APU \cdot mmHg^{-1}$ (CV 2.52) post I-R, which were not significantly different (25.6% [-10.4 to 76.0], p=0.25). EMLA sites were not significantly different from untreated skin sites pre I-R (2.9% [-22.6 to 36.8%], p=0.86), or post I-R (4.4% [-40.4 to 83.1%], p=0.89). Finally, the post I-R, EMLA-treated skin site was not significantly different from the untreated, pre I-R skin site (29.2% [-16.6 to 100.0%], p=0.31).

The true effect of I-R alone on baseline CVC was *possibly trivial* (0.0%/69.9%/30.1%) and the true effect of combined I-R and EMLA treatment was also *possibly trivial* (2.8%/48.8%/48.4%) (Fig. 8.2). The true effect of sensory nerve blockade on baseline CVC was *very likely trivial* (0.6%/98.3%/1.1%) pre I-R and *UNCLEAR* (6.4%/83.7%/9.9%) post I-R (Fig. 8.2).

8.3.2 Initial vasodilatory peak

At the initial vasodilatory peak, the CVC values for untreated skin sites were 1.12 $APU \cdot mmHg^{-1}$ (CV 1.31) pre I-R and 0.77 $APU \cdot mmHg^{-1}$ (CV 1.79) post I-R, demonstrating a significant attenuation of the initial peak following I-R (-31.2% [-51.5 to -2.3%], p=0.08) (Fig. 8.1.B). The initial peak CVC values for the EMLA-treated skin sites were 0.47 $APU \cdot mmHg^{-1}$ (CV 1.73) pre I-R and 0.59 $APU \cdot mmHg^{-1}$ (CV 1.55) post I-R, which were not significantly different (25.9% [-4.4 to 65.7%], p=0.16). The EMLA sites were significantly reduced compared to the untreated skin sites pre I-R (-57.8% [-69.0 to -42.7%], p=0.0006) and post I-R (-22.9% [-40.2 to -0.6%], p=0.09). Finally, the post I-R, EMLA-treated skin site was significantly attenuated, relative to the untreated, pre I-R skin site (-46.9% [-58.0 to -32.9%], p=0.0008).

The true effect of I-R on the initial peak was *likely negative* (76.2%/23.2%/0.5%), and the true effect of combined I-R and EMLA treatment was *almost certainly negative* (99.4%/0.6%/0.0%) (Fig. 8.3). The true effect of sensory nerve blockade on the initial peak was *almost certainly negative* (99.5%/0.5%/0.0%) pre I-R and *possibly* trivial (32.9%/67.0%/0.1%) post I-R (Fig. 8.3).

8.3.3 Plateau

At the plateau, the CVC values for the untreated skin sites were 1.74 $APU \cdot mmHg^{-1}$ (CV 1.38) pre I-R and 1.15 $APU \cdot mmHg^{-1}$ (CV 1.73) post I-R, demonstrating a significant attenuation of the plateau following I-R (-34.1% [-53.4 to -6.7%], p=0.06) (Fig. 8.1.C). The plateau CVC values for the EMLA-treated skin sites were 1.49 $APU \cdot mmHg^{-1}$ (CV 1.70) pre I-R and 1.26 $APU \cdot mmHg^{-1}$ (CV 1.59) post I-R, which were not significantly different (-15.8% [-41.6 to 21.4%], p=0.41).

The EMLA sites were not significantly different from untreated skin sites pre I-R (-14.2% [-39.4 to 21.5%], p=0.44) or post I-R (9.7% [-19.8 to 50.0%], p=0.60). Finally, the post I-R, EMLA-treated skin site was significantly attenuated, relative to the untreated, pre I-R skin site (-27.7% [-44.0 to -6.7%], p=0.04).

The true effect of I-R on the plateau was *likely negative* (82.7%/16.8%/0.5%) and the true effect of combined I-R and EMLA treatment was also *likely negative* (76.2%/23.7%/0.1%) (Fig. 8.4). The true effect of sensory nerve blockade on the plateau was *possibly trivial* (24.5%/73.3%/2.2%) pre I-R and *likely trivial* (2.6%/83.6%/13.9%) post I-R (Fig. 8.4).

8.3.4 Maximum skin heating

At maximum skin heating to 44°C, the CVC values for the untreated skin sites were 2.12 $APU \cdot mmHg^{-1}$ (CV 1.42) pre I-R and 1.40 $APU \cdot mmHg^{-1}$ (CV 1.62) post I-R, demonstrating a significant reduction in CVC at maximum heating following I-R (-33.8% [-52.6 to -7.4%], p=0.05) (Fig. 8.1.D). The maximum CVC values for the EMLA-treated skin sites were 1.83 $APU \cdot mmHg^{-1}$ (CV 1.55) pre I-R and 1.44 $APU \cdot mmHg^{-1}$ (CV 1.59) post I-R, which were not significantly different (-21.4% [-40.9 to 4.5%], p=0.15). The EMLA sites were not significantly different from the untreated skin sites pre I-R (-13.5% [-37.7 to 20.0%] p=0.44) or post I-R (2.6% [-18.1 to 28.6%], p=0.84). Finally, the post I-R, EMLA-treated skin site was significantly attenuated, relative to the untreated, pre I-R skin site (-32.0% [-48.7 to -10.0%], p=0.03).

The true effect of I-R on the CVC at maximum skin heating was *likely negative* (86.6%/13.0%/0.4%) and the true effect of combined I-R and EMLA treatment was also *likely negative* (88.0%/11.8%/0.2%) (Fig. 8.5). The true effect of sensory nerve blockade at maximum skin heating was *likely trivial* (20.1%/78.2%/1.7%) pre I-R and *very likely trivial* (1.3%/96.1%/2.6%) post I-R (Fig. 8.5).

8.3.5 Vasodilatory onset time

The vasodilatory onset times for untreated skin sites were 105.6 s (CV 1.19) pre I-R and 141.5 s (CV 1.23) post I-R, demonstrating a significant delay in the onset of vasodilatation following I-R (34.0% [20.5 to 48.9%], p=0.0007) (Fig. 8.6.A). The

onset times for the EMLA-treated skin sites were 180.5 s (CV 1.23) pre I-R and 172.4 s (CV 1.52) post I-R, which were not significantly different (-4.5% [-22.3 to 17.4%], p=0.69). The EMLA sites were significantly delayed relative to the untreated skin sites pre I-R (71.0% [48.4 to 97.1%], p<0.0001), but not post I-R (21.9% [-3.2 to 53.6%], p=0.15). Finally, the post I-R, EMLA-treated skin site was significantly delayed, relative to the untreated, pre I-R skin site (63.3% [26.5 to 110.9%], p=0.006).

The true effect of I-R on the vasodilatory onset time was *likely positive* (0.0%/11.6%/88.4%) and the true effect of combined I-R and EMLA treatment was *very likely positive* (0.0%/3.9%/96.1%) (Fig. 8.7). The true effect of sensory nerve blockade on vasodilatory onset time was *almost certainly positive* (0.0%/0.0%/100.0%) pre I-R and *likely positive* (2.9%/15.0%/82.2%) post I-R (Fig. 8.7).

8.3.6 Time to initial peak

The time to initial peak for the untreated skin sites were 272.3 s (CV 1.09) pre I-R and 275.1 s (CV 1.13) post I-R, which were not significantly different (1.0% [-7.8 to 10.6%], p=0.85) (Fig. 8.6.B). The time to peak for the EMLA-treated skin sites were 329.0 s (CV 1.25) pre I-R and 305.8 s (CV 1.29) post I-R, which were not significantly different (-7.0% [-15.3 to 2.1%], p=0.19). The EMLA sites were significantly delayed relative to the untreated skin sites pre I-R (20.7% [6.1 to 37.3%], p=0.03), but not post I-R (11.1% [-5.3 to 30.4%], p=0.26). Finally, the post I-R, EMLA-treated skin site was not significantly different from the untreated, pre I-R skin site (12.2% [-4.5 to 31.9%], p=0.22).

The true effect of I-R on the time to initial peak was *UNCLEAR* (10.9%/70.3%/18.8%) and the true effect of the combined I-R and EMLA treatment was *possibly positive* (4.0%/22.4%/73.7%) (Fig. 8.8). The true effect of sensory nerve blockade on the time to initial peak was *very likely positive* (0.5%/3.8%/95.7%) pre I-R and *UNCLEAR* (5.8%/20.4%/73.8%) post I-R (Fig. 8.8).

Table 8.1 Temperature and Haemodynamic Conditions at the start of local skin heating

	Pre	**Post**	**(Post - Pre)**
	Mean (SD)	Mean (SD)	$Mean_{diff}$ [95%CI]
Temperatures			
T_{amb} (°C)	25.2 (0.3)	25.3 (0.2)	0.1 [-0.2, 0.3], p=0.62
T_{fa} (°C)	31.6 (1.1)	31.7 (0.9)	0.1 [-0.3, 0.6], p=0.51
$\overline{T}_{sk}$ (°C)	32.7 (0.6)	32.4 (0.5)	-0.3 [-0.6, 0.1], p=0.10
Haemodynamics			
HR (bpm)	56.3 (9.6)	56.6 (10.1)	0.3 [-2.1, 2.8], p=0.76
MAP (mmHg)	88.1 (5.8)	88.8 (10.2)	0.7 [-5.2, 6.6], p=0.80
S_aO_2 (%)	97.5 (1.3)	97.9 (1.2)	0.4 [-0.2, 1.0], p=0.19

Significance was set to $p<0.05$. SD, standard deviation; CI, confidence interval; $Mean_{diff}$, mean difference between trials; T_{amb}, ambient air temperature; T_{fa}, forearm skin temperature; $\overline{T}_{sk}$, mean skin temperature; HR, heart rate; MAP, mean arterial pressure; S_aO_2, arterial oxygen saturation.

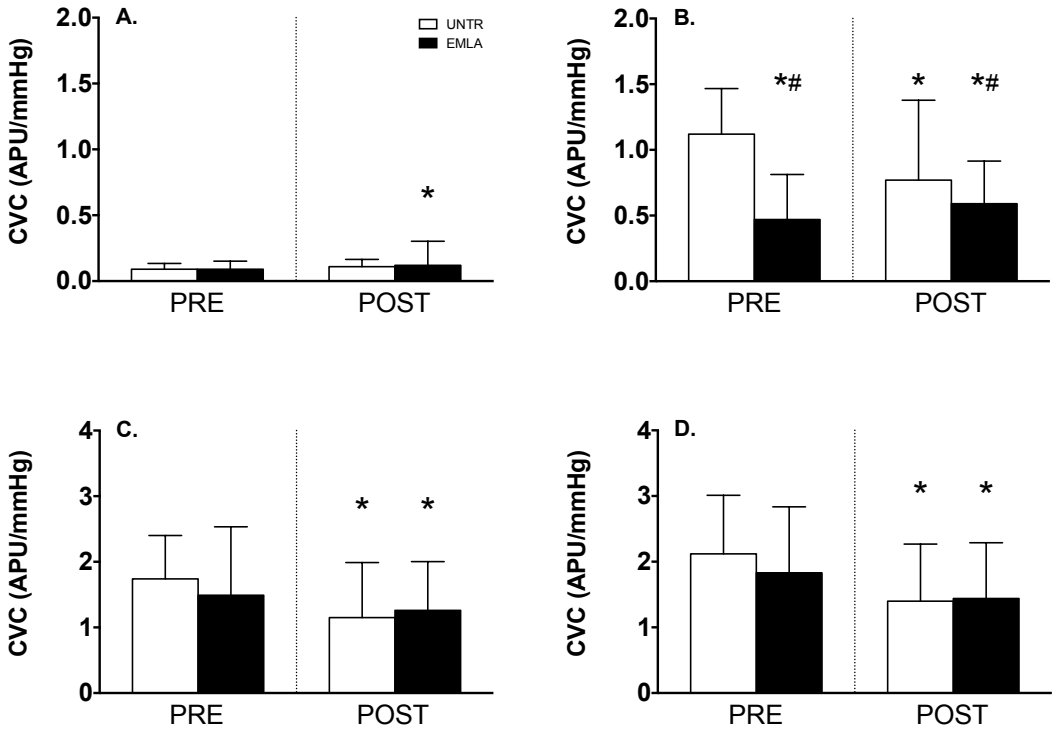

Figure 8.1 Cutaneous vascular conductance for all skin sites in the forearm

A, Baseline; B, Initial vasodilatory peak; C, Plateau; D, Maximum heating at 44°C. APU, arbitrary perfusion units; CVC, cutaneous vascular conductance; UN-PRE, untreated, pre-ischaemia condition; EM-PRE, sensory nerve blockade, pre-ischaemia condition; UN-PST, untreated, post-ischaemia condition; EM-PST, sensory nerve blockade, post-ischaemia condition. *p<0.10 v. UN-PRE; #p<0.10 v. UN-PST.

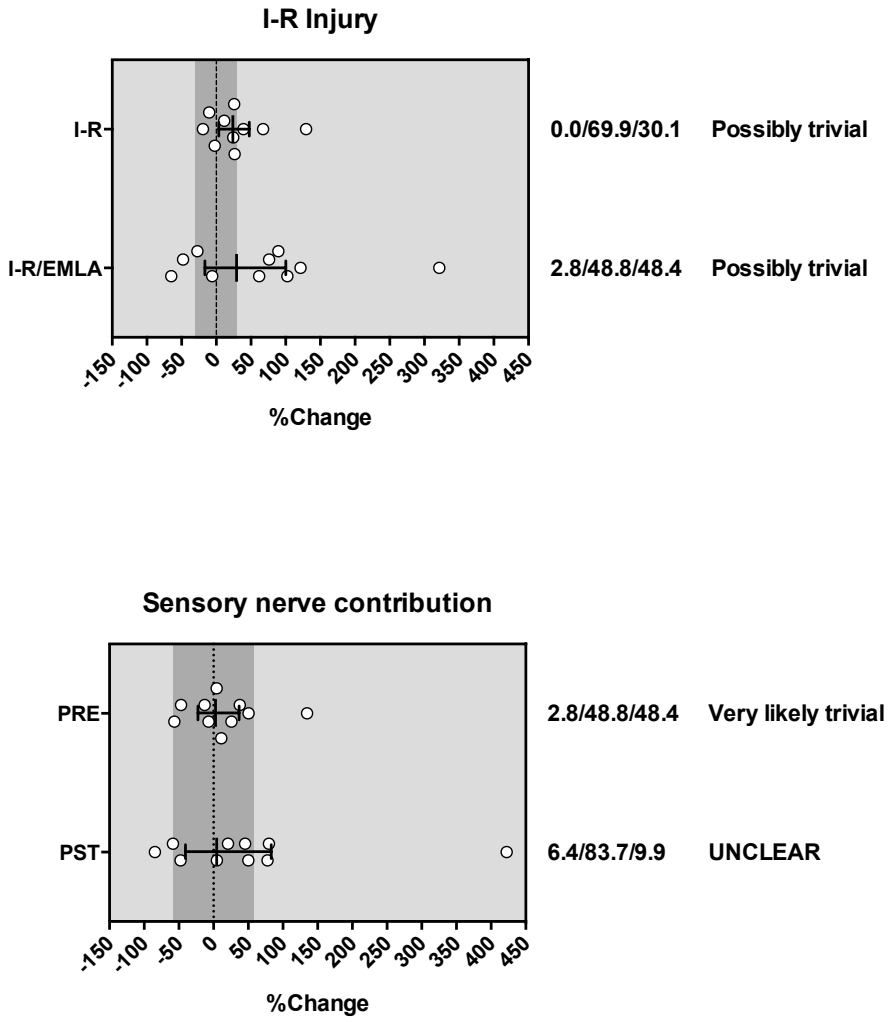

Figure 8.2 Baseline: Percent change for the effects of I-R injury (ISCH-SHAM) and the contribution of sensory nerves (EMLA-UNTR)

Dark shaded areas represents the relevant within-subject coefficient of variation (CV) derived from Chapter 7. I-R, ischaemia-reperfusion; I-R/EMLA, ischaemia-reperfusion and sensory nerve blockade; PRE, pre-ischaemia condition; PST, post-ischaemia condition. Black bar represents mean percentage difference with 90% confidence limits. White circles represent individual responses. Qualitative inferences are based on the presence or absence of a substantial effect, defined as Mean difference being outside of the test-retest CV determined for each variable in Chapter 7. If the chance of being substantially positive and negative were both >5%, true effect was assessed as UNCLEAR (could be positive or negative). Otherwise, chances of being positive or negative were assessed as follows: <1%, almost certainly not; 1-5%, very unlikely; 5-25%, unlikely; 25-75%, possibly; 75-95%, likely; 95-99%, very unlikely; >99%, almost certainly.

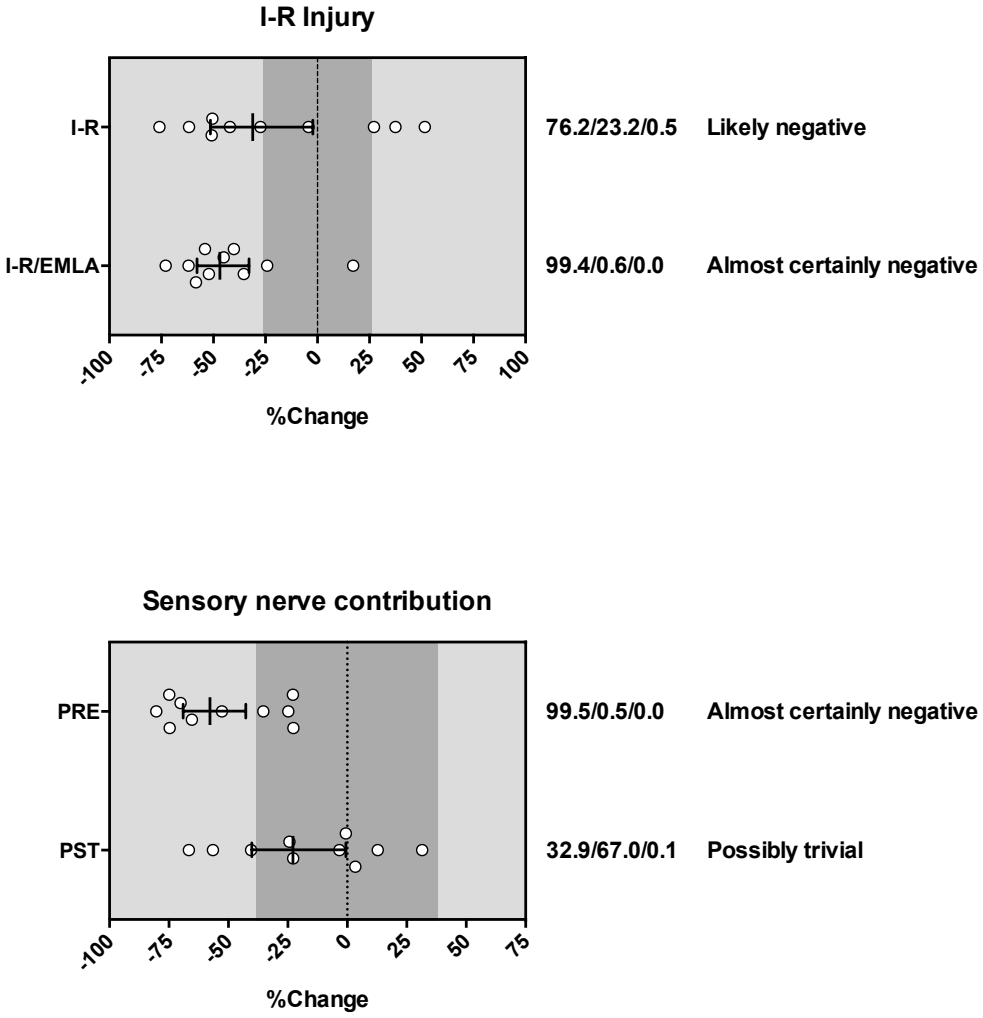

Figure 8.3 Initial vasodilatory peak: Percent change for the effects of I-R injury (ISCH-SHAM) and the contribution of sensory nerves (EMLA-UNTR)

Dark shaded areas represents the relevant within-subject coefficient of variation (CV) derived from Chapter 7. I-R, ischaemia-reperfusion; I-R/EMLA, ischaemia-reperfusion and sensory nerve blockade; PRE, pre-ischaemia condition; PST, post-ischaemia condition. Black bar represents mean percentage difference with 90% confidence limits. White circles represent individual responses. Qualitative inferences are based on the presence or absence of a substantial effect, defined as Mean difference being outside of the test-retest CV determined for each variable in Chapter 7. If the chance of being substantially positive and negative were both >5%, true effect was assessed as UNCLEAR (could be positive or negative). Otherwise, chances of being positive or negative were assessed as follows: <1%, almost certainly not; 1-5%, very unlikely; 5-25%, unlikely; 25-75%, possibly; 75-95%, likely; 95-99%, very unlikely; >99%, almost certainly.

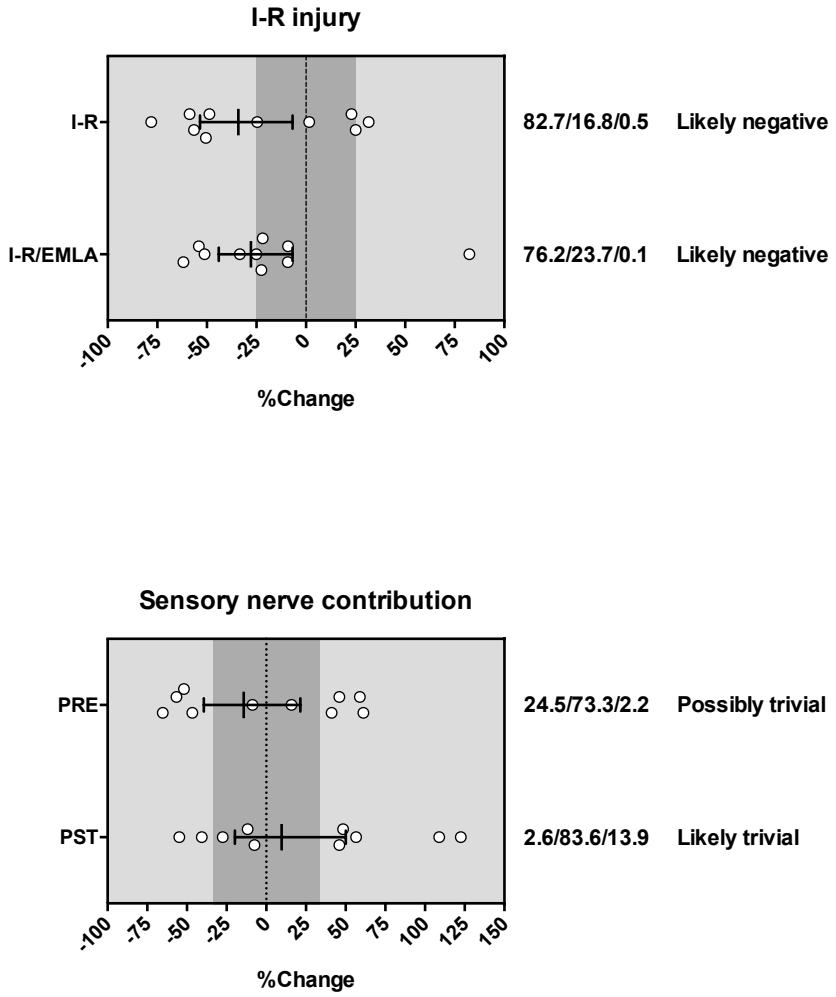

Figure 8.4 Plateau: Percent change for the effects of I-R injury (ISCH-SHAM) and the contribution of sensory nerves (EMLA-UNTR)

Dark shaded areas represents the relevant within-subject coefficient of variation (CV) derived from Chapter 7. I-R, ischaemia-reperfusion; I-R/EMLA, ischaemia-reperfusion and sensory nerve blockade; PRE, pre-ischaemia condition; PST, post-ischaemia condition. Black bar represents mean percentage difference with 90% confidence limits. White circles represent individual responses. Qualitative inferences are based on the presence or absence of a substantial effect, defined as Mean difference being outside of the test-retest CV determined for each variable in Chapter 7. If the chance of being substantially positive and negative were both >5%, true effect was assessed as UNCLEAR (could be positive or negative). Otherwise, chances of being positive or negative were assessed as follows: <1%, almost certainly not; 1-5%, very unlikely; 5-25%, unlikely; 25-75%, possibly; 75-95%, likely; 95-99%, very unlikely; >99%, almost certainly.

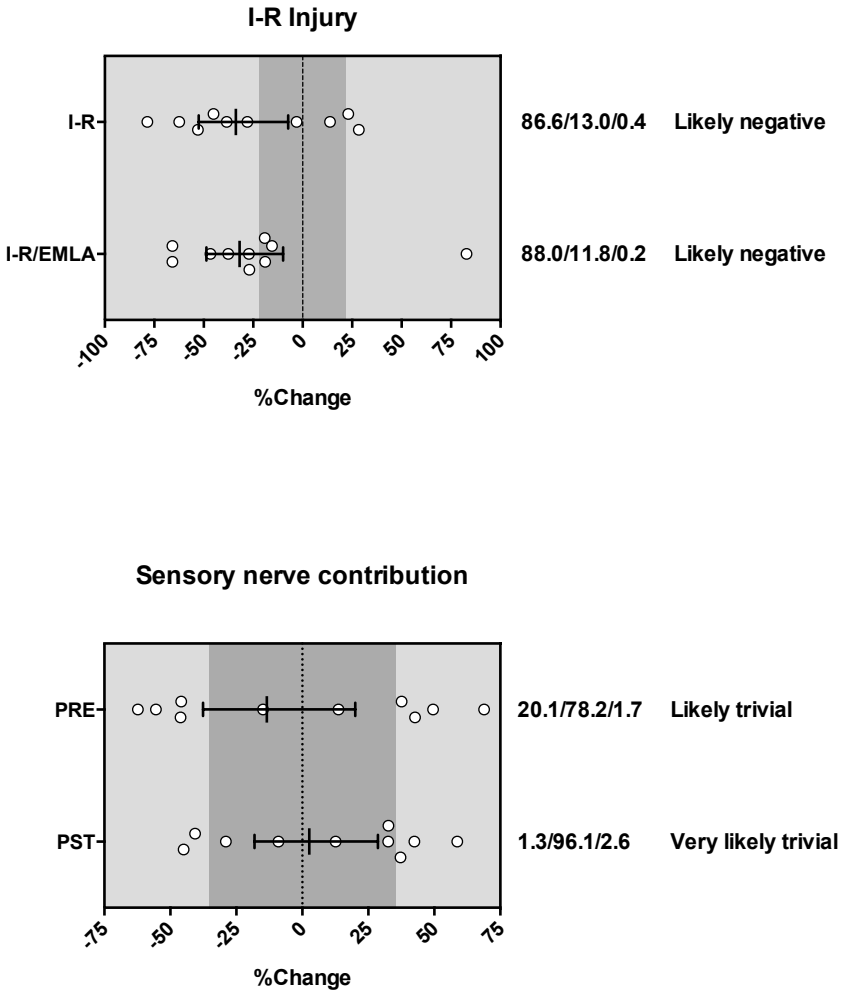

Figure 8.5 Maximum heating: Percent change for the effects of I-R injury (ISCH-SHAM) and the contribution of sensory nerves (EMLA-UNTR)

Dark shaded areas represents the relevant within-subject coefficient of variation (CV) derived from Chapter 7. I-R, ischaemia-reperfusion; I-R/EMLA, ischaemia-reperfusion and sensory nerve blockade; PRE, pre-ischaemia condition; PST, post-ischaemia condition. Black bar represents mean percentage difference with 90% confidence limits. White circles represent individual responses. Qualitative inferences are based on the presence or absence of a substantial effect, defined as Mean difference being outside of the test-retest CV determined for each variable in Chapter 7. If the chance of being substantially positive and negative were both >5%, true effect was assessed as UNCLEAR (could be positive or negative). Otherwise, chances of being positive or negative were assessed as follows: <1%, almost certainly not; 1-5%, very unlikely; 5-25%, unlikely; 25-75%, possibly; 75-95%, likely; 95-99%, very unlikely; >99%, almost certainly.

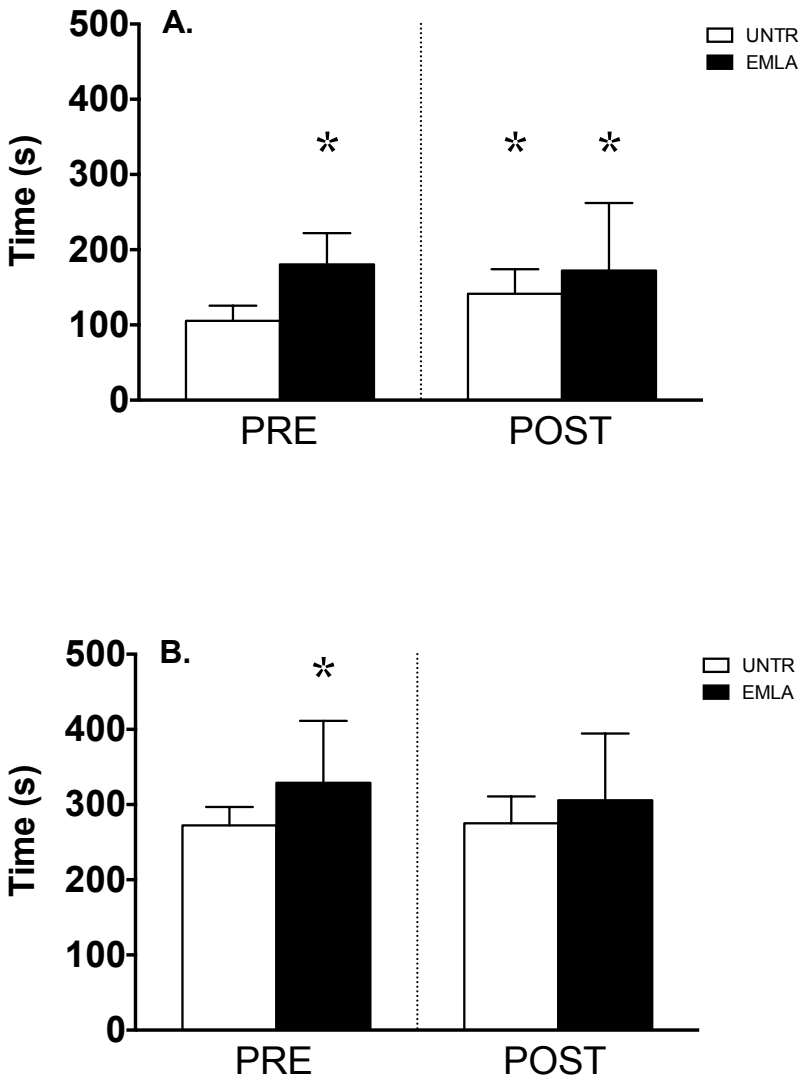

Figure 8.6 Kinetics for all skin sites in the forearm

A, Vasodilatory onset time; B, Time to initial peak; UN-PRE, untreated pre-ischaemia condition; EM-PRE, sensory nerve blockade, pre-ischaemia condition; UN-PST, untreated post-ischaemia condition; EM-PST, sensory nerve blockade, post-ischaemia condition. *p<0.10 v. UN-PRE.

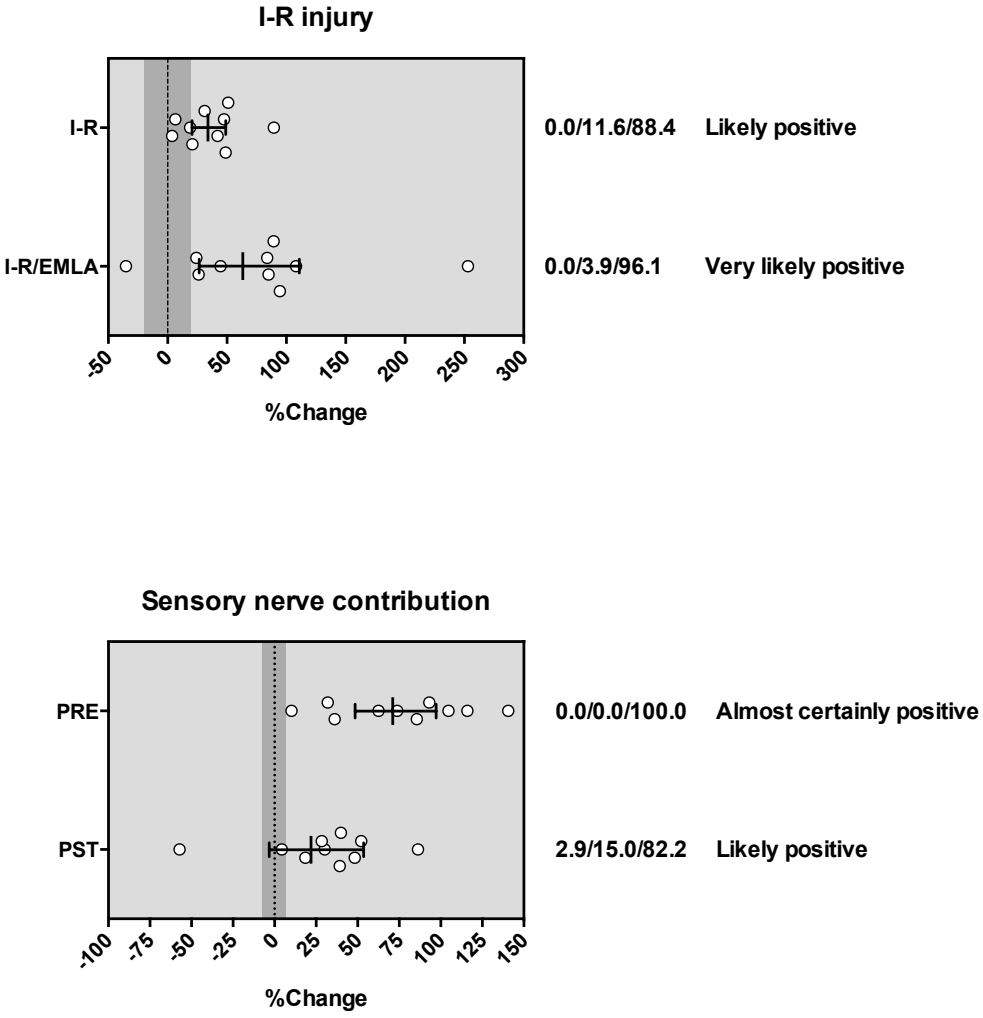

Figure 8.7 Vasodilatory onset time: Percent change for the effects of I-R injury (ISCH-SHAM) and the contribution of sensory nerves (EMLA-UNTR)

Dark shaded areas represents the relevant within-subject coefficient of variation (CV) derived from Chapter 7. I-R, ischaemia-reperfusion; I-R/EMLA, ischaemia-reperfusion and sensory nerve blockade; PRE, pre-ischaemia condition; PST, post-ischaemia condition. Black bar represents mean percentage difference with 90% confidence limits. White circles represent individual responses. Qualitative inferences are based on the presence or absence of a substantial effect, defined as Mean difference being outside of the test-retest CV determined for each variable in Chapter 7. If the chance of being substantially positive and negative were both >5%, true effect was assessed as UNCLEAR (could be positive or negative). Otherwise, chances of being positive or negative were assessed as follows: <1%, almost certainly not; 1-5%, very unlikely; 5-25%, unlikely; 25-75%, possibly; 75-95%, likely; 95-99%, very unlikely; >99%, almost certainly.

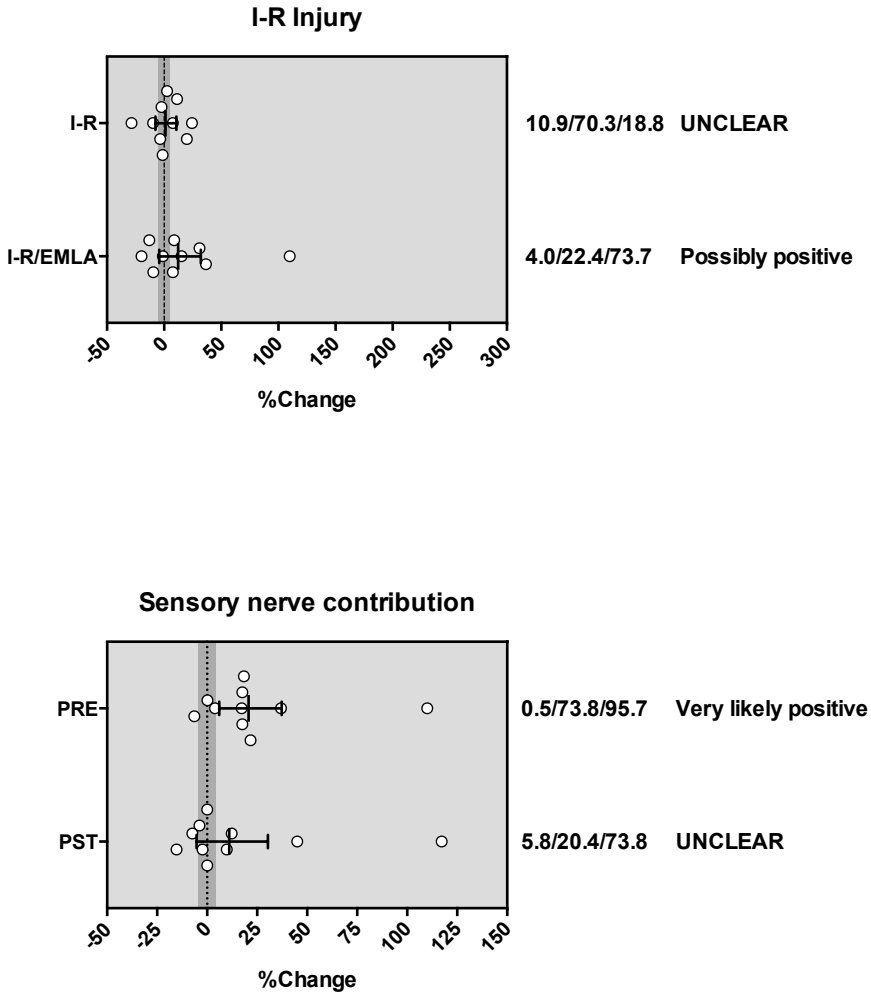

Figure 8.8 Time to initial peak: Percent change for the effects of I-R injury (ISCH-SHAM) and the contribution of sensory nerves (EMLA-UNTR)

Dark shaded areas represents the relevant within-subject coefficient of variation (CV) derived from Chapter 7. I-R, ischaemia-reperfusion; I-R/EMLA, ischaemia-reperfusion and sensory nerve blockade; PRE, pre-ischaemia condition; PST, post-ischaemia condition. Black bar represents mean percentage difference with 90% confidence limits. White circles represent individual responses. Qualitative inferences are based on the presence or absence of a substantial effect, defined as Mean difference being outside of the test-retest CV determined for each variable in Chapter 7. If the chance of being substantially positive and negative were both >5%, true effect was assessed as UNCLEAR (could be positive or negative). Otherwise, chances of being positive or negative were assessed as follows: <1%, almost certainly not; 1-5%, very unlikely; 5-25%, unlikely; 25-75%, possibly; 75-95%, likely; 95-99%, very unlikely; >99%, almost certainly.

8.4 Discussion

In the current study, the influence of upper limb I-R injury on sensory nerve involvement in the subsequent response to local heating in the non-glabrous skin of the forearm was examined. Consistent with the approach taken in Chapter 6, final conclusions were based on inferential statistics emphasizing precision of estimation over null-hypothesis testing. The main findings were (i) I-R injury attenuated the initial vasodilatory peak and delayed the onset of vasodilatation, (ii) I-R injury also attenuated the vasodilatory response to sustained local heating, (iii) pre-ischaemia, sensory nerves contributed prominently to the initial vasodilatory peak and the onset of vasodilatation, but their contribution to sustained local heating was negligible, (iv) post-ischaemia, the contribution of sensory nerves in mediating the initial peak and vasodilatory onset was reduced, while the observed reduction in the plateau was independent of sensory nerve function.

The baseline CVC was not influenced by I-R and, consistent with previous work, sensory nerve blockade with EMLA treatment did not influence the baseline CVC in the non-glabrous skin of the forearm (Minson *et al.*, 2001; Hodges *et al.*, 2015). In contrast, during local skin heating at 42°C, I-R injury was associated with a 34% delay in vasodilatory onset time and a 31% attenuation of the initial vasodilatory peak, while these pre- and post-ischaemia differences were abolished with sensory nerve blockade. The observed delay in vasodilatory onset time and the attenuation of the initial peak during local heating following I-R were approximately half of those demonstrated with complete sensory nerve blockade with EMLA pre-ischaemia. Ultimately, the effects of I-R injury were such that the sensory nerve contribution to the vasodilatory onset time and the magnitude of the initial peak were both reduced considerably post-ischaemia. Combined, these findings strongly indicate that 20 minutes of upper limb ischaemia followed by reperfusion acutely impairs sensory nerve function in the non-glabrous skin of the forearm.

It is well established that sensory nerves play an important role in initiating the cutaneous vasodilatory response to both local (Minson *et al.*, 2001; Hodges *et al.*, 2015; Hodges *et al.*, 2016) and whole-body heating (Wong, 2013). Capsaicin-sensitive C-fibres are stimulated during rapid, local heating (Magerl & Treede,

1996), which occurs via activation of TRPV-1 ion channels and subsequent sensory nerve depolarization (Wong & Fieger, 2010). Moreover, complete sensory nerve blockade with EMLA cream attenuates the initial peak (Minson *et al.*, 2001; Hodges *et al.*, 2015) and also delays the timing of the response during both rapid (Hodges *et al.*, 2015) and gradual (Hodges *et al.*, 2016) local skin heating. Additionally, NK-1 receptors are involved in regulating the initial vasodilatory peak, consistent with an important modulatory role of the sensory neuropeptide SP in this response (Wong & Minson, 2011).

In addition, sensory nerve stimulation is an important functional component of the responses to both ischaemia and reperfusion. In the rodent myocardium, low tissue pH (Franco-Cereceda *et al.*, 1993) and ROS (Ustinova & Schultz, 1994b, a) directly stimulate capsaicin-sensitive C-fibres during ischaemia and reperfusion, respectively. Furthermore, many animal models of I-R have demonstrated that stimulation of these sensory afferents and the consequent release of vasodilatory neuropeptides from their nerve endings is important for modulating both blood flow and inflammation in the affected tissue (Ustinova *et al.*, 1995; Gherardini *et al.*, 1996; Harada *et al.*, 2002; Turchanyi *et al.*, 2005; Wang & Wang, 2005; Mizutani *et al.*, 2009; Wang *et al.*, 2012; Ji *et al.*, 2013). Although important for modulating tissue blood flow and inflammation in response to tissue injury, activation of sensory nerves under these conditions can alter the vasodilatory response to a secondary stimulation. In a series of experiments, Wong and colleagues demonstrated that prior stimulation of the skin with exogenous infusion of SP, blunted subsequent vasodilatory responses to a second SP infusion (Wong *et al.*, 2005) and to whole-body heating (Wong & Minson, 2006), while during local skin heating, prior stimulation with SP rendered both the initial vasodilatory peak and nadir phases indistinguishable from each other (Wong & Minson, 2011).

Alterations in cutaneous sensory axonal conduction may also contribute to the impaired vasodilatory response post-ischaemia. Examination of large myelinated sensory nerves has demonstrated that reperfusion following cuff occlusion of the upper limb in humans is associated with rapid axonal hyperpolarization and a slow return to pre-ischaemic excitability levels (Lin *et al.*,

2002), which is associated with an increase in nerve firing thresholds (Burke *et al.*, 2001). To the best of this author's knowledge, the relationship between I-R and axonal hyperpolarization in cutaneous capsaicin-sensitive C-fibres, which are primarily responsible for mediating the vasodilatory response to rapid local skin heating, has not been directly evaluated in human skin. However, it is plausible that the observed delay in vasodilatory onset time during local heating post-ischaemia is associated with altered axonal conduction properties in these sensory afferents during reperfusion. In support of this, Hodges *et al.* (2016) recently demonstrated a significant increase in the local skin temperature onset threshold for vasodilatation in the arm and leg during gradual local heating under conditions of sensory nerve blockade with EMLA treatment, which inhibits axonal conduction by blocking Na^+ influx via competitive binding with Na^+ channels on the intracellular membrane surface. These findings during gradual local skin heating were consistent with previously observed delays in vasodilatory onset time in both limbs with the same rapid local heating protocol used in the current study (Hodges *et al.*, 2015).

In addition to sensory nerves, noradrenergic nerves are also important in modulating the initial vasodilatory peak (Houghton *et al.*, 2006; Hodges *et al.*, 2008, 2009). The reduction in NO bioavailability associated with I-R injury may contribute to an elevation of sympathetic tone by shifting the balance toward a vasoconstrictive state (Harrison, 1997; Carden & Granger, 2000). Indeed, during local skin heating in the forearm, NO release is directly responsible for inhibiting the vasoconstrictor response to exogenous norepinephrine administration (Wingo *et al.*, 2009). In the same I-R model as that used in the current experiment, Lambert *et al.* (2016) demonstrated an elevation of muscle sympathetic nerve activity in the leg throughout ischaemia and early reperfusion of the upper limb. Thus, if NO-bioavailability is reduced as a result of scavenging by ROS during reperfusion, an increase in sympathetic tone may contribute to the delayed vasodilatory response to local heating.

Following the initial vasodilatory peak, the response to sustained local heating in the forearm skin was attenuated by 34% following I-R injury. Consistent with previous work, the contribution of sensory nerves in mediating the plateau

phase was negligible prior to ischaemia (Minson *et al.*, 2001; Hodges *et al.*, 2015), and this effect was not altered during reperfusion, indicating that other mechanisms were responsible for the post-ischaemic reduction in the CVC. Kellogg *et al.* (1999) demonstrated that the vasodilatory response to sustained local heating is primarily NO-mediated. Accordingly, the observed attenuation of the plateau phase post-ischaemia is consistent with a reduction in NO bioavailability, which is a hallmark of I-R injury (Carden & Granger, 2000). In addition, this response is also consistent with previous findings of impaired radial artery flow-mediated dilation (Kharbanda *et al.*, 2001; Gori *et al.*, 2006) and attenuated resistance artery endothelium-dependent vasodilatation during acetylcholine infusions in the same I-R model (Kharbanda *et al.*, 2001). Furthermore, although the initial vasodilatory peak is mediated primarily by sensory nerves, NO also contributes to the response, and NOS inhibition can modestly attenuate or delay the initial peak during local heating in the non-glabrous skin of the forearm (Minson *et al.*, 2001; Houghton *et al.*, 2006; Hodges *et al.*, 2008). Combined, these findings suggest that inhibition of NO by I-R may be an important contributor to altering both phases of the vasodilatory response to local heating post-ischaemia.

Limitations

The components of the EMLA cream (lidocaine/prilocaine) interfere with the conduction properties of all cutaneous nerve fibres. However, prior work has demonstrated that application of EMLA cream does not measurably influence cutaneous sympathetic nerves during local skin cooling (Johnson *et al.*, 2005; Hodges *et al.*, 2007) or whole-body cooling (Wong, 2013) and, instead only appears to block sensory nerve function. There does not appear to be any current methods that would allow for verification of the effects of EMLA cream on sensory nerves exclusively. As such, there is a potential that sympathetic nerves may also be influenced by the anaesthetic application.

In the current study, core body temperature was not assessed, which may have had an influence on the observed skin blood flow responses. However, the ambient temperature was tightly controlled and participants were examined at the same time of day and each experimental session was time-matched with the same

acclimation period prior to baseline data collection. Furthermore, mean whole-body skin temperature, as well as non-glabrous and glabrous skin temperatures from the middle finger of the experimental limb did not differ significantly between trials, indicating that marked changes in core temperature were very unlikely.

Conclusions

The current data indicate that upper limb I-R has detrimental effects on the vasodilatory response to a subsequent local heating stimulus in the non-glabrous skin of the forearm. The vasodilatory onset time was delayed and the magnitude of the initial vasodilatory peak was attenuated post-ischaemia. In addition, the vasodilatory response to sustained local heating in the forearm was also attenuated. These findings indicate that acute I-R injury of the upper limb is associated with impairments in sensory nerve function and NO bioavailability that negatively impact blood flow in the cutaneous microcirculation.

8.5 References

Batterham AM & Hopkins WG. (2006). Making Meaningful Inferences About Magnitudes. *Int J Sport Physiol Perform* **1,** 50-57.

Burke D, Kiernan MC & Bostock H. (2001). Excitability of human axons. *Clin Neurophysiol* **112,** 1575-1585.

Carden DL & Granger DN. (2000). Pathophysiology of ischaemia-reperfusion injury. *J Pathol* **190,** 255-266.

Franco-Cereceda A, Kallner G & Lundberg JM. (1993). Capsazepine-sensitive release of calcitonin gene-related peptide from C-fiber afferents in the guinea pig heart by low pH and lactic acid. *Eur J Pharmacol* **238,** 311-316.

Gherardini G, Evans GRD, Theodorsson E, Gurlek A, Milner SM, Palmer B & Lundeberg T. (1996). Calcitonin gene-related peptide in experimental ischemia. Implication of an endogenous anti-ischemic effect. *Ann Plast Surg* **36,** 616-620.

Gori T, Di Stolfo G, Sicuro S, Dragoni S, Parker JD & Forconi S. (2006). The effect of ischemia and reperfusion on microvascular function: A human in vivo comparative study with conduit arteries. *Clin Hemorheol Microcirc* **35,** 169-173.

Granger DN. (1999). Ischemia-reperfusion: Mechanisms of microvascular dysfunction and the influence of risk factors for cardiovascular disease. *Microcirculation* **6,** 167-178.

Harada N, Okajima K, Uchiba M & Katsuragi T. (2002). Ischemia/reperfusion-induced increase in the hepatic level of prostacyclin is mainly mediated by activation of capsaicin-sensitive sensory neurons in rats. *J Lab Clin Med* **139,** 218-226.

Harrison DG. (1997). Cellular and molecular mechanisms of endothelial cell dysfunction. *J Clin Invest* **100,** 2153-2157.

Hodges GJ, Del Pozzi AT, McGarr GW, Mallette MM & Cheung SS. (2015). The contribution of sensory nerves to cutaneous vasodilatation of the forearm and leg to local skin heating. *Eur J Appl Physiol* **115,** 2091-2098.

Hodges GJ, Kosiba WA, Zhao K & Johnson JM. (2008). The involvement of norepinephrine, neuropeptide Y, and nitric oxide in the cutaneous vasodilator response to local heating in humans. *Journal of Applied Physiology* **105,** 233-240.

Hodges GJ, Kosiba WA, Zhao K & Johnson JM. (2009). The involvement of heating rate and vasoconstrictor nerves in the cutaneous vasodilator response to skin warming. *Am J Physiol-Heart Circul Physiol* **296,** H51-H56.

Hodges GJ, McGarr GW, Mallette MM, Del Pozzi AT & Cheung SS. (2016). The contribution of sensory nerves to the onset threshold for cutaneous vasodilatation during gradual local skin heating of the forearm and leg. *Microvasc Res* **105,** 1-6.

Hodges GJ, Traeger JA, Tang T, Kosiba WA, Zhao K & Johnson JM. (2007). Role of sensory nerves in the cutaneous vasoconstrictor response to local cooling in humans. *Am J Physiol-Heart Circul Physiol* **293,** H784-H789.

Hopkins WG. (2002). Probabiliites of Clinical or Practical Significance. *Sportscience* **6**.

Hopkins WG. (2007). A Spreadsheet for Deriving a Confidence Interval, Mechanistic Inference and Clinical Inference from a P value. *Sportscience* **11,** 16-20.

Houghton BL, Meendering JR, Wong BJ & Minson CT. (2006). Nitric oxide and noradrenaline contribute to the temperature threshold of the axon reflex response to gradual local heating in human skin. *J Physiol-London* **572,** 811-820.

Ji P, Jiang T, Wang MH, Wang RR, Zhang LQ & Li Y. (2013). Denervation of capsaicin-sensitive C fibers increases pulmonary inflammation induced by ischemia-reperfusion in rabbits. *J Surg Res* **184,** 782-789.

Johnson JM, Minson CT & Kellogg DL. (2014). Cutaneous Vasodilator and Vasoconstrictor Mechanisms in Temperature Regulation. *Compr Physiol* **4,** 33-89.

Johnson JM, Yen TC, Zhao K & Kosiba WA. (2005). Sympathetic, sensory, and nonneuronal contributions to the cutaneous vasoconstrictor response to local cooling. *Am J Physiol Heart Circ Physiol* **288,** H1573-1579.

Kellogg DL, Liu Y, Kosiba IF & O'Donnell D. (1999). Role of nitric oxide in the vascular effects of local warming of the skin in humans. *Journal of Applied Physiology* **86,** 1185-1190.

Kharbanda RK, Peters M, Walton B, Kattenhorn M, Mullen M, Klein N, Vallance P, Deanfield J & MacAllister R. (2001). Ischemic preconditioning prevents endothelial injury and systemic neutrophil activation during ischemia-reperfusion in humans in vivo. *Circulation* **103,** 1624-1630.

Kline RB. (2005). *Principles and Practice of Structural Equation Modeling*. The Guilford Press, New York.

Lambert EA, Thomas CJ, Hemmes R, Eikelis N, Pathak A, Schlaich MP & Lambert GW. (2016). Sympathetic nervous response to ischemia-reperfusion injury in humans is altered with remote ischemic preconditioning. *Am J Physiol-Heart Circul Physiol* **311,** H364-H370.

Lin CSY, Kuwabara S, Cappelen-Smith C & Burke D. (2002). Responses of human sensory and motor axons to the release of ischaemia and to hyperpolarizing currents. *J Physiol-London* **541,** 1025-1039.

Magerl W & Treede RD. (1996). Heat-evoked vasodilatation in human hairy skin: Axon reflexes due to low-level activity of nociceptive afferents. *J Physiol-London* **497,** 837-848.

Minson CT, Berry LT & Joyner MJ. (2001). Nitric oxide and neurally mediated regulation of skin blood flow during local heating. *Journal of Applied Physiology* **91,** 1619-1626.

Mizutani A, Okajima K, Murakami K, Mizutani S, Kudo K, Uchino T, Kadoi Y & Noguchi T. (2009). Activation of Sensory Neurons Reduces Ischemia/Reperfusion-induced Acute Renal Injury in Rats. *Anesthesiology* **110,** 361-369.

Perneger TV. (1998). What's wrong with Bonferroni adjustments. *Br Med J* **316,** 1236-1238.

Turchanyi B, Toth B, Racz I, Vendegh Z, Furesz J & Hamar J. (2005). Ischemia Reperfusion injury of the skeletal muscle after selective deafferentation. *Physiol Res* **54,** 25-31.

Ustinova EE, Bergren D & Schultz HD. (1995). Neuropeptide depletion impairs postischemic recovery of the isolated rat heart - Role of Substance-P. *Cardiovasc Res* **30,** 55-63.

Ustinova EE & Schultz HD. (1994a). Activation of cardiac vagal afferents by oxygen-derived free radicals in rats. *Circulation Research* **74,** 895-903.

Ustinova EE & Schultz HD. (1994b). Activation of cardiac vagal afferents in ischemia and reperfusion - Prostaglandins versus oxygen-derived free radicals. *Circulation Research* **74,** 904-911.

Wang LH & Wang DH. (2005). TRPV1 gene knockout impairs postischemic recovery in isolated perfused heart in mice. *Circulation* **112,** 3617-3623.

Wang MH, Ji P, Wang RR, Zhao LF & Xia ZY. (2012). TRPV1 Agonist Capsaicin Attenuates Lung Ischemia-Reperfusion Injury in Rabbits. *J Surg Res* **173,** 153-160.

Wingo JE, Low DA, Keller DM, Brothers RM, Shibasaki M & Crandall CG. (2009). Effect of elevated local temperature on cutaneous vasoconstrictor responsiveness in humans. *Journal of Applied Physiology* **106,** 571-575.

Wong BJ. (2013). Sensory nerves and nitric oxide contribute to reflex cutaneous vasodilation in humans. *Am J Physiol-Regul Integr Comp Physiol* **304,** R651-R656.

Wong BJ & Fieger SM. (2010). Transient receptor potential vanilloid type-1 (TRPV-1) channels contribute to cutaneous thermal hyperaemia in humans. *J Physiol* **588,** 4317-4326.

Wong BJ & Minson CT. (2006). Neurokinin-1 receptor desensitization attenuates cutaneous active vasodilatation in humans. *J Physiol-London* **577,** 1043-1051.

Wong BJ & Minson CT. (2011). Altered thermal hyperaemia in human skin by prior desensitization of neurokinin-1 receptors. *Exp Physiol* **96,** 599-609.

Wong BJ, Tublitz NJ & Minson CT. (2005). Neurokinin-1 receptor desensitization to consecutive microdialysis infusions of substance P in human skin. *J Physiol-London* **568,** 1047-1056.

Chapter 9: General Discussion

9.1 Experimental synopsis

The present set of experiments was conducted to evaluate the effects of upper limb I-R on the subsequent vasodilatory response to local heating of the skin of the index finger and forearm. It was originally hypothesized that I-R would be associated with impairments in both the timing and magnitude of the initial vasodilatory peak during a subsequent local heating challenge due to a desensitization of the sensory nerves and/or associated neuropeptide receptors resulting from the preceding stimuli of ischaemia and reperfusion. In addition, it was also hypothesized that the vasodilatory response to sustained local heating would be impaired in the non-glabrous skin of the forearm and finger post-ischaemia, due to a reduction in NO bioavailability.

Comprehensive evaluations of the test-retest reliability for all components of the cutaneous LTH response using single-point LDF were described in Chapter 5 for the non-glabrous and glabrous skin of the index finger, and in Chapter 7 for the non-glabrous skin of the forearm. Reliability was assessed for several commonly reported forms of data expression. In addition, test-retest CV measurements derived from these studies were used to define the threshold values for minimally important positive and negative effects for the relevant skin sites in Chapters 6 and 8. This was done in order to make meaningful inferences about the true (population) effects of I-R on each component of the cutaneous LTH response. In Chapter 6, the effects of I-R on the cutaneous LTH response were compared between the non-glabrous and glabrous skin of the index finger. Since these skin types are known to differ in their neurovascular control and microcirculatory organization, it was anticipated that they might respond differently to I-R. In Chapter 8, the effects of I-R were compared to those of complete sensory nerve blockade with topical EMLA cream treatment in the non-glabrous skin of the forearm. This study was conducted to examine further the mechanistic basis for the observed impairments in the early vasodilatory response to local heating in the non-glabrous skin of the index finger in Chapter 6,

and to provide comparative data for non-glabrous skin in the forearm and finger as a means of identifying possible regional post-ischaemic differences in the response to local heating.

9.2 Experimental conclusions

In response to the objectives and hypotheses outlined in Chapter 3, the following conclusions can be made from the current research:

9.2.1 Chapter 5

In general, between-day reliability estimates for each phase of the LTH response were superior when the CVC was normalized to maximum. Using this form of data expression, reliability was typically superior in non-glabrous skin. However, the reliability was generally comparable between skin types for raw CVC. The reliability for the vasodilatory onset time was superior in non-glabrous skin, while that for time to initial peak was identical for both skin types. Finally, the between-day reliability in glabrous skin was comparable to that previously reported by Roustit *et al.* (2010a).

9.2.2 Chapter 6

Contrary to the original hypotheses, I-R had no effects on the initial peak or secondary plateau during local heating in either skin type. However, in non-glabrous skin, the nadir was attenuated post-ischaemia. In addition, both the vasodilatory onset time and the time to initial peak were delayed by ~23% and ~16%, respectively, in non-glabrous skin following I-R.

9.2.3 Chapter 7

Both within- and between-day reliability for the initial peak and secondary plateau phases of the LTH response were generally comparable for all forms of data expression, consistent with the hypothesis that spatial variation in the forearm is the primary contributor to the poor reliability in the forearm. The reliability for the vasodilatory onset time appeared to be superior for the within-day (inter-site) assessment, compared to the within-day (test-retest) and between-day assessments, while the reliability assessments for the time to initial peak were almost identical

for all assessments. Consistent with the original hypothesis, reliability was superior to previous experiments using single-point LDF (Roustit *et al.*, 2010a; Roustit *et al.*, 2010b) when data were expressed as raw CVC and when normalized to maximum. In addition, reliability in the current study was comparable to previous work using integrating-probe LDF (Tew *et al.*, 2011) when the CVC was normalized to maximum, but not for raw CVC.

9.2.4 Chapter 8

Consistent with the original hypotheses, I-R was associated with a ~31% attenuation of the initial peak and a ~34% attenuation during sustained local heating in the forearm. I-R was also associated with a 34% delay in vasodilatory onset time. Combined, these findings indicate that I-R had a greater detrimental effect on the cutaneous microcirculation in the non-glabrous skin of the forearm, compared to the index finger. Post-ischaemia, there were prominent reductions in the contribution of sensory nerves in mediating the initial vasodilatory peak and kinetics of the response. In contrast, the reduction in the secondary plateau was independent of sensory nerve activity, and was more likely the result of an impaired NO bioavailability.

9.3 Synthesis of findings

It has long been recognized that spatial variation in the cutaneous microvascular organization is an important contributor to differences in the LDF responses across skin sites on the forearm (Yen & Braverman, 1976). Despite anatomical evidence that non-glabrous skin in the finger displays similar morphological characteristics to that in the forearm (Sangiorgi *et al.*, 2004), it was anticipated that reliability may still be greater on the dorsal aspect of the index finger due to the smaller absolute surface area for probe placement compared to the volar surface of the forearm. When comparing non-glabrous skin sites, the reliability values for the raw CVC were very similar, and when the CVC values were normalized to maximum heating at 44°C, the reliability for the index finger was modestly superior for both the initial vasodilatory peak and plateau phases of the LTH response. However, examining the overlap of the confidence intervals between the

non-glabrous skin sites suggests that any observed differences in reliability were trivial.

In contrast to the assertion by Roustit *et al.* (2010a) that single-point LDF was useful for examining the LTH response in the finger pad, but not in the forearm, due to a lack of adequate reliability in the case of the forearm, between-day reliability results for the initial vasodilatory peak and plateau phases of the LTH response on the finger pad were generally comparable to both non-glabrous skin sites when data were expressed as raw CVC. Furthermore, when the CVC data were normalized to maximum heating at 44°C, the reliability in non-glabrous skin in both the forearm and finger were generally superior to that of the glabrous skin of the finger pad for the initial vasodilatory peak, while the results were similar among skin sites for the plateau phase. As mentioned previously in Chapters 5 and 7, the longer duration of skin heating at 44°C in the current experiments likely attributed to greater reliability compared to that of Roustit *et al.* (2010a) who only sustained local heating at 44°C for 5 min, which was likely insufficient to establish a true plateau during maximum heating. In addition, the inferior reliability demonstrated for the initial vasodilatory peak on the finger pad was also be due to the fact that local heating to 44°C does not always produce a true maximum vasodilatory response that is greater in magnitude than the initial peak for this skin type, which was clearly demonstrated in Chapter 5, and is consistent with previous work in the finger pad (Roustit *et al.*, 2010a) and palm (Metzler-Wilson *et al.*, 2012).

In Chapter 6, no practical effects of I-R were demonstrated in the glabrous skin of the index finger. Conversely, for the non-glabrous skin on the dorsal aspect of the finger, the timing of the vasodilatory response to local skin heating was clearly delayed post-ischaemia, with the most definitive finding being a delay in the vasodilatory onset time. This response was also demonstrated in the non-glabrous forearm skin in Chapter 8. However, unlike the finger, the attenuations of the initial vasodilatory peak and plateau phases of the LTH response were also observed in the forearm post-ischaemia. The combined delay in vasodilatory onset time and attenuation of the entire vasodilatory response indicate that the detrimental effects of I-R on the cutaneous microcirculation were greater in the forearm than in the

finger. There are several possible reasons why the detrimental effects of I-R appeared to be greater in the forearm relative to the index finger, despite testing non-glabrous skin in both sites. First, there is a greater mass of underlying muscle tissue in the forearm that is also influenced by ischaemia and reperfusion. As such, it is likely that there was a larger build up of metabolic byproducts during ischaemia, and a greater free radical burst during reperfusion, which could have influenced the magnitude of the response in all tissues within the immediate area. Second, in the current experiments, blood flow in the non-glabrous skin of the finger was generally higher than that in the forearm, which may have provided a protective effect on the tissue by rapidly flushing out toxic metabolites. In addition, finger temperatures approximated ambient room temperature by the end of the 20 minutes of ischaemia, while forearm temperatures were relatively stable throughout cuff occlusion (data not shown). Finger skin temperature is influenced by ambient conditions to a much greater extent than forearm skin due to the greater surface area to mass ratio in the fingers. In the forearm, the large mass of underlying skeletal muscle also contributes heat energy to the skin surface, which helps to maintain skin temperature in this region for longer during occlusion. As such, it is also plausible that the reduction in finger skin temperature may have been associated with a lower metabolic rate, the effect of which could have provided modest protection of the finger tissue from metabolic breakdown, contributing to an attenuation of ROS induced injury and NO scavenging.

While the degree to which I-R influenced the magnitude of the vasodilatory response to local heating differed between the non-glabrous skin of the forearm and finger, both regions demonstrated distinct delays in the vasodilatory onset time. In Chapter 8, there was a prominent delay in the vasodilatory onset time in the forearm skin following sensory nerve blockade with EMLA treatment, which is consistent with prior work from our laboratory using the same local heating protocol in the arm and leg (Hodges *et al.*, 2015). The delay caused by I-R was approximately half that induced by complete blockade of sensory nerve conduction with the EMLA cream, indicating that sensory nerve conduction was at least partially impaired post-ischaemia. The current experiment in Chapter 8 and the

study by Hodges *et al.* (2015) both suggest that a stronger temperature stimulus is necessary to induce cutaneous vasodilatation when sensory nerve conduction is impaired. However, the rapid heating rate used in these experiments precluded a clear determination of the local temperature onset threshold. To address this issue, another recent study by our laboratory utilized a gradual local heating protocol to examine the relationship between local skin temperature and vasodilatory onset time (Hodges *et al.*, 2016). In that experiment, sensory nerve blockade with the EMLA cream shifted the local skin temperature onset threshold for vasodilatation up ~1.5°C and ~2.0°C in the arm and leg, respectively, when local skin temperature was increased at a rate of 1°C every 10 minutes. These findings are consistent with previous work in large myelinated sensory nerves demonstrating that reperfusion following cuff occlusion of the upper limb in humans is associated with rapid axonal hyperpolarization and a slow return to pre-ischaemic excitability levels (Lin *et al.*, 2002), which is associated with an increase in nerve firing thresholds (Burke *et al.*, 2001). Combined, these results strongly indicate that the observed delay in vasodilatory onset time post-ischaemia is associated with an impaired cutaneous sensory nerve conduction, resulting in a greater local temperature onset threshold for vasodilatation, due to hyperpolarization of capsaicin-sensitive C-fibres.

Since a reduction in NO bioavailability is a hallmark of I-R injury (Carden & Granger, 2000) and NO is also the primary mediator of the cutaneous response to sustained local heating (Minson *et al.*, 2001), the observed attenuation of the plateau phase during local heating in the forearm post-ischaemia strongly suggests that the current I-R model was associated with an impaired NO release in the non-glabrous skin of the forearm. This finding is consistent with prior work demonstrating impairments in endothelium-dependent vasodilatation in both conduit and resistance arteries in the same I-R model as that used in the current experiments (Kharbanda *et al.*, 2001; Gori *et al.*, 2006). Importantly, NO release also contributes to the initial vasodilatory peak during rapid, local skin heating, albeit to a lesser degree than sensory nerves (Minson *et al.*, 2001). In addition Houghton *et al.* (2006) demonstrated that NOS inhibition delays the temperature threshold for the axon reflex during gradual local skin heating. Combined, these findings indicate that a

reduction in NO bioavailability post-ischaemia may also modestly contribute to the delayed vasodilatory onset in the non-glabrous skin of the forearm and index finger, in addition to attenuating the plateau phase during sustained local heating in the forearm.

Importantly, the role of sensory nerves and NO in mediating the cutaneous vasodilatory response to whole-body heating appear to be similar to those previously described for local skin heating. Indeed, Wong (2013) demonstrated that application of the EMLA cream delayed the oral temperature onset threshold for vasodilatation in non-glabrous forearm skin during whole body heating, while it had no measurable effect on the overall magnitude of the response. Conversely, NOS inhibition was associated with a delay in vasodilatory onset, in addition to a reduction in the magnitude of the response. The similarities between the mechanisms involved in local skin heating and whole body heating suggest that in addition to impairing the response to local skin heating, I-R may also be associated with an impaired cutaneous vasodilatory response to whole-body heating. However, this has yet to be confirmed experimentally.

9.4 Upper limb I-R model

The current findings demonstrate that the upper limb I-R model used in the preceding experiments is a safe and useful experimental approach for investigating the influence of ischaemia and reperfusion on the cutaneous microcirculation in otherwise healthy participants. Protocols utilizing 20 min of ischaemia followed by reperfusion have been widely used and functional impairments in conduit arteries were demonstrated in multiple studies with no prolonged side effects in otherwise healthy, young participants (Kharbanda *et al.*, 2001; Gori *et al.*, 2006; Seeger *et al.*, 2015; Brunt *et al.*, 2016). Since the microcirculation is more sensitive than large blood vessels to the effects of I-R (Carden & Granger, 2000), it was anticipated that the 20 min ischaemic insult followed by reperfusion would induce a sufficient microcirculatory strain to observe alterations in the cutaneous LTH response.

Due to the fact that ischaemic injury is directly related to the duration of the insult (Wang *et al.*, 2011; Schmidt *et al.*, 2012; Granger & Kvietys, 2015), it is

reasonable to assume that a period of cuff occlusion longer than the 20 min could have been safely adopted for the current experiments in order to induce a greater level of cutaneous microcirculatory dysfunction. This may have been associated with greater impairments in the LTH response, especially in the glabrous skin of the index finger, which did not appear to be negatively impacted by the I-R stimulus. While there is no clear consensus on safe tourniquet times for limb ischaemia (Pedowitz, 1991), operative time limits of up to ~2-3 h are commonly adhered to (Pedowitz, 1991; Sharma & Salhotra, 2012). Indeed, prominent tissue oedema only develops when cuff occlusion time exceeds 1 h (Wilgis, 1971) and the 2-3 h safety window is associated with impairments in neuromuscular function lasting as long as 5-7 d post-operatively, in the absence of overt histological damage of the affected tissue (Turchanyi *et al.*, 2005; Sharma & Salhotra, 2012). That said, while a longer cuff occlusion may have been possible, and was more likely to induce a greater level of tissue injury, it would not have been ethical to significantly prolong the ischaemic period in the current experiments since neurological complications are 3 times more likely to develop for every additional 30 min of cuff inflation time (Horlocker *et al.*, 2006). Furthermore, longer exposure times would have likely been associated with greater participant dropout, due to increasing pain associated with more prolonged ischaemic exposure in conscious participants.

In the current experiments, all participants tolerated the I-R stimulus well, with the most common complaints being minor muscle tightening during ischaemia, cold sensations during ischaemia, and hot sensations during reperfusion, as well as "pins-and-needles" sensations throughout. In addition, minor muscle weakness in the affected limb was reported by some participants within the first 1-2 h of reperfusion. Overall, the results indicate that the upper limb I-R model used is sufficient to cause measurable impairments in the cutaneous microcirculation and transient muscle weakness lasting at least 1-2 h post-ischaemia. It appears that upper limb I-R has a stronger influence on the function of non-glabrous skin than it does on glabrous skin, at least with the duration of ischaemia and reperfusion used in the current protocol. In addition, the negative effects of I-R appear to be greater in the forearm than in the finger. As such, future studies examining potential clinical

interventions for I-R induced cutaneous microcirculatory dysfunction should focus on examining non-glabrous forearm skin when using the current I-R model in order to ensure that a sufficient level of microvascular injury is applied. An added benefit of examining the forearm is the larger surface area for measuring multiple skin sites at the same time, which allows for the addition of various pharmacological manipulations in order to further elucidate the underlying pathophysiological mechanism(s) involved.

9.5 Clinical relevance

An important limitation when evaluating the cutaneous LTH response or any other microvascular reactivity test is the inherently integrative nature of the physiological response, which involves multiple and often redundant signaling mechanisms, including neural, endothelial, and vascular smooth muscle contributions (Holowatz *et al.*, 2008). Indeed, although the response to local skin heating is dominated by sensory nerves during the early vasodilatory phase and NO during sustained heating (Minson *et al.*, 2001), a variety of other mediators are also involved (Johnson *et al.*, 2014), and since the response to I-R is also multifactorial in nature (Eltzschig & Collard, 2004; Kalogeris *et al.*, 2012; Widgerow, 2014), it is very likely that the negative effects on the LTH response in non-glabrous skin also involve other mechanisms beyond sensory nerves. It is, therefore, suggested that the role of NO in this response needs to be evaluated in future studies.

Regardless of the specific underlying mechanism(s) involved, or their relative pathophysiological contribution(s), it is clear from the preceding experiments that the current upper limb I-R model is associated with an impaired functional vasodilatory response to local heating in non-glabrous skin. Such a finding indicates that the cutaneous LTH response may be a useful clinical tool for tracking general microcirculatory function and tissue viability over time following limb surgery, replantations, or skin grafting procedures. In addition, it may be a useful approach for identifying the effects of pharmaceutical or other clinical interventions aimed at improving tissue viability under these conditions. Indeed, the LTH test has already demonstrated prognostic value as an independent predictor of

mortality and morbidity in end-stage renal disease (Kruger *et al.*, 2006), and has been used as a predictor of digital ulcer formation in sclerosis patients (Blaise *et al.*, 2014). However, in the context of I-R, the predictive value of the test remains to be confirmed in clinical populations.

Beyond its potential utility as a clinical marker of microcirculatory function, the finding of impaired LTH responses in the non-glabrous skin of the forearm and index finger post-ischaemia may also shed new light on the relationship between local skin and core body temperatures and the development of chronic wounds, such as pressure-induced ulcers, which are associated with repeated cycles of ischaemia and reperfusion (Mustoe, 2004). Indeed, elevated local skin (Kokate *et al.*, 1995) and core body (Bergstrom & Braden, 1992; Nixon *et al.*, 2000) temperatures are both associated with an increased risk of pressure ulcer formation. It is well established that increasing tissue temperature increases metabolic demand and under conditions of I-R where tissue perfusion is compromised, there is a greater risk of ischaemia for a given reduction in blood flow when temperature is elevated, relative to when it remains stable (Clark *et al.*, 2010). As such, the general consensus is that elevated tissue temperature increases the susceptibility to ischaemia and tissue injury with shorter durations and lower levels of pressure-induced occlusion relative to normothermic conditions (Clark *et al.*, 2010).

In addition, during the reperfusion phase, tissue hypoxia will persist if oxygen delivery falls below the increased metabolic demand associated with elevated local temperature. As such, the finding of a delayed vasodilatory onset time in the non-glabrous skin of the index finger and forearm in Chapters 6 and 8, indicates that in addition to the increased metabolic demand associated with elevated tissue temperature, I-R also contributes to the temperature-induced tissue damage by directly impairing the functional ability of the cutaneous microcirculation to initiate an effective vasodilatory response to the increased temperature stimulus. Indeed, in the forearm skin, even after vasodilatation was initiated, the magnitude of the response was still attenuated post-ischaemia. The combined influence of increasing metabolic demand under higher local temperature, along with an impaired vasodilatory response to that stimulus, is likely

to exacerbate tissue hypoxia during reperfusion and further underscores the importance of keeping local and core body temperatures stable during recovery from an acute ischaemic injury, and in patients that are susceptible to pressure ulcers such as those that use wheelchairs or are confined to their beds. In chronic wounds, where I-R occurs in a cyclical fashion (Mustoe, 2004), the ability of the cutaneous microcirculation to vasodilate adequately in response to a local heating stimulus is likely to be further impaired under the influence of repeated exposures to ischaemia and reperfusion, underlying the importance of appropriate temperature control under such conditions.

9.6 Statistical Approach

In Chapters 6 and 8, statistical evaluation of the impact of I-R injury on the cutaneous LTH response was ultimately based on the examination of magnitude-based inferences (MBI), which emphasize precision of estimation over the more traditional approach of null hypothesis significance testing (NHST) (Batterham & Hopkins, 2006). The primary advantage of MBI is that it requires the researcher to define and justify values of an effect that are practically (mechanistically) meaningful, in contrast to the more traditional NHST, in which effects are deemed relevant only when the observed probability value for an effect is below a previously defined threshold for statistical significance (Batterham & Hopkins, 2015). In the context of the preceding experiments, the effects of I-R injury were only identified as meaningful under the MBI approach when they were greater than the typical test-retest variation, defined by the %CV from the relevant reliability studies that were performed in Chapters 5 and 7. Thus, MBI goes one step further by providing a framework for describing the level of uncertainty in the effects of I-R injury in relation to these experimentally derived (%CV) values for a trivial effect (Batterham & Hopkins, 2006, 2015).

The primary criticism of MBI is that it is a deliberately less conservative approach to evaluating the data, which may lead to an increase in the Type-I error (false positive) rate, thus making it more likely that the researcher will declare an effect to be meaningful than when it is based on chance alone (Welsh & Knight,

2015). This concern is based on the fact that MBI allows the researcher to evaluate the practical importance of a given effect even when it has been deemed statistically non-significant. If one only considers the statistical results under a strict accept-reject paradigm, as is the case with NHST, then this is a legitimate criticism. However, it is more appropriate to evaluate the importance of a given effect on a continuum by examining the entire length of its surrounding CI, which identifies the uncertainty of the effect estimate. In this regard, the use of MBI is appropriate. It should be recognized that under conditions where an effect is deemed non-significant by NHST, the practical effect identified by MBI would not support a definitive statement regarding the importance of a particular finding, since a portion of the CI will cross the zone defined as trivial. Furthermore, with a wider trivial zone, a greater portion of the CI is likely to cross this region and the effect becomes less definitive. These realities are clearly reflected in the relative probabilities of an effect being negative/trivial/positive and the associated qualitative descriptive statements. Under these circumstances, the weight of evidence may warrant further evaluation of a particular effect in a larger, more powerful follow-up study, limiting scenarios where potentially important findings are erroneously assumed to be of no practical importance simply because they were statistically non-significant. In this context, the MBI approach provides a more nuanced strategy for identifying the practical significance of an effect, but care should be taken not to ascribe more practical importance than is actually supported by the data. In addition, the requirement for establishing a clear practical effect of an intervention based on experimental (real-world) evidence, rather than a threshold for statistical significance, tempers the concern for Type-I error addressed by its critics (Batterham & Hopkins, 2015).

The argument that MBI is a less conservative strategy than NHST also ignores the fact that statistically significant findings may ultimately be shown to have little to no practical relevance when evaluating the size of an effect. This can be illustrated by evaluating the effect of I-R injury on vasodilatory onset time during LTH from Chapter 6. A statistically significant delay ($p=0.04$) in onset time was identified in glabrous skin following I-R injury. However, when the typical test-retest variation

(%CV) was taken into consideration, MBI demonstrated that there was a 93.8% chance that the real effect of I-R injury on this response was actually trivial in glabrous skin (Fig 6.7). In addition, while minimizing Type-I error rate is important in order to avoid making erroneous conclusions, it must be appreciated that any effort to reduce this problem is necessarily associated with a concomitant increase in Type-II error rate, which makes it more difficult to identify truly meaningful effects when they do exist (Perneger, 1998; Sterne & Smith, 2001). This is particularly a problem in studies with relatively small samples sizes, such as the ones performed in the preceding chapters, where efforts to reduce Type-1 error often compromise the utility of the experiment due to significant reductions in power (Perneger, 1998; Button *et al.*, 2013).

In the preceding experiments, the effects of I-R injury were evaluated using both MBI and the more traditional NHST approach, allowing the reader to interpret the findings using whichever statistical framework they deem most appropriate. Ultimately, interpretation of the findings for each experiment should be based on the entire weight of evidence provided, including what is already known from prior work and whether or not a particular finding is biologically plausible (Sterne & Smith, 2001). In addition, caution should be used when attempting to place undue emphasis on the p-value or effect size estimate of any particular measurement, since both are derived from sampled data, which may not ultimately accurately represent the true population effect. In this regard, the reader should appreciate that if both statistical approaches are interpreted correctly, and the results are evaluated in the context of what is already known about the effects of I-R injury on sensory nerve function and tissue blood flow, the ultimate conclusions from the experiments in Chapters 6 and 8 are consistent and each approach should tell the same story.

9.7 Limitations

In addition to those previously described in Chapters 5-8, the following limitations should also be considered for the current research:

The reliability studies performed in Chapters 5 and 7 used a small (n=10) sample of individuals to examine the cutaneous LTH response in the forearm and

finger, which was consistent with the sample size used in previous reliability studies examining this response (Agarwal *et al.*, 2010; Roustit *et al.*, 2010a; Roustit *et al.*, 2010b; Tew *et al.*, 2011). Although the current results were in line with these prior experiments, all of these studies likely suffer from a lack of precision. This is demonstrated in Chapters 5 and 7 by examining the wide 95% CIs for all calculated reliability measures. As such, future work could examine a larger sample of participants in order to provide more precise effect size estimates for all reliability measures.

In the current thesis, maximum vasodilatation was operationally defined as the response achieved when the skin was locally heated to 44°C, consistent with many previous studies (Roustit *et al.*, 2010a; Roustit *et al.*, 2010b; Tew *et al.*, 2011; Hodges *et al.*, 2015; Hodges *et al.*, 2016). This temperature was the highest set point possible with the available equipment, which is restricted to avoid burn injuries. The main disadvantage of this approach for achieving maximum vasodilatation is that it requires a fully functional endogenous response to the local heating stimulus, which may not occur following I-R due to NO scavenging. A commonly used alternate approach for obtaining maximum vasodilatation is the infusion of the exogenous NO donor SNP, either through iontophoresis or microdialysis. Since SNP acts directly on vascular smooth muscle, which is not negatively influenced by I-R (Banda *et al.*, 1997), this approach may offer a more reliable strategy for achieving maximum vasodilatation in this context. As such, it may also allow for the identification of more subtle differences in the local heating response by taking advantage of the greater test-retest reliability achieved when normalizing the CVC to maximum, at least in the non-glabrous skin where a true maximum value is consistently obtained.

For the current thesis, SNP infusions were not used due to the fact that direct comparisons between all skin sites would not have been possible since microdialysis cannot be performed in the finger safely, and iontophoresis is not generally reliable in glabrous skin due to poor current-induced transfer of the drug, which is likely due to a thicker connective tissue component in this skin type. In addition, beyond the effects of endothelial or vascular smooth muscle induced

vasodilatation, I-R is also associated with leukocyte plugging, coagulation, and oedema formation, all of which may also contribute to altering maximum vasodilatation. In order to account for all potential influences on skin blood flow, an absolute measure of total forearm vascular responses can be achieved by passively warming the entire forearm in a water bath or misting device, and assessing changes with venous plethysmography. During passive limb heating, the majority of blood flow changes are isolated to the skin, and as such, alterations in total skin blood flow can be assessed using this approach, which would provide the most informative assessment of whether the current model of I-R injury influences total skin blood flow (Minson, 2010; Johnson *et al.*, 2014).

9.8 Suggestions for future research

The present research has raised the following questions for future investigation:

1. Does I-R shift the onset threshold for cutaneous vasodilatation to a higher local temperature during gradual local skin heating?
2. Does I-R shift the onset threshold for cutaneous vasodilatation to a higher core temperature during whole-body heating?
3. Is the observed delay in vasodilatory onset with I-R associated with a greater influence of cutaneous adrenergic nerves under this condition?
4. How does I-R influence maximum skin blood flow during passive heating of the entire forearm?
5. Are the observed impairments in the vasodilatory response to local skin heating in non-glabrous skin associated with a reduction in NO-bioavailability in the current I-R model and can these impairments be reversed with the introduction of ROS inhibitors such as SOD?

9.9 References

Agarwal SC, Allen J, Murray A & Purcell IF. (2010). Comparative reproducibility of dermal microvascular blood flow changes in response to acetylcholine iontophoresis, hyperthermia and reactive hyperaemia. *Physiol Meas* **31,** 1-11.

Banda MA, Lefer DJ & Granger DN. (1997). Postischemic endothelium-dependent vascular reactivity is preserved in adhesion molecule-deficient mice. *Am J Physiol-Heart Circul Physiol* **273,** H2721-H2725.

Batterham AM & Hopkins WG. (2006). Making Meaningful Inferences About Magnitudes. *Int J Sport Physiol Perform* **1,** 50-57.

Batterham AM & Hopkins WG. (2015). The Case for Magnitude-based Inference. *Med Sci Sports Exerc* **47,** 885-885.

Bergstrom N & Braden B. (1992). A prospective study of pressure sore risk among institutionalized elderly. *J Am Geriatr Soc* **40,** 747-758.

Blaise S, Roustit M, Carpentier P, Seinturier C, Imbert B & Cracowski JL. (2014). The digital thermal hyperemia pattern is associated with the onset of digital ulcerations in systemic sclerosis during 3 years of follow-up. *Microvasc Res* **94,** 119-122.

Brunt VE, Jeckell AT, Ely BR, Howard MJ, Thijssen DHJ & Minson CT. (2016). Acute hot water immersion is protective against impaired vascular function following forearm ischemia-reperfusion in young healthy humans. *Am J Physiol-Regul Integr Comp Physiol* **311,** R1060-R1067.

Burke D, Kiernan MC & Bostock H. (2001). Excitability of human axons. *Clin Neurophysiol* **112,** 1575-1585.

Button KS, Ioannidis JPA, Mokrysz C, Nosek BA, Flint J, Robinson ESJ & Munafo MR. (2013). Power failure: why small sample size undermines the reliability of neuroscience. *Nat Rev Neurosci* **14,** 365-376.

Carden DL & Granger DN. (2000). Pathophysiology of ischaemia-reperfusion injury. *J Pathol* **190,** 255-266.

Clark M, Romanelli M, Reger SI, Ranganathan VK, Black J & Dealey C. (2010). Microclimate in context. In *International review Pressure ulcer prevention: pressure, shear, friction and microclimate in context*. Wounds International, London.

Eltzschig HK & Collard CD. (2004). Vascular ischaemia and reperfusion injury. *Br Med Bull* **70,** 71-86.

Gori T, Di Stolfo G, Sicuro S, Dragoni S, Parker JD & Forconi S. (2006). The effect of ischemia and reperfusion on microvascular function: A human in vivo comparative study with conduit arteries. *Clin Hemorheol Microcirc* **35,** 169-173.

Granger DN & Kvietys PR. (2015). Reperfusion injury and reactive oxygen species: The evolution of a concept. *Redox Biol* **6,** 524-551.

Hodges GJ, Del Pozzi AT, McGarr GW, Mallette MM & Cheung SS. (2015). The contribution of sensory nerves to cutaneous vasodilatation of the forearm and leg to local skin heating. *Eur J Appl Physiol* **115,** 2091-2098.

Hodges GJ, McGarr GW, Mallette MM, Del Pozzi AT & Cheung SS. (2016). The contribution of sensory nerves to the onset threshold for cutaneous vasodilatation during gradual local skin heating of the forearm and leg. *Microvasc Res* **105,** 1-6.

Holowatz LA, Thompson-Torgerson CS & Kenney WL. (2008). The human cutaneous circulation as a model of generalized microvascular function. *J Appl Physiol (1985)* **105,** 370-372.

Horlocker TT, Hebl JR, Gali B, Jankowski CJ, Burkle CM, Berry DJ, Zepeda FA, Stevens SR & Schroeder DR. (2006). Anesthetic, patient, and surgical risk factors for neurologic complications after prolonged total tourniquet time during total knee arthroplasty. *Anesth Analg* **102,** 950-955.

Houghton BL, Meendering JR, Wong BJ & Minson CT. (2006). Nitric oxide and noradrenaline contribute to the temperature threshold of the axon reflex response to gradual local heating in human skin. *J Physiol-London* **572,** 811-820.

Johnson JM, Minson CT & Kellogg DL. (2014). Cutaneous Vasodilator and Vasoconstrictor Mechanisms in Temperature Regulation. *Compr Physiol* **4,** 33-89.

Kalogeris T, Baines CP, Krenz M & Korthuis RJ. (2012). Cell biology of ischemia/reperfusion injury. In *International Review of Cell and Molecular Biology, Vol 298*, ed. Jeon KW, pp. 229-317. Elsevier Academic Press Inc, San Diego.

Kharbanda RK, Peters M, Walton B, Kattenhorn M, Mullen M, Klein N, Vallance P, Deanfield J & MacAllister R. (2001). Ischemic preconditioning prevents endothelial injury and systemic neutrophil activation during ischemia-reperfusion in humans in vivo. *Circulation* **103,** 1624-1630.

Kokate JY, Leland KJ, Held AM, Hansen GL, Kveen GL, Johnson BA, Wilke MS, Sparrow EM & Iaizzo PA. (1995). Temperature modulated pressure ulcers - A porcine model. *Arch Phys Med Rehabil* **76,** 666-673.

Kruger A, Stewart J, Sahityani R, O'Riordan E, Thompson C, Adler S, Garrick R, Vallance P & Goligorsky MS. (2006). Laser Doppler flowmetry detection of

endothelial dysfunction in end-stage renal disease patients: correlation with cardiovascular risk. *Kidney Int* **70,** 157-164.

Lin CSY, Kuwabara S, Cappelen-Smith C & Burke D. (2002). Responses of human sensory and motor axons to the release of ischaemia and to hyperpolarizing currents. *J Physiol-London* **541,** 1025-1039.

Metzler-Wilson K, Kellie LA, Tomc C, Simpson C, Sammons D & Wilson TE. (2012). Differential vasodilatory responses to local heating in facial, glabrous and hairy skin. *Clin Physiol Funct Imaging* **32,** 361-366.

Minson CT. (2010). Thermal provocation to evaluate microvascular reactivity in human skin. *J Appl Physiol (1985)* **109,** 1239-1246.

Minson CT, Berry LT & Joyner MJ. (2001). Nitric oxide and neurally mediated regulation of skin blood flow during local heating. *Journal of Applied Physiology* **91,** 1619-1626.

Mustoe T. (2004). Understanding chronic wounds: a unifying hypothesis on their pathogenesis and implications for therapy. *Am J Surg* **187,** 65S-70S.

Nixon J, Brown J, McElvenny D, Mason S & Bond S. (2000). Prognostic factors associated with pressure sore development in the immediate post-operative period. *Int J Nurs Stud* **37,** 279-289.

Pedowitz RA. (1991). Tourniquet-induced neuromuscular injury - A recent review of rabbit and clinical experiments. *Acta Orthop Scand* **62,** U1-U33.

Perneger TV. (1998). What's wrong with Bonferroni adjustments. *Br Med J* **316,** 1236-1238.

Roustit M, Blaise S, Millet C & Cracowski JL. (2010a). Reproducibility and methodological issues of skin post-occlusive and thermal hyperemia assessed by single-point laser Doppler flowmetry. *Microvascular Research* **79,** 102-108.

Roustit M, Millet C, Blaise S, Dufournet B & Cracowski JL. (2010b). Excellent reproducibility of laser speckle contrast imaging to assess skin microvascular reactivity. *Microvasc Res* **80,** 505-511.

Sangiorgi S, Manelli A, Congiu T, Bini A, Pilato G, Reguzzoni M & Raspanti M. (2004). Microvascularization of the human digit as studied by corrosion casting. *J Anat* **204,** 123-131.

Schmidt Y, Bannasch H & Eisenhardt SU. (2012). Ischemia-Reperfusion Injury Leads to Significant Tissue Damage in Free Flap Surgery. *Plast Reconstr Surg* **129,** 174E-175E.

Seeger JPH, Lenting CJ, Schreuder THA, Landman TRJ, Cable NT, Hopman MTE & Thijssen DHJ. (2015). Interval exercise, but not endurance exercise, prevents endothelial ischemia-reperfusion injury in healthy subjects. *Am J Physiol-Heart Circul Physiol* **308,** H351-H357.

Sharma JP & Salhotra R. (2012). Tourniquets in orthopedic surgery. *Indian J Orthop* **46,** 377-383.

Sterne JAC & Smith GD. (2001). Sifting the evidence - what's wrong with significance tests? *Br Med J* **322,** 226-+.

Tew GA, Klonizakis M, Moss J, Ruddock AD, Saxton JM & Hodges GJ. (2011). Reproducibility of cutaneous thermal hyperaemia assessed by laser Doppler flowmetry in young and older adults. *Microvasc Res* **81,** 177-182.

Turchanyi B, Toth B, Racz I, Vendegh Z, Furesz J & Hamar J. (2005). Ischemia Reperfusion injury of the skeletal muscle after selective deafferentation. *Physiol Res* **54,** 25-31.

Wang WZ, Baynosa RC & Zamboni WA. (2011). Update on Ischemia-Reperfusion Injury for the Plastic Surgeon: 2011. *Plast Reconstr Surg* **128,** 685E-692E.

Welsh AH & Knight EJ. (2015). "Magnitude-based Inference'': A Statistical Review. *Med Sci Sports Exerc* **47,** 874-884.

Widgerow AD. (2014). Ischemia-Reperfusion Injury Influencing the Microcirculatory and Cellular Environment. *Ann Plast Surg* **72,** 253-260.

Wilgis EFS. (1971). Observations on effects of tourniquet ischemia. *J Bone Joint Surg-Am Vol* **A 53,** 1343-&.

Wong BJ. (2013). Sensory nerves and nitric oxide contribute to reflex cutaneous vasodilation in humans. *Am J Physiol-Regul Integr Comp Physiol* **304,** R651-R656.

Yen A & Braverman IM. (1976). Ultrastructure of human dermal microcirculation - horizontal plexus of papillary dermis. *J Invest Dermatol* **66,** 131-142.

Appendix 1 – Certificates of ethics clearance

Brock University
Research Ethics Office
Tel: 905-688-5550 ext. 3035
Email: reb@brocku.ca

Bioscience Research Ethics Board

Certificate of Ethics Clearance for Human Participant Research

DATE: 11/18/2015

PRINCIPAL INVESTIGATOR: CHEUNG, Stephen - Kinesiology

FILE: 15-077 - CHEUNG

TYPE: Ph. D. STUDENT: Gregory McGarr
SUPERVISOR: Stephen Cheung

TITLE: Contribution of sensory nerves to skin blood flow responses during forearm ischaemia and reperfusion (EEL- 092)

ETHICS CLEARANCE GRANTED

Type of Clearance: NEW Expiry Date: 11/30/2016

The Brock University Bioscience Research Ethics Board has reviewed the above named research proposal and considers the procedures, as described by the applicant, to conform to the University's ethical standards and the Tri-Council Policy Statement. Clearance granted from **11/18/2015** to **11/30/2016**.

The Tri-Council Policy Statement requires that ongoing research be monitored by, at a minimum, an annual report. Should your project extend beyond the expiry date, you are required to submit a Renewal form before 11/30/2016. Continued clearance is contingent on timely submission of reports.

To comply with the Tri-Council Policy Statement, you must also submit a final report upon completion of your project. All report forms can be found on the Research Ethics web page at http://www.brocku.ca/research/policies-and-forms/research-forms.

In addition, throughout your research, you must report promptly to the REB:

a) Changes increasing the risk to the participant(s) and/or affecting significantly the conduct of the study;
b) All adverse and/or unanticipated experiences or events that may have real or potential unfavourable implications for participants;
c) New information that may adversely affect the safety of the participants or the conduct of the study;
d) Any changes in your source of funding or new funding to a previously unfunded project.

We wish you success with your research.

Approved: _____

Sandra Peters, Chair
Bioscience Research Ethics Board

Note: Brock University is accountable for the research carried out in its own jurisdiction or under its auspices and may refuse certain research even though the REB has found it ethically acceptable.

If research participants are in the care of a health facility, at a school, or other institution or community organization, it is the responsibility of the Principal Investigator to ensure that the ethical guidelines and clearance of those facilities or institutions are obtained and filed with the REB prior to the initiation of research at that site.

Brock University
Research Ethics Office
Tel: 905-688-5550 ext. 3035
Email: reb@brocku.ca

Bioscience Research Ethics Board

Certificate of Ethics Clearance for Human Participant Research

DATE: March 15, 2016

PRINCIPAL INVESTIGATOR: CHEUNG, Stephen - Kinesiology

FILE: 15-077 - CHEUNG

TYPE: Ph. D. STUDENT: Gregory McGarr
SUPERVISOR: Stephen Cheung

TITLE: Contribution of sensory nerves to skin blood flow responses during forearm ischaemia and reperfusion (EEL- 092)

ETHICS CLEARANCE GRANTED

Type of Clearance: MODIFICATION Expiry Date: 11/30/2016

The Brock University Bioscience Research Ethics Board has reviewed the above named research proposal and considers the procedures, as described by the applicant, to conform to the University's ethical standards and the Tri-Council Policy Statement.

Modification: New measurement sites and addition of testing trials to assess reliability of measures.

The Tri-Council Policy Statement requires that ongoing research be monitored by, at a minimum, an annual report. Should your project extend beyond the expiry date, you are required to submit a Renewal form before **11/30/2016**. Continued clearance is contingent on timely submission of reports.

To comply with the Tri-Council Policy Statement, you must also submit a final report upon completion of your project. All report forms can be found on the Research Ethics web page at http://www.brocku.ca/research/policies-and-forms/research-forms.

In addition, throughout your research, you must report promptly to the REB:

a) Changes increasing the risk to the participant(s) and/or affecting significantly the conduct of the study;
b) All adverse and/or unanticipated experiences or events that may have real or potential unfavourable implications for participants;
c) New information that may adversely affect the safety of the participants or the conduct of the study;
d) Any changes in your source of funding or new funding to a previously unfunded project.

We wish you success with your research.

Approved:

_____
Sandra Peters, Chair
Bioscience Research Ethics Board

Note: Brock University is accountable for the research carried out in its own jurisdiction or under its auspices and may refuse certain research even though the REB has found it ethically acceptable.

If research participants are in the care of a health facility, at a school, or other institution or community organization, it is the responsibility of the Principal Investigator to ensure that the ethical guidelines and clearance of those facilities or institutions are obtained and filed with the REB prior to the initiation of research at that site.